

# On a Prototype of an Optimal Control Problem Governed by Ordinary and Partial Differential Equations

Von der Universität Bayreuth  
zur Erlangung des Grades eines  
Doktors der Naturwissenschaften (Dr. rer. nat.)  
genehmigte Abhandlung

vorgelegt von

Stefan Wendl

geboren am 14.11.1980

Betreuer/ 1. Gutachter: Prof. Dr. Hans-Josef Pesch  
Universität Bayreuth  
2. Gutachter: Prof. Dr. Lars Grüne  
Universität Bayreuth  
3. Gutachter: Prof. Dr. Wolf von Wahl  
Universität Bayreuth

Tag der Einreichung : 06.12.2013

Tag des Kolloquiums: 28.07.2014



# Contents

<b>1</b>	<b>The hypersonic rocket car problems</b>	<b>1</b>
<b>2</b>	<b>The state-unconstrained hypersonic rocket car problem</b>	<b>5</b>
2.1	The ODE-part . . . . .	5
2.2	Semi-analytical solution of the heat equation . . . . .	7
<b>3</b>	<b>Theoretical analysis</b>	<b>11</b>
3.1	A short summary of the properties of the coupled ODE-PDE system . . . . .	11
3.2	Analysis of the switching structure for the hypersonic rocket car problems . . . . .	16
3.3	Some new aspects of ODE-PDE optimal control . . . . .	18
<b>4</b>	<b>Necessary optimality conditions</b>	<b>25</b>
4.1	Problem 1 as ODE-PDE optimal control problem . . . . .	26
4.2	Problem 1 as ODE optimal control problem . . . . .	29
4.3	Problem 1 as PDE optimal control problem . . . . .	32
<b>5</b>	<b>Numerical solution of the hypersonic rocket car problems</b>	<b>35</b>
5.1	Results for Problem 1 . . . . .	38
5.2	Results for Problem 2 . . . . .	41
5.3	A side note on discretizations . . . . .	44
5.4	Approximate verification of optimality conditions . . . . .	46
5.5	Solution via an indirect method . . . . .	54
5.5.1	Primal dual active set strategy . . . . .	54
5.5.2	Switching point optimization . . . . .	56
<b>6</b>	<b>Conclusion and outlook</b>	<b>61</b>
<b>A</b>	<b>Compact overview over the different optimality systems</b>	<b>63</b>
A.1	Problem 1: ODE formulation . . . . .	63
A.2	Problem 1: PDE formulation . . . . .	64
A.3	Problem 1: ODE-PDE formulation . . . . .	65
A.4	Problem 2: ODE formulation . . . . .	66
A.5	Problem 2: PDE formulation . . . . .	67
A.6	Problem 2: ODE-PDE formulation . . . . .	68
<b>B</b>	<b>List of symbols and abbreviations</b>	<b>69</b>
<b>C</b>	<b>On a Prototype Class of ODE-PDE State-constrained Optimal Control Problems Part 1: Analysis of the State-unconstrained Problems</b>	<b>71</b>



# List of Figures

1.1	Scheme of dependencies . . . . .	2
2.1	Phase diagram of the historic ODE optimal control problem . . . . .	6
2.2	Optimal controls $u$ for the highlighted trajectories of Fig. (2.1) . . . . .	6
2.3	Temperature profiles for Problem 1 along state-unconstrained trajectories . . . . .	9
2.4	Temperature profiles for Problem 2 along state-unconstrained trajectories . . . . .	9
5.1	Temperature $T(x, t)$ and cross-section $T(\frac{l}{2}, t)$ for Problem 1 along a state- and control-constrained trajectory . . . . .	38
5.2	State-constrained control-constrained optimal trajectory for Problem 1 in the phase-plane with associated optimal control $u$ . . . . .	38
5.3	Cross-sections of the temperature profiles at $\frac{l}{2}$ and according optimal controls $u$ for Problem 1 ("single hump"-case) featuring different values for $T_{\max}$ . . . . .	39
5.4	Cross-sections of the temperature profiles at $\frac{l}{2}$ and according optimal controls $u$ for Problem 1 ("double hump"-case) featuring different values for $T_{\max}$ . . . . .	40
5.5	Temperature $T(x, t)$ and cross-section $T(l, t)$ for Problem 2 along a state- and control-constrained trajectory . . . . .	41
5.6	State-constrained control-constrained optimal trajectory for Problem 2 in the phase-plane with associated optimal control $u$ . . . . .	41
5.7	Cross-sections of the temperature profiles at $x = l$ for Problem 2 featuring different values for $T_{\max}$ . . . . .	42
5.8	Closeups of the "first hump" of the bottom right pictures of Fig. (5.4) and (5.7) . . . . .	43
5.10	Optimal control $u$ with simpson rule as quadrature formula . . . . .	45
5.11	Optimality check showing the perfect coincidence with the projection formula (4.7h) . . . . .	47
5.12	Illustration of the left and right hand side of equation (4.7a) . . . . .	48
5.13	Adjoint state $p_3$ and associated measure $\mu$ for Problem 1 ("single-hump" case) . . . . .	48
5.14	Adjoint state $p_3$ and associated measure $\mu$ for Problem 1 ("double-hump" case) . . . . .	49
5.15	Adjoint state $q$ of the temperature . . . . .	49
5.16	Cross section of $q$ at $t = 3$ . . . . .	50
5.17	Adjoint state $q$ of the temperature . . . . .	50
5.18	Adjoint state $q$ of the temperature (Problem 2) . . . . .	51
5.19	Illustration of the left and right hand side of equation (4.14b) . . . . .	53
5.20	Illustration of the left and right hand side of equation (4.14d) . . . . .	53
5.21	Hamiltonian for Problem 1 . . . . .	53

# List of Tables

- 5.1 Performance and accuracy of rocketcar\_ode\_pde.txt . . . . . 46
- 5.2 Performance and accuracy of rocketcar\_ode.txt . . . . . 46
- 5.3 Performance and accuracy of indirect2.m . . . . . 59

## Abstract

This thesis is concerned with optimal control problems governed by a system of partial as well as ordinary differential equations. As this is yet a relatively untouched field of mathematical research, the limited scope here was to get first insights by creating and studying an academical prototype example in the following dubbed the “hypersonic rocketcar problem“.

Additionally, this prototype also features control as well as state constraints, with the mathematical focus being on the latter ones. In conjunction with the two different kinds of differential equations those will lead to some new effects that, to the authors knowledge, have so far not been witnessed in optimal control of either ordinary or partial differential equations.

The first chapter will describe said prototype problem in details as well as motivate its creation by expanding a classical problem from the pioneering days of optimal control of ordinary differential equations.

Chapter 2 will expand a bit on the rocketcar’s state-unconstrained solution to form a base for comparison with the final results, while the third chapter will try to anticipate some of those by analysis of the switching structure of the full blown version. Here we will also encounter the new aspects of optimal control problems with ordinary and partial differential equations mentioned above.

Necessary first order optimality conditions will be briefly sketched in chapter 4. As we will see there, the rocketcar can not just be interpreted as an optimal control problem with both ordinary and partial differential equations, but can also be reformulated into one with either just ordinary or just partial differential equations, albeit those reformulations will lead to highly nonstandard versions of their respective kind. Nevertheless this will naturally be a good opportunity for comparison between those 3 related fields of optimal control.

The last and most important chapter number 5 will deal with all the numerical aspects, i.e. solving the optimal control problem via a direct (first discretize, then optimize) method and a subsequent comparison to the results derived beforehand, the approximate verification of the optimality conditions from the previous chapter and finally the much more demanding solving of the problem with an indirect (first optimize, then discretize) method. In addition the 3 sets of necessary conditions of the aforementioned different versions of the problem will of course be matched and cross-referenced.

## Kurzfassung

Diese Arbeit befasst sich mit Optimalsteuerungsproblemen, welche sowohl gewöhnliche als auch partielle Differentialgleichungen als Nebenbedingungen aufweisen. Da es sich hierbei um ein noch vergleichsweise unerforschtes mathematisches Gebiet handelt, beschränkt sich die Arbeit auf das Erstellen und Analysieren eines Beispielprototyps, welcher im Folgenden "Hyperpersonisches Rocketcar-Problem" genannt wird.

Zusätzlich beinhaltet dieses Prototypproblem noch Steuerungs- sowie Zustandsbeschränkungen, wobei der mathematische Fokus auf Letzteren liegen wird. Gemeinsam mit den beiden oben erwähnten Arten von Differentialgleichungsnebenbedingungen werden diese zu einigen neuen Effekten führen, welche nach Kenntnis der Autors bis jetzt weder in der Optimalsteuerung mit gewöhnlichen noch mit partiellen Differentialgleichungen aufgetreten sind.

Kapitel 1 beinhaltet eine ausführliche Beschreibung des besagten Beispielprototyps sowie seine Entstehung durch Erweiterung eines bekannten Modellproblems aus den frühen Tagen der Optimalsteuerung gewöhnlicher Differentialgleichungen.

Im 2. Kapitel wird zunächst die Lösung des nicht zustandsbeschränkten Rocketcars hergeleitet, welche eine Vergleichsbasis mit den Endergebnissen bilden wird. Einige dieser Ergebnisse werden wir in Kapitel 3 schon versuchen vorwegzunehmen, indem wird die Schaltstruktur des kompletten Problems analysieren. An dieser Stelle werden wir auf die bereits erwähnten neuen Effekte der Optimalsteuerung mit gewöhnlichen und partiellen Differentialgleichungen treffen.

Notwendige Optimalitätsbedingungen erster Ordnung werden in Kapitel 4 kurz hergeleitet. Dabei werden wir sehen, dass das Rocketcar nicht nur als Optimalsteuerungsproblem mit gewöhnlichen und partiellen Differentialgleichungen interpretiert werden kann, sondern auch in eines mit nur gewöhnlichen oder nur partiellen umformuliert werden kann. Diese beiden Alternativversionen werden allerdings keine "Standardvertreter" ihrer jeweiligen Art sein. Nichtsdestotrotz wird sich daraus natürlich eine hervorragende Gelegenheit zum Vergleich dieser 3 Gebiete der Optimalsteuerung ergeben.

Das Hauptkapitel Nummer 5 beinhaltet schliesslich alle numerischen Aspekte: das Lösen des Rocketcar-Problems durch eine direkte (erst diskretisieren, dann optimieren) Methode sowie der Vergleich mit den vorher hergeleiteten Resultaten von Kapitel 3, die numerische Verifikation der Optimalitätsbedingungen aus Kapitel 4, sowie das erneute (und wesentlich anspruchsvollere) Lösen mit einer indirekten (erst optimieren, dann diskretisieren) Methode. Zusätzlich wird noch auf die Verbindungen zwischen den Optimalitätsbedingungen der 3 verschiedenen Versionen eingegangen.

## Preface

While the mathematical model problem discussed in this thesis was conceived by the author himself, most of the actual research was done in a team effort at the chair of mathematics in engineering sciences of the University of Bayreuth.

As the authors main task within the working group were numerical calculations, those will also be the focus of the thesis and be featured in the entire main chapter number 5. However a lot of the theoretical results leading up to said chapter 5 have either been achieved by the entire team or by the author's coworkers.

To keep the thesis readable and self-contained some heavy citing in the early chapters was therefore unfortunately unavoidable. The exact amount is detailed in the introductions of chapters 2 - 4.

Additionally it should be mentioned, that the main sources (chiefly [25], [29] and to a lesser extent [27] and [28]) also contain quite some further results considering regularities etc. that, while not immediately necessary here, might prove insightful to the interested reader.

The same holds true for [26], which is currently in preparation and still has some unresolved issues.

[25] is a preprint and has been added to the appendix.

## Acknowledgement

First I would like to thank my supervisor Prof. Dr. Hans-Josef Pesch for his great mentoring and considerable patience, for providing me with a really great job the last years and for his sustained support in things both mathematical and beyond.

Furthermore I would like to thank Prof. Dr. Kurt Chudej and Prof. Dr. Wolf von Wahl for their assistance in some tricky numerical resp. theoretical questions.

And last but not least I want to express my gratitude towards my current and former colleagues, my friends and my family for bearing with me all those years.

Bayreuth, 06.12.2013

Stefan Wendl

# Chapter 1

## The hypersonic rocket car problems

A good starting point to explain the hypersonic rocket car problems might be etymology: the title bears very much resemblance to the “rocketcar on a railtrack“ problem, an academic problem investigated by Bushaw [8] in the early days of optimal control of ordinary differential equations roughly 60 years ago. Its objective was to drive said rocketcar on a railtrack from some arbitrarily given initial position and speed to the origin of the phase-plane in minimal time. Based on newtonian mechanics the problem features a second order ODE governing the car’s movement depending on its acceleration, which plays the role of the problems control. For regularisation purposes the acceleration also enters the objective functional.

Having a by todays standards relatively easy to compute analytical solution, as well as being rather benign from the numerical point of view, the rocketcar on a railtrack problem has proven to be an ideal ingredient for our aim to create a comprehensive ODE-PDE optimal control problem.

The second part of the name, ”hypersonic“ stems from the ODE-PDE optimal control problem *Instationary Heat Constrained Trajectory Optimization of a Hypersonic Space Vehicle* investigated by Chudej at al. in 2008 [12]. As the name suggests it deals with flight path optimization under a further constraint imposed by the vehicle heating up due to its speed. Featuring the already relatively complex flight mechanics equations plus the temperature constraint however, this problem was way to complex to do anything but basic numeric calculations.

The idea of the hypersonic rocket car now was rather straightforward: simply complement Bushaw’s old rocket car with a heat equation, mimicking the car’s heating due to friction, which has to stay under a given maximum temperature. Thereby one creates an ODE-PDE optimal control problem similar in overall structure to the Hypersonic Space Vehicle yet with considerably simpler underlying mechanics. Together with the usual simplifications for mathematical model problems (all in a mathematical sense nonessential constants set to 1 etc.) we hoped to create a prototype problem that, while still retaining a somewhat reproducible physical background (physicists and engineers might take this with a pinch of salt), was nevertheless uncomplicated enough to allow more in depth analysis of its structure and mathematical properties.

Before we start with any formulae, a few preliminary remarks on the setting: In the following the spatial variable  $x$  shall denote the *position within the car*, with  $x = 0$  resp.  $x = l$  ( $l \leq 1$ ) being the rear resp. nose of the (one-dimensional) car. This variable will only be relevant for the PDE.  $w = w(t)$  on the other hand will denote the *position of the car*, starting at a given location  $w_0$  and with a given initial speed  $\dot{w}_0$ . The control shall as usual be  $u = u(t)$  and the temperature  $T = T(x, t)$ . Heating is achieved either by a source term  $g(\dot{w}(t))$  in the PDE’s right hand side (in the following dubbed Problem 1) or  $h(\dot{w}(t))$  in the PDE’s boundary condition at the car’s nose  $x = l$  (Problem 2, heating of the car’s front). As  $g(\dot{w}(t))$  only depends on time, Problem 1 represents distributed and even heating in all  $[0, l]$  which is of course somewhat unphysical and

can be seen as a further of the aforementioned simplifications. Despite their similarities Problems 1 and 2 will show some interesting differences later on.

Altogether one finally arrives at the following scheme of dependencies:

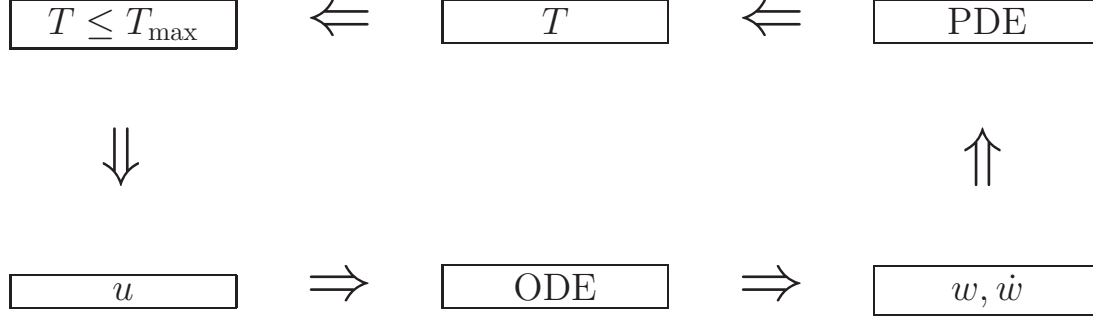


Figure 1.1: Scheme of dependencies

Based on the acceleration  $u(t)$  the ODE delivers the car's position  $w(t)$  and speed  $\dot{w}(t)$ . The latter yields the car's temperature  $T(x, t)$  via the PDE. The temperature is bounded by the maximal temperature  $T_{\max}$ , in turn influencing the control  $u(t)$  and completing the circle. Both versions also feature a control constraint, which was omitted here, as it is relatively harmless compared to the temperature constraint and can be dealt with a mere projection later on.

The hypersonic rocket car problems are now given as follows:

$$\min_{u \in U} \left\{ t_f + \frac{1}{2} \lambda \int_0^{t_f} u^2 dt \right\}, \quad \lambda > 0, \quad (1.1)$$

subject to

$$\ddot{w}(t) = u(t) \quad \text{in } (0, t_f), \quad (1.2a)$$

$$w(0) = w_0, \quad \dot{w}(0) = \dot{w}_0, \quad (1.2b)$$

$$w(t_f) = 0, \quad \dot{w}(t_f) = 0, \quad (1.2c)$$

$$U := \{u \in L^2(0, t_f) : |u(t)| \leq u_{\max} \text{ in } [0, t_f]\}, \quad (1.2d)$$

and either

1st Problem: *Distributed control of the PDE via an ODE state variable:*

$$T_t(x, t) - T_{xx}(x, t) = g(\dot{w}(t)) \text{ in } (0, l) \times (0, t_f), \quad (1.3a)$$

$$T(x, 0) = T_0 \text{ on } (0, l), \quad (1.3b)$$

$$-T_x(0, t) = -(T(0, t) - T_0), \quad T_x(l, t) = -(T(l, t) - T_0) \text{ in } [0, t_f], \quad (1.3c)$$

or

2nd Problem: *Boundary control of the PDE via an ODE state variable:*

$$T_t(x, t) - T_{xx}(x, t) = 0 \text{ in } (0, l) \times (0, t_f), \quad (1.4a)$$

$$T(x, 0) = T_0 \text{ on } (0, l), \quad (1.4b)$$

$$-T_x(0, t) = -(T(0, t) - T_0), \quad T_x(l, t) = -(T(l, t) - T_0) + h(\dot{w}(t)) \text{ in } [0, t_f], \quad (1.4c)$$

and finally subject to a pointwise state constraint of type

$$T(x, t) \leq T_{\max} \text{ in } [0, l] \times [0, t_f]. \quad (1.5)$$

---

The ambient temperature, which is also the car's initial temperature, is given by the constant  $T_0$ .  $\lambda > 0$  shall denote the problem's Tychonoff parameter modelling the control cost and  $t_f \geq 0$  its free end time.

For the aforementioned functions  $g$  and  $h$  we need some additional properties (identical for both, so here only noted for  $g$ ):

i)  $g(z) \geq 0$  and  $g(z) = 0 \Leftrightarrow z = 0$

ii)  $g(z) = g(-z)$

iii)  $|z_1| < |z_2| \Leftrightarrow g(z_1) < g(z_2)$

iv)  $g \in C^\infty(\mathbb{R} \setminus \{0\}) \cap C(\mathbb{R})$

Thereby we ensure that the friction depends continuously and monotonically on the absolute value of the car's velocity and is naturally only zero if the car is at rest.

Item ii) may appear a bit bewildering, especially for Problem 2. Unfortunately the necessary remedy, an additional second source term at  $x = 0$  that kicks in if  $\dot{w}$  drops below 0, would make the whole model just too awkward. The same goes for further effects like inertia etc.

Some reasonable choices for  $g$  and  $h$  are, for example,  $z \mapsto |z|^n$ ,  $n = 1, 2, 3$ , according to Coulomb, Stokes, and Newton friction. All numerical calculations later on will feature  $n = 2$ .



## Chapter 2

# The state-unconstrained hypersonic rocket car problem

For better illustration and to allow comparison with the results of the full-blown ODE-PDE problem let's first have a brief look at the state-unconstrained problem. The following section is only a short summary of results achieved nearly 60 years prior to this thesis and hence is of course not the authors contribution. It can also be found in [25].

### 2.1 The ODE-part

Rewriting the second-order ODE as a system of two first-order ODEs in  $\mathbf{w} := (w_1, w_2) := (w, \dot{w})$ ,  $\dot{w}_1 = w_2$ ,  $\dot{w}_2 = u$ , and defining the Hamiltonian by

$$H(\mathbf{w}, \mathbf{p}, u) = 1 + \frac{1}{2} \lambda u^2 + p_1 w_2 + p_2 u,$$

the ODE adjoint equations are

$$\dot{p}_1 = -H_{w_1} = 0, \quad \dot{p}_2 = -H_{w_2} = -p_1.$$

The minimum principle yields

$$u(t) = P_{[-u_{\max}, u_{\max}]} \left( -\frac{1}{\lambda} p_2 \right),$$

where  $P_{[a,b]}(z) := \min \{b, \max \{a, z\}\}$  denotes the projection of  $\mathbb{R}$  onto the interval  $[a, b]$ . Furthermore, the terminal time  $t_f$  is determined by

$$H|_{t_f} = 1 + \frac{1}{2} \lambda u(t_f)^2 + p_1(t_f) \underbrace{w_2(t_f)}_{=0} + p_2(t_f) u(t_f) = 0.$$

An elementary calculation shows that  $p_2(t) = -C(t - t_f) + p_2(t_f)$  with  $p_1(t) = C = \text{const}$ . Hence  $p_2$  is linear; cf. [24]. Due to this linearity, the optimal control law induces at most two junction points, when taking box constraints on the control  $u$  into account. If  $\lambda$  is sufficiently small, the switching structure generally consists either of the three subarcs  $u(t) = u_{\max}$ ,  $u(t) = u^{\text{free}}(t) := -\frac{1}{\lambda} p_2(t)$ , and  $u(t) = -u_{\max}$  with the two junction points  $t_1$  and  $t_2$  or the other way around. Herewith, an analytical solution of the state-unconstrained problem can be obtained, however the necessary computations are rather longsome yet basic and are therefore omitted here. Their results are shown in the following phase diagram:

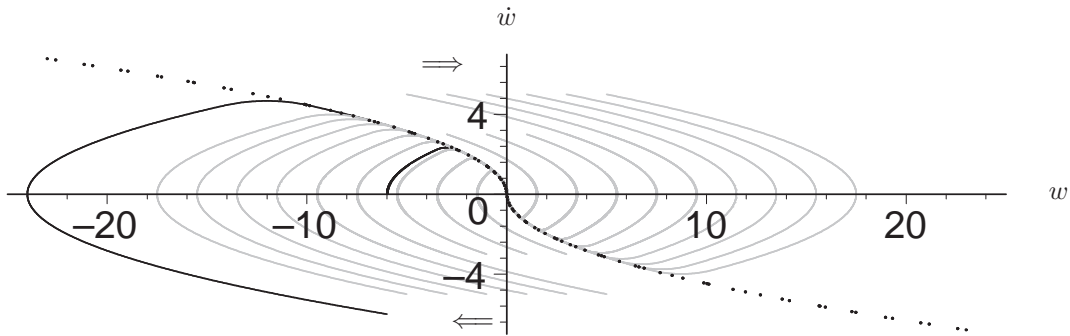


Figure 2.1: Optimal trajectories of the regularized minimum-time problem in the phase plane (grey) with  $\lambda = 10^{-1}$  and box constraints  $|u| \leq u_{\max} = 1$ . The dotted black curve is the envelope curve and coincides with the switching curve for  $\lambda = 0$ . The black curves are the optimal solutions for the starting conditions  $w_0 = -6$  and  $\dot{w}_0 = 0$  resp.  $w_0 = -6$  and  $\dot{w}_0 = -6$ . Those will be picked up again later on. (Source: [25])

Due to the linear  $\dot{p}_2$ , the control  $u$  is either  $\pm u_{\max}$  or linear in between.

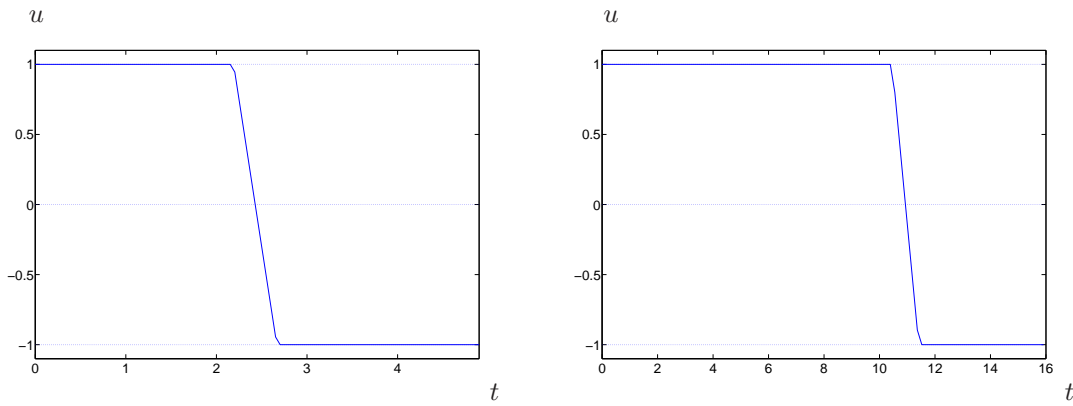


Figure 2.2: Optimal controls  $u$  for the highlighted trajectories of Fig. (2.1) with  $\dot{w}_0 = 0$  (left) and  $\dot{w}_0 = -6$  (right).

## 2.2 Semi-analytical solution of the heat equation

Furthermore it is also possible to derive a semi-analytical solution of the heat equation for both problems (of course still depending on the input  $\dot{w} = w_2$  from the ODE).

This was originally done by Pesch in the course of writing [25]. The authors only contribution in this section is Lemma 2.2.1.

Without loss of generality, we may choose  $T_0 := 0$ . Additionally, in the second problem a transformation to homogeneous Robin conditions can be achieved by  $\hat{T} := T - \frac{1}{2} e^{x-l} h(\dot{w})$ . Then the second problem reads, again replacing  $\hat{T}$  by  $T$ , as

$$T_t(x, t) - T_{xx}(x, t) = \frac{1}{2} e^{x-l} (h(\dot{w}(t)) - \frac{d}{dt} h(\dot{w}(t))) \text{ in } (0, l) \times (0, t_f), \quad (2.1a)$$

$$T(x, 0) = -\frac{1}{2} e^{x-l} h(\dot{w}(0)) \text{ in } (0, l), \quad (2.1b)$$

$$-T_x(0, t) = -T(0, t), \quad T_x(l, t) = -T(l, t) \text{ in } [0, t_f]. \quad (2.1c)$$

Considering the homogeneous parts of the PDEs of the two problems, a separation of variables,  $T(x, t) = \xi(x) \tau(t)$ , leads to the eigenvalue problem

$$\xi'' + \mu \xi = 0 \quad \text{with} \quad 0 < \mu =: k^2$$

with the associated boundary conditions  $-\xi'(0) = -\xi(0)$  and  $\xi'(l) = -\xi(l)$ . In addition, one obtains a differential equation for  $\tau$ ,  $\dot{\tau} + \mu \tau = 0$ . For both problems, the analysis yields the same eigenfunctions

$$\varphi_n(x) = k_n \cos k_n x + \sin k_n x$$

and the same eigenvalues determined by either

$$\frac{2k}{k^2 - 1} = \tan kl \quad (\text{if } l \neq \frac{1}{2k} (2m - 1)\pi) \quad (2.2a)$$

or

$$\frac{k^2 - 1}{2k} = \cot kl \quad (\text{if } l \neq \frac{1}{2k} (2m + 1)\pi). \quad (2.2b)$$

### Lemma 2.2.1.

For the (positive)  $k_n$  the following properties hold:

- a)  $k_n \in \left] (n-1)\frac{\pi}{l}, (n-1)\frac{\pi}{l} + \frac{\pi}{2l} \right[ \quad n \in \mathbb{N}$ ,
- b)  $\lim_{n \rightarrow \infty} \left( k_n - (n-1)\frac{\pi}{l} \right) = 0$  and
- c) the sequence  $\left( k_n - (n-1)\frac{\pi}{l} \right)$  is positive and strictly monotonically decreasing.

### Proof:

One has to intersect the graphs of  $\frac{2x}{x^2 - 1}$  and  $\tan(xl)$ .

$\frac{2x}{x^2 - 1}$  is positive and strictly monotonically decreasing for  $x > 1$  and  $\lim_{x \rightarrow \infty} \frac{2x}{x^2 - 1} = 0$ .

$\tan(xl)$  is only positive in  $\left] (n-1)\frac{\pi}{l}, (n-1)\frac{\pi}{l} + \frac{\pi}{2l} \right[ \quad n \in \mathbb{N}$ , and strictly monotonically increasing in each of the intervals.

Together with the fact that  $(n-1)\frac{\pi}{l}$ ,  $n \in \mathbb{N}$ , are roots of  $\tan(xl)$  the properties a)-c) follow immediately.  $\diamond$

The dependence of  $k_n$  on  $l$  will from now on be suppressed.

Because of the symmetry of the boundary conditions, the above eigenfunctions are orthogonal, but not normalized with respect to the usual Hilbert space scalar product. To facilitate further calculations, we mainly use the normalized eigenfunctions from now on,

$$\phi_n(x) = \frac{1}{N_n} (k_n \cos k_n x + \sin k_n x) \text{ with } N_n^2 := \|\varphi_n\|_{L^2(0,l)}^2 = \int_0^l \varphi_n^2(x) dx = \frac{l}{2} k_n^2 + \frac{l}{2} + 1.$$

By Fourier's method one finally obtains the following solutions:

For the 1st problem, Eqs. (1.3):

$$\begin{aligned} T(x, t) &= \sum_{n=1}^{\infty} \left[ \int_0^t g(\dot{w}(s)) e^{-k_n^2(t-s)} ds \right] \cdot \left( \int_0^l \phi_n(y) dy \right) \phi_n(x) \\ &= \sum_{n=1}^{\infty} \left[ \int_0^t g(\dot{w}(s)) e^{-k_n^2(t-s)} ds \right] \cdot \frac{1}{N_n} \left[ \sin k_n l + \frac{1}{k_n} (1 - \cos k_n l) \right] \phi_n(x). \end{aligned} \quad (2.3)$$

For the 2nd problem, Eqs. (2.1):

$$\begin{aligned} T(x, t) &= -\frac{1}{2} e^{-l} \sum_{n=1}^{\infty} \left[ h(\dot{w}(0)) e^{-k_n^2 t} - \int_0^t (h(\dot{w}(s)) - \frac{d}{ds} h(\dot{w}(s))) e^{-k_n^2(t-s)} ds \right] \\ &\quad \cdot \left( \int_0^l e^{y} \phi_n(y) dy \right) \phi_n(x) + \frac{1}{2} h(\dot{w}(t)) e^{x-l} \end{aligned} \quad (2.4a)$$

$$= \frac{1}{2} \sum_{n=1}^{\infty} \left[ (1 + k_n^2) \int_0^t h(\dot{w}(s)) e^{-k_n^2(t-s)} ds \right] \frac{1}{N_n} \sin k_n l \phi_n(x). \quad (2.4b)$$

However it should be noted, that evaluating these solution formulas is significantly more taxing than simply solving the heat equations with a finite element solver. Nevertheless they shall prove indispensable during the later analysis and reformulation of the problem.

## 2.2 Semi-analytical solution of the heat equation

To conclude this section let's have a look at the temperature profiles for the trajectories of Fig. (2.1) for the problems 1 and 2 (In all computations the length  $l$  of the car has been set to 1):

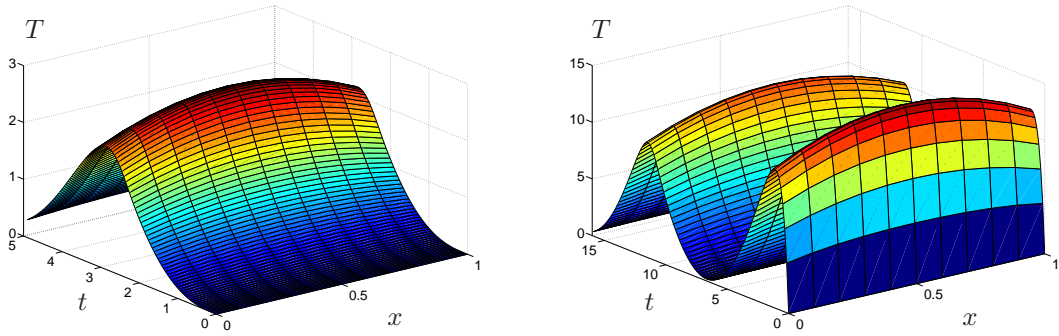


Figure 2.3: Temperature profiles for Problem 1 along state-unconstrained trajectories; cf. Fig. (2.1). Data:  $\lambda = 10^{-1}$ ,  $u_{\max} = 1$ ,  $w_0 = -6$ ,  $\dot{w}_0 = 0$  (left), resp.  $\dot{w}_0 = -6$  (right), and  $g(z) := z^2$ .

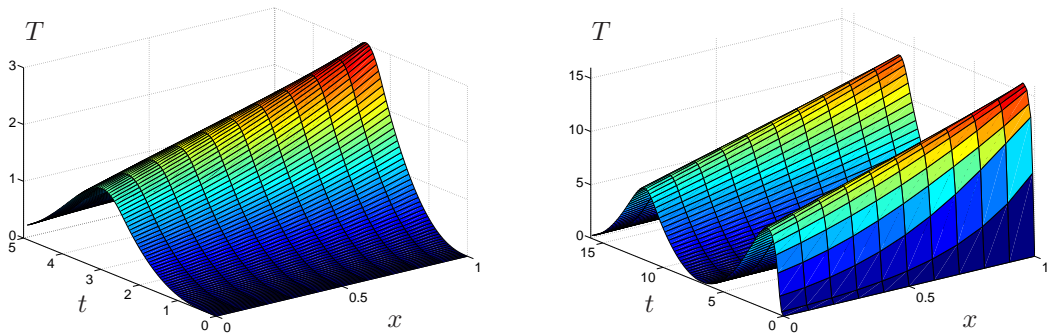


Figure 2.4: Temperature profiles for Problem 2 along state-unconstrained trajectories; cf. Fig. (2.1). Data:  $\lambda = 10^{-1}$ ,  $u_{\max} = 1$ ,  $w_0 = -6$ ,  $\dot{w}_0 = 0$  (left), resp.  $\dot{w}_0 = -6$  (right), and  $h(z) := z^2$ .

Please note that for Problem 1 the temperature is symmetric in space with respect to  $x = \frac{1}{2}$ , where the spatial maximum for each time  $t$  is situated. For Problem 2 there is unfortunately no such symmetry, but one can observe that the absolute maximum of the temperature is always at  $x = l$ . The latter implies that the coordinate  $x^*$  of the maximum of  $T$  for arbitrary  $t \in [0, t_f]$  satisfies  $x^* < l$ , if and only if the state constraint is not active. Those observations will come in very handy later on.



# Chapter 3

## Theoretical analysis

### 3.1 A short summary of the properties of the coupled ODE-PDE system

In depth theoretical analysis of the system has been done mainly in [25]. Some useful additional regularity results for Problem 1 can be found in [29]. The following just sums up the most essential of the results (itemized ones are citations), which are crucial for later analysis and numerics.

- For any admissible control  $u$  the resulting  $w$ ,  $\dot{w}$  and  $T$  are continuous<sup>1</sup>.
- *Theorem 4.1 from [25]*

Let  $g$  and  $h$  be continuously differentiable real valued functions satisfying  $g(0) = h(0) = 0$ . Let  $t_f$  be fixed. Then Problems 1 and 2 given by Eqs. (1.2), (1.3), resp. (1.2), (1.4) possess each one and only one solution  $(w, T)$  in the space  $W_2^1(0, t_f) \times W_2^{1,0}(Q)$ . This solution also belongs to the space  $W_2^1(0, t_f) \times (W_2^{1,0}(Q) \cap C([0, t_f], L^2(0, l)))$  for all  $u \in U$ .

Moreover, the solutions depend continuously on the data, for example,

$$\begin{aligned} & \|w\|_{W_2^1(0, t_f)} + \max_{[0, t_f]} \|T(\cdot, t)\|_{L^2(0, l)} + \|T\|_{W_2^{1,0}(Q)} \\ & \leq c_{\text{ODE}} (|w_0| + |\dot{w}_0| + \|u\|_{L^2(0, t_f)}) + c_{\text{PDE}} \|g(\dot{w})\|_{L^2(0, t_f)} \end{aligned}$$

with constants  $c_{\text{ODE}}$ , resp.  $c_{\text{PDE}}$  independent of  $u$ , resp.  $g$  or  $h$ .

As usual we define the Banach spaces  $W_p^m(0, t_f) := \{w \in L^p(0, t_f) : \frac{d^m}{dt^m} w \in L^p(0, t_f)\}$ . In particular,  $W_p^1(0, t_f)$ ,  $p = 2$ , resp.  $p = \infty$ , denote the Banach space of all absolutely continuous functions, both equipped with the usual norms. Moreover,  $W_2^{1,0}(Q)$  denotes the Banach space of all functions in  $L^2(Q)$  with weak first-order partial derivative w. r. t.  $x$  in  $L^2(Q)$ , and  $C([0, t_f], L^2(0, l))$  is the space of abstract continuous functions with values in  $L^2(0, l)$ .  $Q$  stands for the space-time cylinder  $(0, l) \times (0, t_f)$ . For later use, we define  $V_2^{1,0}(Q) := W_2^{1,0}(Q) \cap C([0, t_f], L^2(0, l))$ .

This gives rise to continuous, generally non-linear solution operators

$$S: U \rightarrow W_2^1(0, t_f) \times V_2^{1,0}(Q), \quad u \mapsto (w, T).$$

Note that the nonlinearity of  $S$  is solely induced by the nonlinearities of  $g$ , resp.  $h$ .

---

<sup>1</sup>Actually the regularities are much higher, see for example [29] p43 Satz 3.3.4

For Problem 1 it holds:

- *Theorem 4.5 from [25]*

Let  $T$  be the unique weak solution of

$$T_t + \mathcal{L}T = g(\dot{w}), \quad (3.1a)$$

$$T(0) = 0, \quad (3.1b)$$

i. e.,  $T \in C^0([0, t_f], L^2(0, l)) \cap L^2(0, t_f; \mathcal{D}(\mathcal{L}^{\frac{1}{2}}))$ , such that

$$-\int_0^{t_f} (T, \psi_t) ds + \int_0^{t_f} (\mathcal{L}^{\frac{1}{2}}T, \mathcal{L}^{\frac{1}{2}}\psi) ds = \int_0^{t_f} (g(\dot{w}), \psi) ds + (T(0) = 0, \psi(0)) \quad (3.2)$$

for all test functions  $\psi \in C^1([0, t_f], \mathcal{D}(\mathcal{L}^{\frac{1}{2}}))$  with  $\psi(t_f) = 0$ .

Then

$$T(t) = \int_0^t e^{-(t-s)\mathcal{L}} g(\dot{w}(s)) ds, \quad (3.3)$$

and  $T$  has the following additional regularity properties:

$$T(t) \in \mathcal{D}(\mathcal{L}), \quad 0 \leq t \leq t_f, \quad (3.4a)$$

$$\mathcal{L}T \in C^0([0, t_f], L^2(0, l)), \quad (3.4b)$$

$$T \in C^1([0, t_f], L^2(0, l)), \quad (3.4c)$$

$$T \in \bigcap_{\eta, 0 \leq \eta < \frac{1}{2}} C^0((0, t_f], C^{3+\eta}([0, l])), \quad (3.4d)$$

$$T_t \in \bigcap_{\eta, 0 \leq \eta < \frac{1}{2}} C^0((0, t_f], C^{1+\eta}([0, l])). \quad (3.4e)$$

In particular,  $T$  is a classical solution of (3.1) in  $[0, l] \times (0, t_f]$  and satisfies (3.1) in the strong sense, i. e.,  $\frac{d}{dt}T + \mathcal{L}T = g(\dot{w})$  in  $[0, t_f]$ .

- *Theorem 4.6 from [25]*

For any  $\varepsilon$ ,  $0 < \varepsilon < t_f$ , and any  $r \geq 2$  we have

$$T_{tt} \in L^r(\varepsilon, t_f; L^2(0, l)),$$

$$\partial_x^4 T \in L^r(\varepsilon, t_f; L^2(0, l)).$$

In the next step we will show the symmetry of  $T$  as already gleaned in figures (2.3). An elegant proof can again be found in [25] (Theorem 4.3), but one can also do it with the solution formula (2.3). It is more cumbersome and requires some auxiliary results, however those necessary steps will prove helpful later on:

**Lemma 3.1.1.**

*Every even mode of the series in (2.3) vanishes.*

**Proof:**

$$\sin k_n l + \frac{1}{k_n} (1 - \cos k_n l) = \frac{2}{k_n} \sin \frac{k_n l}{2} \left( k_n \cos \frac{k_n l}{2} + \sin \frac{k_n l}{2} \right) \quad (3.5)$$

### 3.1 A short summary of the properties of the coupled ODE-PDE system

---

For the  $k_n$  it holds

$$\frac{2k_n}{k_n^2 - 1} = \tan k_n l = \frac{2 \tan \frac{k_n l}{2}}{1 - \tan^2 \frac{k_n l}{2}},$$

which implies either

- i)  $\tan \frac{k_n l}{2} = -k_n$  or
- ii)  $\tan \frac{k_n l}{2} = \frac{1}{k_n}$ .

Case i) immediately yields that the bracket in (3.5) equals 0 in this case. Due to the  $\frac{2\pi}{l}$  periodicity of  $\tan \frac{x l}{2}$  it holds <sup>2</sup>

$$\begin{aligned} \tan \frac{x l}{2} &= -x, \quad x > 0 \\ \implies x_i &\in \left] (2i-1)\frac{\pi}{l}, 2i\frac{\pi}{l} \right[ , \quad i \in \mathbb{N}. \end{aligned}$$

Together with the already known fact that

$$k_n \in \left] (n-1)\frac{\pi}{l}, (n-1)\frac{\pi}{l} + \frac{\pi}{2l} \right[ \quad n \in \mathbb{N}, n \geq 2 \quad (\text{from Lemma 2.2.1})$$

one obtains that case i) occurs for all even  $n$ . ◇

#### Theorem 3.1.1.

It holds  $T\left(\frac{l}{2} - x, t\right) = T\left(\frac{l}{2} + x, t\right)$ .

#### Proof:

In face of Lemma 3.1.1 we have to show that

$$k_n \cos k_n \left(\frac{l}{2} - x\right) + \sin k_n \left(\frac{l}{2} - x\right) = k_n \cos k_n \left(\frac{l}{2} + x\right) + \sin k_n \left(\frac{l}{2} + x\right)$$

in case ii) of the above proof.

Sorting in sin and cos terms and applying standard addition Theorem yields the desired result:

$$\begin{aligned} k_n \left( \cos k_n \left(\frac{l}{2} - x\right) - \cos k_n \left(\frac{l}{2} + x\right) \right) &= - \left( \sin k_n \left(\frac{l}{2} - x\right) - \sin k_n \left(\frac{l}{2} + x\right) \right) \\ 2k_n \sin k_n \frac{l}{2} \cdot \sin(k_n x) &= 2 \sin(k_n x) \cdot \cos k_n \frac{l}{2} \end{aligned}$$

which is fulfilled for case ii). ◇

The next result is probably the most important for Problem 1 in this section. It was originally conceived by W. von Wahl.

- *Theorem 4.4 from [25]*

$T$  takes its strong maximum in  $x = \frac{l}{2}$  for each  $t_0 \in (0, t_f)$ .  $T(x, t_0)$  increases strictly monotonic in  $[0, \frac{l}{2}]$  and decreases strictly monotonic in  $[\frac{l}{2}, l]$ .

---

<sup>2</sup>For this and some of the following conclusions based on properties of trigonometric functions it might be best for comprehension to simply behold a plot of the functions in question.

This result is as expected from figures (2.3) and also hardly surprising given the physics behind it: In Problem 1 we have distributed heating independent of  $x$  and cooling can only occur at  $x = 0$  and  $x = l$  due to the Robin-type boundary conditions.

Nevertheless this is an extremely useful result. Before doing any further analysis, we already know that the active set  $\mathcal{A}_1$  for the temperature constraint of Problem 1 is a subset of the line  $\{(x, t) : x = \frac{l}{2}, t \in [0, t_f]\}$ . This has a good and a bad side:

On the good side we can replace (1.5) with

$$T\left(\frac{l}{2}, t\right) \leq T_{\max}, \quad t \in [0, t_f] \quad (3.6)$$

and in case we utilize the solution formula (2.3) we only have to evaluate it at  $x = \frac{l}{2}$ .

On the bad side  $\mathcal{A}_1$  will have empty interior with respect to  $(x, t)$ .

Furthermore Lemma 3.1.1, Theorem 3.1.1 and Theorem 4.4 from [25] together with the appropriate regularity and continuity results from above (resp. [25] and [29]) lead to

**Theorem 3.1.2.**

For Problem 1 it holds:

- a) For each point of time  $t$  the temperature  $T$  takes its absolute minima with respect to space symmetrically at  $x = 0$  and  $x = l$ .
- b)  $T(x, t) \geq 0 \quad \forall x, t$  and if  $T(x, \tilde{t}) = 0$  it must hold that  $\dot{w}(t) \equiv 0 \quad \forall t \in [0, \tilde{t}]$ <sup>3</sup>.

**Proof:**

a) follows immediately from Theorem 4.4 of [25] and Theorem 3.1.1.

For b) we now only have to examine (2.3) at  $x = 0$ :

$$\begin{aligned} T(0, t) &= \sum_{n=1}^{\infty} \left[ \int_0^t g(\dot{w}(s)) e^{-k_n^2(t-s)} ds \right] \cdot \frac{1}{N_n} \left[ \sin k_n l + \frac{1}{k_n} (1 - \cos k_n l) \right] \phi_n(0) \\ &= \sum_{n=1}^{\infty} \left[ \int_0^t g(\dot{w}(s)) e^{-k_n^2(t-s)} ds \right] \cdot \frac{k_n}{N_n^2} \left[ \sin k_n l + \frac{1}{k_n} (1 - \cos k_n l) \right] \\ &\stackrel{(2.2a)}{=} \sum_{n=1}^{\infty} \left[ \int_0^t g(\dot{w}(s)) e^{-k_n^2(t-s)} ds \right] \cdot \frac{k_n}{N_n^2} \left[ \frac{1}{k_n} + \frac{k_n^2 + 1}{2k_n} \sin k_n l \right]. \end{aligned} \quad (3.7)$$

$\sin$  shares its roots with  $\tan$  and  $\sin k_n l$  is therefore positive for all odd  $n$  and negative for all even ones, which fortunately vanish due to Lemma 3.1.1.

This implies

$$T(0, t) = 0 \Leftrightarrow \int_0^t g(\dot{w}(s)) e^{-k_n^2(t-s)} ds = 0.$$

Due to the required properties of  $g$ , a standard variational argument is enough to conclude the proof.  $\diamond$

---

<sup>3</sup>  $\lim_{t \rightarrow \infty} T(x, t)$  is of course 0, provided there exists a point of time  $t'$  with  $\dot{w}(t) \equiv 0 \quad \forall t \in [t', \infty[$ .

### 3.1 A short summary of the properties of the coupled ODE-PDE system

For Problem 2 we have:

- *Part of Theorem 4.7 from [25]*  
There is one and only one solution for  $T$ . (Regularity results are a bit more involved here and best digested in the whole context of the source  $\Rightarrow$  Appendix C)
- *Theorem 4.8 from [25]* with the additional simplification  $T_0 = 0$   
 $T$  as well as  $T_x$  of problem (1.4) are continuous in  $[0, l] \times [0, t_f]$ . Moreover,  $T \geq 0$  in  $[0, l] \times [0, t_f]$  and assumes its global maximum in  $[0, l] \times [0, t_f]$  on  $x = l$ .

This does not mean, that we can pinpoint the maximum of  $T$  with respect to  $x$  in advance for any given point of time, like we could for Problem 1 before!

So the latter result seems somewhat weaker than its Problem 1 counterpart. But looks are deceptive here: For all times  $t$  with said maximum below  $T_{\max}$  its exact location is absolutely inconsequential, while in the constrained case the global maximum will of course be  $T_{\max}^4$  and will be situated at  $x = l$ . So in essence we know, that the spatial maximum will be at  $x = l$  for all "interesting times" and therefore the active set  $\mathcal{A}_2$  of Problem 2's temperature constraint will be a subset of  $\{(x, t) : x = l, t \in [0, t_f]\}$ . Just as before we can now substitute (1.5) with

$$T(l, t) \leq T_{\max}, \quad t \in [0, t_f] \quad (3.8)$$

and the solution formula (2.4) has only to be evaluated at  $x = l$ .

But again  $\mathcal{A}_2$  will have empty interior with respect to  $(x, t)$ .

Finally, as a Corollary to Theorem 4.8 from [25] we have

**Corollary 3.1.1.**

$T(l, t) \geq 0 \quad \forall t$  and if  $T(l, \tilde{t}) = 0$  it must hold that  $\dot{w}(t) \equiv 0 \quad \forall t \in [0, \tilde{t}[$

**Proof:**

$$\begin{aligned} T(l, t) &= \frac{1}{2} \sum_{n=1}^{\infty} \left[ (1 + k_n^2) \int_0^t h(\dot{w}(s)) e^{-k_n^2(t-s)} ds \right] \frac{1}{N_n} \sin k_n l \phi_n(l) \\ &= \sum_{n=1}^{\infty} \left[ \int_0^t h(\dot{w}(s)) e^{-k_n^2(t-s)} ds \right] \frac{1 + k_n^2}{2N_n^2} \sin k_n l (k_n \cos k_n l + \sin k_n l) \\ &\stackrel{(2.2a)}{=} \sum_{n=1}^{\infty} \left[ \int_0^t h(\dot{w}(s)) e^{-k_n^2(t-s)} ds \right] \frac{(1 + k_n^2)^2}{4N_n^2} \sin^2 k_n l \end{aligned} \quad (3.9)$$

Obviously every summand is  $\geq 0$ , therefore the claim follows analogously to the proof of Theorem 3.1.2.  $\diamond$

This result seems considerably weaker than its Problem 1 counterpart Theorem 3.1.2 as its only concerned with  $x = l$ . In fact it is possible to show precisely the same results as in Theorem 3.1.2 for Problem 2. Due to some rather technical difficulties it would however be ridiculously tedious and time consuming while, in the light of the results already at hand, precious little new insight would be gained from it.

With those results and the ones borrowed from [25] we can now tackle the switching structure induced by the temperature constraint.

<sup>4</sup>As long as the constraint gets active, of course.

### 3.2 Analysis of the switching structure for the hypersonic rocket car problems

The following section again follows by and large the section of the same name to appear in [26], done mostly by Pesch.

As the analysis of switching structures for constrained ODE optimal control <sup>5</sup> is already very advanced, our main aim here is to transfer as much as possible into the ODE-PDE context, or should that be impossible, at least show up the parallels as well as the differences <sup>6</sup>.

The main source here is Jacobson, Lele and Speyer [16], also utilized in [26]. A crucial assumption therein is the regularity of the Hamiltonian, which is fulfilled here as both problems are regularized ( $\lambda > 0$ ). Those results say that, in case of effective state constraints,<sup>7</sup> there exist either only boundary subarcs, if the order of the state constraint is odd, resp. there may exist both boundary subarcs and/or touch points, if the order is even. Here, the order of a point-wise scalar state constraint of type  $S(t, \mathbf{w}(t)) \leq S_{\max}$  denotes the minimum number  $q$  of total differentiations w. r. t. time, after which the control appears explicitly for the first time, if the components of  $\dot{\mathbf{w}}$  are substituted by the right hand sides of their associated ODEs,

$$\frac{\partial}{\partial u} \left( \frac{d^q}{dt^q} S(t, \mathbf{w}) \right) \neq \mathbf{0}. \quad (3.10)$$

Here, the notation *order* is used in the sense of order with respect to a function, i. e., w. r. t. the right hand sides of the underlying ODEs; see [21].

Now we investigate the structure of the active sets  $\mathcal{A}_1$  and  $\mathcal{A}_2$  associated with the state constraint (1.5).

Obviously, we may assume that  $T(x^*(t), t)$  is sufficiently often continuously differentiable w. r. t.  $t$  on the interior of state-constrained (non-empty) subarcs. Indeed,  $T$  is a classical solution in  $[0, l] \times (0, t_f]$  for both problems; see Theorem 4.5, resp. Theorem 4.8 of [25] (both mentioned in the previous section).

#### *Problem 1: 2nd order state constraint*

As we already know, the active set will be a subset of  $\{(x, t) : x = \frac{l}{2}, t \in [0, t_f]\}$ . Defining  $S(t, \mathbf{w}, T) := T\left(\frac{l}{2}, t\right) - T_{\max}$  with  $\mathbf{w} := (w, \dot{w}^\top)$  two (total) differentiations w. r. t.  $t$  yield

$$\frac{d}{dt} S[t] = T_t \left( \frac{l}{2}, t \right) = T_{xx} \left( \frac{l}{2}, t \right) + g(\dot{w}(t)), \quad (3.11a)$$

$$\frac{d^2}{dt^2} S[t] = T_{tt} \left( \frac{l}{2}, t \right) = T_{xxt} \left( \frac{l}{2}, t \right) + g'(\dot{w}(t)) u(t), \quad (3.11b)$$

with  $[t]$  denoting a list of all arguments evaluated at time  $t$  that apply to the respective function. Here, both the ODE (1.2) and the PDE (1.3a) are substituted whenever possible.

Hence, two differentiations w. r. t.  $t$  are necessary to meet (3.10), if  $g'(\dot{w}(\cdot)) \neq 0$  on  $(t_{\text{on}}, t_{\text{off}})$ , where  $t_{\text{on}}$  and  $t_{\text{off}}$  shall denominate the entry- resp. exitpoint of a boundary subarc. Under this assumption, the constraint (1.5) constitutes a second order state constraint. Therefore, we have to expect boundary subarcs and/or touch points.

Note that  $T_{xxt}$ , resp.  $\partial_x^4 T$  are real analytic in  $(0, l) \times (0, t_f)$  according to Theorem 4.5 of [25], but  $T_{tt}$  is only of class  $L^\infty$  on a subset of  $(0, l) \times (0, t_f)$  according to Theorem 4.6 of [25].

<sup>5</sup>This and all further references to ODE optimal control are only to be understood in the context of ODE optimal control with scalar control.

<sup>6</sup>The main difference will be explored in detail in the next section.

<sup>7</sup>A state constraint is said to be effective, if the optimal solutions of the state-unconstrained and the state-constrained problem differ in cases where the constraint is chosen in such a way that the active set contains exactly one point.

### 3.2 Analysis of the switching structure for the hypersonic rocket car problems

---

On a constrained subarc, we must have  $T_t(\frac{l}{2}, t) \equiv T_{tt}(\frac{l}{2}, t) \equiv 0$  for all  $t \in (t_{\text{on}}, t_{\text{off}})$ ,  $0 < t_{\text{on}} < t_{\text{off}} < t_f$ . In general, one obtains a candidate optimal boundary control in feedback form

$$u(t) = u^{\text{bound}}(t) := -\frac{T_{xxt}(\frac{l}{2}, t)}{g'(\dot{w}(t))} \quad \text{on } t \in (t_{\text{on}}, t_{\text{off}}), \quad (3.12)$$

assuming  $g'(\dot{w}(t)) \neq 0$  on  $(t_{\text{on}}, t_{\text{off}})$ , of course. Fortunately  $g'(\dot{w}(t)) = 0$  is equivalent to  $\dot{w}(t) = 0$ , which is highly unlikely on a boundary arc, to say the least.

There is precious little practical use for (3.12) anyway, as it is a rather involved integro type equation, not the speak of the convergence- and computation problems  $T_{xxt}$  is bound to create in the sin-cos-series. Its unwieldy structure will again become apparent in the next section.

Nevertheless we immediately see that the boundary control (3.12) is continuous on  $(t_{\text{on}}, t_{\text{off}})$ .

Since the results of Theorem 4.4 of [25] are independent of the trajectory  $w$ , the above results yield either ridges (weak global maximum points) or peaks (isolated global maximum points) of  $T$  in  $Q$ .

#### *Problem 2: 1st order state constraint*

In order to proceed as for Problem 1, we have to exploit the formulation (2.1a) of Problem 2 with homogeneous Robin boundary conditions. Because of Theorem 4.8, there holds  $S(t, \mathbf{w}, T) := T(l, t) - T_{\text{max}}$ . By Eq. (2.1a), one obtains

$$\frac{d}{dt}S[t] = T_t(l, t) = T_{xx}(l, t) + \frac{1}{2}\left(h(\dot{w}(t)) - h'(\dot{w}(t))u(t)\right). \quad (3.13)$$

Assuming  $h'(w(\cdot)) \neq 0$  on  $(t_{\text{on}}, t_{\text{off}})$ , we have

$$\frac{\partial}{\partial u}\left(\frac{d}{dt}S(t, \mathbf{w}(t), T(l, t))\right) \neq 0,$$

and thus a first order state constraint w.r.t. the right hand sides of the ODE and the PDE:  $\bar{q}_t = 1$ . Therefore, we have to expect only boundary arcs except at trivial contact or touch points. Such points exist, if the state-unconstrained optimal solution coincides with the state-constrained solution when choosing  $T_{\text{max}}$  as global maximum of  $T$  in  $Q$ . The general situation for first order state constraints is that a slight decrease of  $T_{\text{max}}$  immediately results in a boundary subarc  $T(l, t) \equiv T_{\text{max}}$  on  $(t_{\text{on}}, t_{\text{off}})$ .

The boundary control on  $(t_{\text{on}}, t_{\text{off}})$  is determined by setting the right hand side of Eq. (3.13) to zero,

$$u(t) = u^{\text{bound}}(t) = \frac{1}{h'(\dot{w}(t))} (h(\dot{w}(t)) + 2T_{xx}(l, t)), \quad (3.14)$$

just like before under the assumption  $h'(\dot{w}(t)) \neq 0$  i.e.  $\dot{w}(t) \neq 0$  on  $(t_{\text{on}}, t_{\text{off}})$ . Its practical use is as doubtful as with its Problem 1 pendant (3.12) for the same reasons.

Again, the boundary control is continuous on the subarc  $(t_{\text{on}}, t_{\text{off}})$ .

In summary, the order concept for state-constrained ODE problems is generalizable to the distributed control problems investigated here. Obviously, boundary control problems can only be treated this way, if the boundary control can be shifted into a source term by an appropriate transformation.

### 3.3 Some new aspects of ODE-PDE optimal control

In this section we will at first have a further look at the series from the solution formulae (2.3) and (2.4). Thanks to Theorems 4.4 and 4.8 from [25] as well as Theorem 3.1.2, it is sufficient to examine Problem 1 at  $x = \frac{l}{2}$  and Problem 2 at  $x = l$ , as the rest is sandwiched between those and 0 anyway. Therefore we introduce:

For Problem 1:

$$\begin{aligned}
 T\left(\frac{l}{2}, t\right) &= \sum_{n=1}^{\infty} \left[ \int_0^t g(\dot{w}(s)) e^{-k_n^2 (t-s)} ds \right] \cdot \left( \int_0^l \phi_n(y) dy \right) \phi_n\left(\frac{l}{2}\right) \\
 &= \sum_{n=1}^{\infty} \left[ \int_0^t g(\dot{w}(s)) e^{-k_n^2 (t-s)} ds \right] \cdot \frac{1}{N_n} \left[ \sin k_n l + \frac{1}{k_n} (1 - \cos k_n l) \right] \phi_n\left(\frac{l}{2}\right) \\
 &= \sum_{n=1}^{\infty} \left[ \int_0^t g(\dot{w}(s)) e^{-k_n^2 (t-s)} ds \right] \cdot \alpha_n, \tag{3.15}
 \end{aligned}$$

$$\begin{aligned}
 \text{with } \alpha_n &= \frac{1}{N_n} \left[ \sin k_n l + \frac{1}{k_n} (1 - \cos k_n l) \right] \phi_n\left(\frac{l}{2}\right) \\
 &= \frac{1}{N_n^2} \left[ \sin k_n l + \frac{1}{k_n} (1 - \cos k_n l) \right] \cdot \left[ k_n \cos \frac{k_n l}{2} + \sin \frac{k_n l}{2} \right], \tag{3.16}
 \end{aligned}$$

and

$$\sum_{n=1}^{\infty} \alpha_n = 1,$$

and for Problem 2:

$$\begin{aligned}
 T(l, t) &= \frac{1}{2} \sum_{n=1}^{\infty} \left[ (1 + k_n^2) \int_0^t h(\dot{w}(s)) e^{-k_n^2 (t-s)} ds \right] \frac{1}{N_n} \sin k_n l \phi_n(l) \\
 &\stackrel{(3.9)}{=} \sum_{n=1}^{\infty} \left[ \int_0^t h(\dot{w}(s)) e^{-k_n^2 (t-s)} ds \right] \frac{(1 + k_n^2)^2}{4N_n^2} \sin^2 k_n l \\
 &= \sum_{n=1}^{\infty} \int_0^t h(\dot{w}(s)) e^{-k_n^2 (t-s)} ds \cdot \beta_n \tag{3.17}
 \end{aligned}$$

$$\text{with } \beta_n = \frac{(1 + k_n^2)^2}{4N_n^2} \sin^2 k_n l > 0. \tag{3.18}$$

### 3.3 Some new aspects of ODE-PDE optimal control

The structure of the  $\alpha_n$  of Problem 1 is plainly the more complicated one, requiring some elaboration.

**Theorem 3.3.1.**

The sequence  $\alpha_n$  is of the structure  $\{p_1, 0, n_1, 0, p_2, 0, n_2, 0, \dots\}$  and

- a)  $p_n$  is a strictly monotonically decreasing positive sequence with  $\lim_{n \rightarrow \infty} p_n = 0$ ,
- b)  $n_n$  is a strictly monotonically increasing negative sequence with  $\lim_{n \rightarrow \infty} n_n = 0$ ,
- c)  $p_n > |n_n| \quad \forall n \in \mathbb{N}$ ,
- d)  $\sum_{n=1}^{\infty} \alpha_n$  converges absolutely.

**Proof:**

$$\begin{aligned}
 \alpha_n &= \frac{1}{N_n^2} \left[ \sin k_n l + \frac{1}{k_n} (1 - \cos k_n l) \right] \cdot \left[ k_n \cos \frac{k_n l}{2} + \sin \frac{k_n l}{2} \right] \\
 &= \frac{1}{N_n^2} \left[ 2 \sin \frac{k_n l}{2} \cos \frac{k_n l}{2} + \frac{2}{k_n} \sin^2 \frac{k_n l}{2} \right] \cdot \left[ k_n \cos \frac{k_n l}{2} + \sin \frac{k_n l}{2} \right] \\
 &= \frac{2}{k_n N_n^2} \sin \frac{k_n l}{2} \left[ k_n \cos \frac{k_n l}{2} + \sin \frac{k_n l}{2} \right]^2
 \end{aligned} \tag{3.19}$$

From Lemma 3.1.1 we already know that  $\alpha_n = 0$  for  $n$  even and  $\tan \frac{k_n l}{2} = \frac{1}{k_n}$  for  $n$  odd.

Inserting this in (3.19) one gets

$$\begin{aligned}
 \alpha_n &= \frac{2}{k_n^2 N_n^2} \cos \frac{k_n l}{2} \left[ k_n \cos \frac{k_n l}{2} + \frac{1}{k_n} \cos \frac{k_n l}{2} \right]^2 \\
 &= 2 \cos^3 \frac{k_n l}{2} \left[ \frac{1}{N_n} + \frac{1}{k_n^2 N_n} \right]^2 \\
 &= 2 \cos^3 \frac{k_n l}{2} \left[ \frac{1}{0.5l k_n^2 + 0.5l + 1} + \frac{2}{0.5l k_n^4 + (0.5l + 1)k_n^2} + \frac{1}{0.5l k_n^6 + (0.5l + 1)k_n^4} \right]
 \end{aligned} \tag{3.20}$$

Applying the majorant criterion to  $|\alpha_n|$  now effortlessly yields absolute convergence of  $\sum_{n=1}^{\infty} \alpha_n$ .

Utilizing Lemma 2.2.1 once more, one obtains that the sign of  $\cos \frac{k_n l}{2}$ ,  $n$  odd, is alternating.

$\lim_{n \rightarrow \infty} k_n = (n-1) \frac{\pi}{l}$ , which is a root of  $\sin \frac{x l}{2}$  for  $n$  odd and consequently  $\lim_{n \rightarrow \infty} \left| \cos \frac{k_n l}{2} \right| = 1$ . As the sequence  $\left( k_n - (n-1) \frac{\pi}{l} \right)$  is strictly monotonically decreasing one additionally gets that  $\left| \cos \frac{k_n l}{2} \right|$ ,  $n$  odd, is unfortunately strictly monotonically increasing. Therefore we need one last reformulation (again with  $\tan \frac{k_n l}{2} = \frac{1}{k_n}$  for  $n$  odd):

$$\alpha_n = 2 \sin \frac{k_n l}{2} \cos^2 \frac{k_n l}{2} \left[ \frac{k_n}{0.5l k_n^2 + 0.5l + 1} + \frac{2k_n}{0.5l k_n^4 + (0.5l + 1)k_n^2} + \frac{k_n}{0.5l k_n^6 + (0.5l + 1)k_n^4} \right] \tag{3.21}$$

As the bracket is obviously monotonically decreasing, we are left with  $\sin \frac{k_n l}{2} \cos^2 \frac{k_n l}{2}$ , which is alternating and whose absolute value is monotonically decreasing for the odd  $k_n$ <sup>8</sup>.  $\diamond$

<sup>8</sup>This can again best be seen when comparing the properties of Lemma 2.2.1 to a plot of  $\sin(x) \cos^2(x)$ .

**Corollary 3.3.1.**

$\sum_{n=1}^{\infty} g(\dot{w}(s)) e^{-k_n^2 (t-s)} \cdot \alpha_n$ ,  $s \in [0, t]$ , is absolutely convergent, too.

**Proof**

For each  $s$   $g(\dot{w}(s))$  is just a fixed number ( $\geq 0, < \infty$ ) and not relevant for the question of convergence.  $e^{-k_n^2 (t-s)}$  is  $\in ]0, 1]$  and monotonically decreasing because of the properties of the  $k_n$  from Lemma 2.2.1. This together with the properties of  $\alpha_n$  from Theorem 3.3.1 results in the desired absolute convergence.  $\diamond$

**Corollary 3.3.2.**

$\sum_{n=1}^{\infty} g(\dot{w}(s)) e^{-k_n^2 (t-s)} \cdot \alpha_n \geq 0 \quad \forall t$  and, if  $\sum_{n=1}^{\infty} g(\dot{w}(s)) e^{-k_n^2 (t-s)} \cdot \alpha_n = 0$ , it must hold  $\dot{w}(t) = 0$ .

**Proof**

$$\begin{aligned} \sum_{n=1}^{\infty} g(\dot{w}(s)) e^{-k_n^2 (t-s)} \cdot \alpha_n &\stackrel{\alpha_{2n}=0}{=} \sum_{n=1}^{\infty} g(\dot{w}(s)) e^{-k_{2n-1}^2 (t-s)} \cdot \alpha_{2n-1} \\ &= g(\dot{w}(s)) \sum_{i=1}^{\infty} \left( e^{-k_{4i-3}^2 (t-s)} \cdot \alpha_{4i-3} + e^{-k_{4i-1}^2 (t-s)} \cdot \alpha_{4i-1} \right) \\ &\geq g(\dot{w}(s)) \sum_{i=1}^{\infty} e^{-k_{4i-3}^2 (t-s)} \cdot \underbrace{(\alpha_{4i-3} + \alpha_{4i-1})}_{>0}. \end{aligned}$$

For the last 2 steps the properties of the  $k_n$  from Lemma 2.2.1 and the properties of the  $\alpha_n$  from Theorem 3.3.1 were crucial.  $\diamond$

Together with the properties of  $g(\cdot)$  we now have, that the integrand of

$$\int_0^t \sum_{n=1}^{\infty} g(\dot{w}(s)) e^{-k_n^2 (t-s)} \cdot \alpha_n \, ds$$

is  $\geq 0$  and only 0 at points with velocity 0. Ironically this is very much the same result we already obtained in Theorem 3.1.2 for  $T(0, t)$ , albeit with considerably less effort.

Nevertheless this all is crucial for a very important question: How does cooling down work?

At an arbitrary but fixed point of time  $t^*$  with  $\dot{w}(t^*) > 0$  one has the temperature

$$T\left(\frac{l}{2}, t^*\right) = \int_0^{t^*} \sum_{n=1}^{\infty} g(\dot{w}(s)) e^{-k_n^2 (t^*-s)} \cdot \alpha_n \, ds \quad (3.22)$$

and beyond

$$T\left(\frac{l}{2}, t\right) = \int_0^{t^*} \sum_{n=1}^{\infty} g(\dot{w}(s)) e^{-k_n^2 (t-s)} \cdot \alpha_n \, ds + \int_{t^*}^t \sum_{n=1}^{\infty} g(\dot{w}(s)) e^{-k_n^2 (t-s)} \cdot \alpha_n \, ds \quad (3.23)$$

### 3.3 Some new aspects of ODE-PDE optimal control

---

Because of Corollary 3.3.2 the second integral of (3.23) is positive, however the first one is smaller than the one in (3.22) because of the previously covered properties of the integrand and the fact that  $e^{-k_n^2 t^*} - e^{-k_n^2 t}$ ,  $t > t^*$ , is also a positive monotonically decreasing sequence with  $\lim_{n \rightarrow \infty} e^{-k_n^2 t^*} - e^{-k_n^2 t} = 0$ . Consequently cooldown is only viable if

$$\int_0^{t^*} \sum_{n=1}^{\infty} g(\dot{w}(s)) (e^{-k_n^2 t^*} - e^{-k_n^2 t}) e^{k_n^2 s} \cdot \alpha_n \, ds > \int_{t^*}^t \sum_{n=1}^{\infty} g(\dot{w}(s)) e^{-k_n^2 (t-s)} \cdot \alpha_n \, ds.$$

For a boundary arc as mentioned in the previous section<sup>9</sup> it must therefore hold

$$\int_0^{t_{\text{on}}} \sum_{n=1}^{\infty} g(\dot{w}(s)) (e^{-k_n^2 t_{\text{on}}} - e^{-k_n^2 t}) e^{k_n^2 s} \cdot \alpha_n \, ds = \int_{t_{\text{on}}}^t \sum_{n=1}^{\infty} g(\dot{w}(s)) e^{-k_n^2 (t-s)} \cdot \alpha_n \, ds$$

$$\forall t \in [t_{\text{on}}, t_{\text{off}}], \quad (3.24)$$

with the latter expression being bounded from below by

$$\int_{t_{\text{on}}}^t \sum_{n=1}^{\infty} g\left(\max\left(\underbrace{|\dot{w}(t_{\text{on}}) - u_{\text{max}}(t - t_{\text{on}})|}_{\text{max.deceleration}}, 0\right)\right) e^{-k_n^2 (t-s)} \cdot \alpha_n \, ds, \quad (3.25)$$

assuming  $\dot{w}(t_{\text{on}}) > 0$ .

Physically the left hand term of (3.24) is the heat loss over time after  $t_{\text{on}}$  if the source term was 0 from that point of time on, while the right hand term is the residual heat created during the deceleration<sup>10</sup>.

This introduces a completely new facet to the concept of switching points, as already hinted in the previous section.

$\dot{w}(t)$ ,  $t \leq t_{\text{on}}$  already determines the velocity in  $[t_{\text{on}}, t_{\text{off}}]$  via (3.24), and some trajectories for  $\dot{w}(t)$ ,  $t \leq t_{\text{on}}$  can make a violation of the temperature constraint during  $[t_{\text{on}}, t_{\text{off}}]$  unavoidable:

For example let  $u$  be given by

$$u(s) = \begin{cases} u_{\text{max}} & s \in [0, 2] \\ -u_{\text{max}} & s > 2 \end{cases}$$

and consequently

$$\dot{w}(s) = \begin{cases} u_{\text{max}} \cdot s & s \in [0, 2] \\ u_{\text{max}}(2 - (s - 2)) & s > 2 \end{cases}$$

with  $u_{\text{max}} = 1$ ,  $\dot{w}_0 = 0$  and  $l = 1$ . One obtains  $T(\frac{l}{2}, 2.2) - T(\frac{l}{2}, 2) \approx 0.16$ .

All in all this means that the temperature constraint will also effect times  $t$  even before it gets active in the “traditional” way (i.e.  $T(\frac{l}{2}, t) = T_{\text{max}}$ ). Therefore a structure of the control  $u$  like

---

<sup>9</sup>and shown in figure (5.1) (right) in chapter 5

<sup>10</sup>Created by the remaining velocity, not by the deceleration itself, as such an effect is not contained in the model.

the one shown in figure (2.2) plus an additional singular arc between  $t_{\text{on}}$  and  $t_{\text{off}}$ , as one might have expected with some knowledge in ODE optimal control<sup>11</sup> is out of the question here<sup>12</sup>.

To the authors knowledge this phenomenon has not been observed before. Utilizing first order necessary conditions, we will try to analytically locate the time of the heat constraints beginning "indirect influence" in the course of the next chapter.

As a last remark before we continue to Problem 2 it should be mentioned that (3.24) is way more potent and (at least numerics wise) easier to handle than the feedback formula (3.12).

The main advantage is, that this is much more than a feedback formula, as it yields complete a priori knowledge for an entire boundary arc, provided one knows the complete history up to the arc's entry point. Additionally there is no need for any higher partial derivatives of  $T$ , which can cause numerical problems due to the extra  $k_n$ -terms.

Contrary to the sequence  $\alpha_n$  from Problem 1, the  $\beta_n$  of Problem 2 are strictly positive and do not converge to 0:

As by (2.2a)

$$\tan(k_n l) = \frac{2k_n}{k_n^2 - 1} \xrightarrow{n \rightarrow \infty} 0, \quad \text{we get} \quad \sin(k_n l) \xrightarrow{n \rightarrow \infty} 0.$$

Because  $\frac{2k_n}{k_n^2 - 1} \approx \frac{2}{k_n}$  for large  $n$  and  $\sin$  is approx. linear near its roots, we have

$$|\sin k_n l| \approx \frac{2}{k_n}$$

for large  $n$ . Together with Lemma 2.2.1 we finally can conclude, that (3.18) is strictly monotonically increasing and

$$\lim_{n \rightarrow \infty} \beta_n = \lim_{n \rightarrow \infty} \frac{1}{2} \cdot \frac{(k_n^2 + 1)^2}{lk_n^2 + l + 2} \sin^2 k_n l = \frac{2}{l}.$$

(3.17) obviously possesses analogous attributes to those shown in Corollary 3.3.2 for its Problem 1 counterpart (3.15). Absolute convergence can be shown rather uncomplicated, too:

**Corollary 3.3.3.**

Let  $\dot{w}_0 \geq 0$ . For any given finite  $t$  the series  $\sum_{n=1}^{\infty} \int_0^t h(\dot{w}(s)) e^{-k_n^2(t-s)} ds \cdot \beta_n$  converges absolutely.

**Proof**

$$\begin{aligned} \sum_{n=1}^{\infty} \int_0^t h(\dot{w}(s)) e^{-k_n^2(t-s)} ds \cdot \beta_n &\leq h(\dot{w}_0 + u_{\text{max}} \cdot t) \cdot \sum_{n=1}^{\infty} \int_0^t e^{-k_n^2(t-s)} ds \cdot \beta_n \\ &= h(\dot{w}_0 + u_{\text{max}} \cdot t) \cdot \sum_{n=1}^{\infty} \left( \frac{1}{k_n^2} - \frac{1}{k_n^2} e^{-k_n^2 t} \right) \cdot \beta_n \end{aligned}$$

<sup>11</sup>In ODE optimal control it is a commonly known fact, that a control can only be nonlinear in sections with an active state constraint.

<sup>12</sup>For Problem 2 we will prove, that full acceleration until  $t_{\text{on}}$  will guarantee a violation of  $T_{\text{max}}$ , the according proof here however is technically extremely complicated due to the structure of the  $\alpha_n$  while being not very insightful and is therefore omitted.

### 3.3 Some new aspects of ODE-PDE optimal control

The boundedness of  $h(\cdot)$ , which follows simply from its properties and the continuity of  $\dot{w}(\cdot)$ , together with the properties of the  $\beta_n$  from above easily yield the desired result.  $\diamond$

Additionally it is possible to prove the necessity of "driving with foresight" in this case:

**Theorem 3.3.2.**

Let  $\dot{w}_0 = 0$ ,  $w_0 < 0$  and  $h(\dot{w}) = \dot{w}^2$ <sup>13</sup>. A control  $u(t) \equiv u_{\max}$  in  $[0, t_{\text{on}}]$  will prompt a violation of  $T(x, t) \leq T_{\max}$  right after  $t_{\text{on}}$ .

**Proof**

In face of the previous results, it is enough to prove

$$\int_0^{t_{\text{on}}} \sum_{n=1}^{\infty} h(\dot{w}(s)) (e^{-k_n^2 t_{\text{on}}} - e^{-k_n^2 t}) e^{k_n^2 s} \cdot \beta_n \, ds < \int_{t_{\text{on}}}^t \sum_{n=1}^{\infty} h(\dot{w}(s)) e^{-k_n^2 (t-s)} \cdot \beta_n \, ds \quad (3.26)$$

for a  $t > t_{\text{on}}$  with  $u$  (similar to the example given for Problem 1) given by

$$u(s) = \begin{cases} u_{\max} & s \in [0, t_{\text{on}}] \\ -u_{\max} & s > t_{\text{on}} \end{cases}$$

and consequently

$$\dot{w}(s) = \begin{cases} u_{\max} \cdot s & s \in [0, t_{\text{on}}] \\ u_{\max}(t_{\text{on}} - (s - t_{\text{on}})) & s > t_{\text{on}}. \end{cases}$$

(3.26) then reads as

$$u_{\max}^2 \cdot \int_0^{t_{\text{on}}} \sum_{n=1}^{\infty} s^2 (e^{-k_n^2 t_{\text{on}}} - e^{-k_n^2 t}) e^{k_n^2 s} \cdot \beta_n \, ds < u_{\max}^2 \cdot \int_{t_{\text{on}}}^t \sum_{n=1}^{\infty} (2t_{\text{on}} - s)^2 e^{-k_n^2 (t-s)} \cdot \beta_n \, ds. \quad (3.27)$$

Calculating both  $s$ -integrals with iterated partial integration one arrives at

$$\begin{aligned} & \sum_{n=1}^{\infty} \left( \frac{t_{\text{on}}^2}{k_n^2} - \frac{t_{\text{on}}^2}{k_n^2} e^{k_n^2 (t_{\text{on}}-t)} - \frac{2t_{\text{on}}}{k_n^4} + \frac{2t_{\text{on}}}{k_n^4} e^{k_n^2 (t_{\text{on}}-t)} \right. \\ & \quad \left. + \frac{2}{k_n^6} - \frac{2}{k_n^6} e^{k_n^2 (t_{\text{on}}-t)} - \frac{2}{k_n^6} (e^{-k_n^2 t_{\text{on}}} - e^{-k_n^2 t}) \right) \cdot \beta_n \\ & < \sum_{n=1}^{\infty} \left( \frac{(2t_{\text{on}} - t)^2}{k_n^2} - \frac{t_{\text{on}}^2}{k_n^2} e^{k_n^2 (t_{\text{on}}-t)} - \frac{2t - 4t_{\text{on}}}{k_n^4} - \frac{2t_{\text{on}}}{k_n^4} e^{k_n^2 (t_{\text{on}}-t)} + \frac{2}{k_n^6} - \frac{2}{k_n^6} e^{k_n^2 (t_{\text{on}}-t)} \right) \cdot \beta_n \end{aligned}$$

which is rather unwieldy. Due to  $\beta_n > 0$  it is fortunately sufficient to just compare both brackets. Cancelling all terms that appear on both sides, one finally has to show

$$\left( (2t_{\text{on}} - t)^2 - t_{\text{on}}^2 \right) \frac{1}{k_n^2} + (3t_{\text{on}} - t) \frac{2}{k_n^4} - \frac{4t_{\text{on}}}{k_n^4} e^{k_n^2 (t_{\text{on}}-t)} + \frac{2}{k_n^6} (e^{-k_n^2 t_{\text{on}}} - e^{-k_n^2 t}) > 0. \quad (3.28)$$

Since (3.28) is (naturally) 0 at  $t = t_{\text{on}}$ , continuous and its derivative with respect to  $t$  evaluated at  $t_{\text{on}}$  given by

$$\frac{2}{k_n^4} (t_{\text{on}} k_n^2 + e^{-t_{\text{on}} k_n^2} - 1)$$

<sup>13</sup>The same holds true for any arbitrary  $h$  possessing the required properties mentioned earlier, the proof however gets extremely tedious.

is positive<sup>14</sup>, there exists an  $\varepsilon > 0$  such that (3.28) holds for  $t \in ]t_{\text{on}}, t_{\text{on}} + \varepsilon[$ .  $\diamond$

The full ramifications of this phenomenon will become even more apparent when beholding the necessary optimality conditions, which we are going to derive in the next chapter.

---

<sup>14</sup>Simply behold  $x + e^{-x} - 1$ ,  $x > 0$ .

## Chapter 4

# Necessary optimality conditions

As already hinted previously, the rocketcar problems can be interpreted not only as ODE-PDE optimal control problems. Some slight reformulations can transform them either into a pure ODE or pure PDE optimal control problem, resulting in an opportunity to draw comparisons and identify differences between those two already comparably well known fields and the rather unexplored ODE-PDE optimal control.

Such a transformation of course comes at a steep price. The resulting ODE optimal control problem will have a very involved integro state constraint replacing the PDE, while the PDE optimal control problem will feature a control nested in integro terms replacing the ODE, making both alternative versions highly nonstandard specimen of their respective fields.

For Problem 1 we would again like to direct the reader to the main sources:

Necessary optimality conditions of the ODE version can be found in [27], the PDE version is featured in [28] and last but not least the ODE-PDE conditions can in detail be found in [29]. Therefore we will limit ourselves to just briefly motivating and sketching them. The interested reader can find further in depth theory results mainly in [29] and hopefully in the near future in the yet to be released [26].

To facilitate comparison between the different formulations and grant at least a minimum of oversight, Appendix A contains a compact compendium of the 3 variants for each of the 2 versions of the rocket car. The following derivations here are only for Problem 1.

Provided one is mainly interested in simply obtaining necessary optimality conditions, the most convenient method currently known is no doubt the formal Lagrange technique. One might go as far as saying that this makes the technique nearly peerless from a users perspective, but naturally such ease of use does not come without an equally big (and for a mathematician maybe even bigger) drawback: In most cases, especially more complex “real life“ problems<sup>1</sup>, its validity can at least a priori not be justified in a strict mathematical way. Existence as well as indispensable regularity properties of the featured Lagrange multipliers simply have to be assumed. Furthermore the uniqueness of any candidate optimal solution obtained this way is not guaranteed<sup>2</sup>.

---

<sup>1</sup>A prime example would be the fuel cell model found e.g. in chapter 4 of [29].

<sup>2</sup>During all numerical calculations we never encountered any hint of ambiguity, though.

## 4.1 Problem 1 as ODE-PDE optimal control problem

With those disadvantages still in mind we will now nevertheless derive the necessary first order conditions for the original ODE-PDE version. To that end it is best to utilize the system of two first order ODEs instead of the second order ODE with  $w_1 := w$  being the position and  $w_2 := \dot{w}$  being the velocity of the car, just like in section 1 of chapter 2. The according adjoints shall be denoted by  $p_1$  and  $p_2$ , the temperature  $T$ 's adjoint will be called  $q$  and the multiplier associated with the temperature state constraint (1.5) will be dubbed  $\bar{\mu}$ . As the control constraint (1.2d) can relatively effortlessly be dealt with by a mere projection later on, it was decided to not include it in the Lagrangian. The same goes for the ODEs initial- and terminal conditions (1.2b) and (1.2d), which will instead be utilized in the following calculations whenever suitable.

Let the Lagrangian be defined by

$$\begin{aligned}
 \mathcal{L} = & t_f + \frac{1}{2} \lambda \int_0^{t_f} u^2 dt - \int_0^{t_f} (\dot{w}_1 - w_2) p_1 + (\dot{w}_2 - u) p_2 dt \\
 & - \int_0^l \int_0^{t_f} (T_t - T_{xx} - g(w_2)) q dt dx - \int_0^{t_f} (-T_x(0, t) + T(0, t)) q(0, t) dt \\
 & - \int_0^{t_f} (T_x(l, t) + T(l, t)) q(l, t) dt \\
 & - \int_0^l \int_0^{t_f} (T - T_{\max}) \bar{\mu} dt dx. \tag{4.1}
 \end{aligned}$$

Integration by parts yields

$$\begin{aligned}
 = & t_f + \frac{1}{2} \lambda \int_0^{t_f} u^2 dt + \int_0^{t_f} w_1 \dot{p}_1 dt + w_0 p_1(0) + \dot{w}_0 p_2(0) + \int_0^{t_f} w_2 (\dot{p}_2 + p_1) dt \\
 & + \int_0^{t_f} u p_2 dt - \int_0^l T(x, t_f) \cdot q(x, t_f) dx + \int_0^l \int_0^{t_f} T \cdot (q_t + q_{xx}) dt dx \\
 & + \int_0^{t_f} g(w_2) \int_0^l q dx dt - \int_0^{t_f} T(0, t) (q(0, t) - q_x(0, t)) dt \\
 & - \int_0^{t_f} T(l, t) (q(l, t) + q_x(l, t)) dt - \int_0^l \int_0^{t_f} (T - T_{\max}) \bar{\mu} dt dx. \tag{4.2}
 \end{aligned}$$

#### 4.1 Problem 1 as ODE-PDE optimal control problem

---

As a next step, we have to calculate all the required directional derivatives, bearing in mind that there is a further constraint on  $u$ :

$$\begin{aligned}
 D_{w_1} \mathcal{L} h_1 &= \int_0^{t_f} h_1 \dot{p}_1 dt \stackrel{!}{=} 0 \\
 D_{w_2} \mathcal{L} h_2 &= \int_0^{t_f} h_2 (\dot{p}_2 + p_1) dt + \int_0^{t_f} g'(w_2) \cdot h_2 \int_0^l q dx dt \stackrel{!}{=} 0 \\
 D_T \mathcal{L} h_T &= - \int_0^l h_T(x, t_f) \cdot q(x, t_f) dx + \int_0^l \int_0^{t_f} h_T \cdot (q_t + q_{xx}) dt dx \\
 &\quad - \int_0^{t_f} h_T(0, t) \cdot (q(0, t) - q_x(0, t)) dt - \int_0^{t_f} h_T(l, t) \cdot (q(l, t) + q_x(l, t)) dt \\
 &\quad - \int_0^l \int_0^{t_f} h_T \bar{\mu} dt dx \stackrel{!}{=} 0, \\
 D_u \mathcal{L} (u - u^*) &= \lambda \int_0^{t_f} u^* (u - u^*) dt + \int_0^{t_f} p_2 (u - u^*) dt \\
 &= \int_0^{t_f} (\lambda u^* + p_2) (u - u^*) dt \geq 0 \quad \text{for all admissible controls } u.
 \end{aligned}$$

Having a problem with free endtime, an additional derivative with respect to  $t_f$  is required, resulting in

$$1 + \frac{\lambda}{2} u^2(t_f) + u(t_f) p_2(t_f) \stackrel{!}{=} 0, \quad (4.3)$$

which corresponds to  $H(t_f) = 0$  with the Hamiltonian defined according to [29].

So the projection formula and adjoint system (formally<sup>3</sup>) read as

$$\dot{p}_1 = 0 \quad (4.4a)$$

$$\dot{p}_2 = -p_1 - g'(w_2) \int_0^l q dx \quad (4.4b)$$

$$-q_t - q_{xx} = \bar{\mu} \quad (4.4c)$$

$$q(x, t_f) = 0 \quad (4.4d)$$

$$q_x(0, t) = q(0, t) \quad (4.4e)$$

$$q_x(l, t) = -q(l, t) \quad (4.4f)$$

$$u = P_{[-u_{\max}, u_{\max}]} \left( -\frac{p_2}{\lambda} \right) \quad (4.4g)$$

with  $P_{[-u_{\max}, u_{\max}]}$  being the aforementioned projection.

---

<sup>3</sup>Strictly speaking the adjoint PDE is of course not to be understood in the classical strong sense, its weak form can be found in [29], equation 3.8. However the above version is the most beneficial for interpretation (and later for chapter 5).

Finally the measure  $\bar{\mu}$  is subject to the complementarity condition

$$\int_0^l \int_0^{t_f} (T - T_{\max}) \bar{\mu} \, dt \, dx = 0, \quad \bar{\mu} \geq 0.$$

Due to Theorem 4.4 from [25] we already know, that  $\bar{\mu}(x, t) \equiv 0$  for all  $x \neq \frac{l}{2}$ , i.e. the active set  $\mathcal{A}_1$  will be a set of intervals and/or points along  $x = \frac{l}{2}$ . Under some additional basic assumptions A. Rund could prove some rather intriguing structural results for  $\bar{\mu}$  ([29], Lemma 3.4.6 and Satz 3.4.13). In essence  $\bar{\mu}$  will be a Dirac delta impulse in space and time for touch points while for boundary arcs it will consist of an impuls in space plus impulses in time at the entry and exit point.

As the adjoint PDE is backward in time, this allows for some predictions on the structure of the temperature's adjoint  $q$ . Assuming for example the switching structure of one single boundary arc,  $q$  will be identical to zero in the last section  $(t_{\text{off}}, t_f]$  as the constraint (1.5) exerts no more influence there, because the car is slowing down anyway to meet the terminal conditions for  $w_{1,2}$ . This of course changes in the middle section between  $t_{\text{on}}$  and  $t_{\text{off}}$ , where (1.5) is directly active and we can expect (positive) peaks of  $q$  at the entry and exit point. However the most interesting interval is naturally  $[0, t_{\text{on}})$  with the expected "indirect" influence of the temperature constraint. Here we can expect  $q$  to have its maximal values close to  $t_{\text{on}}$ , while it will be waning towards  $t = 0$ , as said "indirect" influence will accumulate, the closer we approach the state constraint.

For a touch point similar deliberations can be made. All in all one can always expect a symmetrical adjoint  $q(x, t^* - \varepsilon) \neq 0$  shortly before the first point of time  $t^*$  with  $T\left(\frac{l}{2}, t^*\right) = T_{\max}$ . As from that point on the adjoint is only a heat equation backwards in time without any further source terms, the only thing affecting  $q$  between  $t = 0$  and  $t = t^* - \varepsilon$  is the heat loss due to the robin type boundary conditions, causing  $q$  to slowly drop to zero, however not reaching it in finite time. From that we can infer, that  $q(x, t) > 0$  between  $t = 0$  and  $t = t^*$ .

Finally via (4.4b) and (4.4g) this will influence the control  $u$  from the get-go, preventing a linear behaviour (and consequently an overshooting of  $T$ ) in all of  $[0, t^*)$ . As it is however more than likely, that the control constraint will also be active from the start, the nonlinearity will initially be obscured by the resulting projection. The first point actually witnessing a nonlinear  $u$  can be anticipated somewhere between  $t = 0$  and  $t = t^*$ , depending on the restrictiveness of the control constraint.

## 4.2 Problem 1 as ODE optimal control problem

An alternative way to tackle the necessary conditions is to use Theorem 4.4. from [25] and (3.15)/(3.16) to define an auxiliary state variable

$$w_3(t) := T\left(\frac{l}{2}, t\right) = \int_0^t \sum_{n=1}^{\infty} \alpha_n g(w_2(s)) e^{-k_n^2(t-s)} ds. \quad (4.5)$$

Lets for a start work under the assumption, that exactly one boundary arc  $(t_{\text{on}}, t_{\text{off}})$ ,  $t_{\text{on}} < t_{\text{off}}$  exists.

Then this new state variable must satisfy the following constraints:

$$\dot{w}_3(t) = \frac{d}{dt}T\left(\frac{l}{2}, t\right), \quad (4.6a)$$

$$w_3(0) = 0, \quad (4.6b)$$

$$w_3(t_{\text{on}}) = T_{\text{max}} \quad \text{and} \quad w_3(t_{\text{off}}) = T_{\text{max}}, \quad (4.6c)$$

$$w_3(t) - T_{\text{max}} \leq 0. \quad (4.6d)$$

While getting rid of the PDE is a considerable boon, we have traded it against (4.6a), a Volterra integro-differential equation. This leads to the demanding area of research of optimal control problems with integro-differential equations. The authors knowledge on this field is unfortunately rather limited, therefore we would like to direct the interested reader to some sources where he can find additional information, for example Kappel, Stettner [17], Schmidt [30] and Warga [36] or, as a more recent source, Bonnans, de la Vega and Dupuis [6].

However we can at least confirm, that the new state constraint (4.6d) is of second-order.

To derive the adjoint equations we again apply the formal Lagrange technique:

Let the Lagrangian this time be defined by

$$\begin{aligned} \mathcal{L}(\mathbf{w}, u, \mathbf{p}, t_{\text{on}}, t_{\text{off}}, t_f) &:= \int_0^{t_f} 1 + \frac{\lambda}{2} u^2 dt - \int_0^{t_f} (\dot{w}_1 - w_2) p_1 dt - \int_0^{t_f} (\dot{w}_2 - u) p_2 dt \\ &\quad - \int_0^{t_f} \left[ \dot{w}_3 - \frac{d}{dt}T\left(\frac{l}{2}, t\right) \right] p_3 dt + \int_0^{t_f} (w_3 - T_{\text{max}}) \mu(t) dt \\ &\quad + (w_3(t_{\text{on}}) - T_{\text{max}}) \sigma_{\text{on}} + (w_3(t_{\text{off}}) - T_{\text{max}}) \sigma_{\text{off}}. \end{aligned}$$

Integration by parts then yields, while substituting (1.2b), (1.2c) and (4.6b),

$$\begin{aligned} \mathcal{L}(\mathbf{w}, u, \mathbf{p}, t_{\text{on}}, t_{\text{off}}, t_f) &= \int_0^{t_f} 1 + \frac{\lambda}{2} u^2 dt + w_0 p_1(0) + \int_0^{t_f} w_1 \dot{p}_1 + w_2 p_1 dt \\ &\quad + \dot{w}_0 p_2(0) + \int_0^{t_f} w_2 \dot{p}_2 + u p_2 dt - w_3(t_f) p_3(t_f) \\ &\quad + \int_0^{t_f} w_3 \dot{p}_3 + \frac{d}{dt}T\left(\frac{l}{2}, t\right) p_3 dt + \int_0^{t_f} (w_3 - T_{\text{max}}) \mu(t) dt \\ &\quad + (w_3(t_{\text{on}}) - T_{\text{max}}) \sigma_{\text{on}} + (w_3(t_{\text{off}}) - T_{\text{max}}) \sigma_{\text{off}}. \end{aligned}$$

To avoid getting to repetitive, we only give the derivation of the "most intriguing" adjoint  $p_2$ :

$$\begin{aligned}
 D_{w_2} \mathcal{L}(\dots) h_2 &= \int_0^{t_f} p_1(t) h_2(t) dt + \int_0^{t_f} \dot{p}_2(t) h_2(t) dt \\
 &\quad + \int_0^{t_f} g'(w_2(t)) h_2(t) p_3(t) dt \\
 &\quad - \int_0^{t_f} \left( \int_0^t \sum_{n=1}^{\infty} k_n^2 \alpha_n g'(w_2(s)) e^{-k_n^2 (t-s)} h_2(s) ds \right) p_3(t) dt \\
 &\stackrel{\text{Fubini}}{\implies} \int_0^{t_f} p_1(t) h_2(t) dt + \int_0^{t_f} \dot{p}_2(t) h_2(t) dt \\
 &\quad + \int_0^{t_f} \left( g'(w_2(t)) p_3(t) \right. \\
 &\quad \left. - \int_t^{t_f} \sum_{n=1}^{\infty} k_n^2 \alpha_n g'(w_2(t)) e^{-k_n^2 (s-t)} p_3(s) ds \right) h_2(t) dt \stackrel{!}{=} 0.
 \end{aligned}$$

This yields

$$\dot{p}_2 = -p_1 - g'(w_2(t)) \left( p_3(t) - \int_t^{t_f} \sum_{n=1}^{\infty} k_n^2 \alpha_n e^{-k_n^2 (s-t)} p_3(s) ds \right), \quad (4.7a)$$

again an integro-differential equation of Volterra type, retrograde in time as expected from an adjoint.

All other necessary conditions turn out to coincide with those of Theorem 4.1 from [14], in particular

$$p_1 = \text{const}, \quad (4.7b)$$

$$\dot{p}_3 = -\mu \quad \text{with} \quad p_3(t_f) = 0 \quad \text{and} \quad p_3(t_{\text{on/off}}^+) = p_3(t_{\text{on/off}}^-) - \sigma_{\text{on/off}}, \quad (4.7c)$$

$$\text{with} \quad \sigma_{\text{on/off}} > 0, \quad (4.7d)$$

$$H[t_f] = 0, \quad H[t_{\text{on/off}}^+] = H[t_{\text{on/off}}^-] \quad (4.7e)$$

$$\text{with} \quad H(\mathbf{w}, u, \mathbf{p}) := 1 + \frac{\lambda}{2} u^2 + w_2 p_1 + u p_2 + \frac{d}{dt} T \left( \frac{l}{2}, t \right) p_3 \quad (4.7f)$$

$$\text{and} \quad L(\mathbf{w}, u, \mathbf{p}, \mu) := H(\mathbf{w}, u, \mathbf{p}) + \mu (w_3 - T_{\text{max}}), \quad (4.7g)$$

$$u(t) = P_{[-u_{\text{max}}, u_{\text{max}}]} \left( -\frac{1}{\lambda} p_2 \right), \quad (4.7h)$$

$$\mu = \begin{cases} 0 & \text{on } [0, t_{\text{on}}) \cup (t_{\text{off}}, t_f] \\ \geq 0 & \text{on } [t_{\text{on}}, t_{\text{off}}] \end{cases} \quad \text{and} \quad \mu (w_3 - T_{\text{max}}) = 0. \quad (4.7i)$$

## 4.2 Problem 1 as ODE optimal control problem

---

(4.6d) (together with (4.6a)) constitutes an integro state constraint depending on the entire history of  $w_2$ , as expected. This is mirrored in the structure of the adjoints: bearing in mind, that those are backward in time, (4.7a) shows  $p_2$  depending on  $p_3$ 's behaviour in the interval  $[t, t_f]$ .

Considering (4.7c), (4.7d) and (4.7i) one can deduce some of the structure of the new adjoint  $p_3$  associated with the new version of the heat constraint, just like we did in the ODE-PDE case before. On  $(t_{\text{off}}, t_f]$  it must again hold  $p_3 = 0$ , nicely mirroring the fact, that (1.5) will not effect this interval, as the car is slowing down there anyway. In the middle interval, where (4.6 d) is directly active, this again changes and  $p_3$  is monotonically decreasing there. Additionally we can expect jumps at the entry and exit point, similar to the behaviour of  $T$ 's adjoint  $q$ . And finally  $p_3$  will be constant (and  $\neq 0$ , as both jumps are downward) in  $[0, t_{\text{on}})$ , exerting its "indirect" influence as already anticipated in section 3.3.

Thus we can expect the (continuous) control to be linear on  $(t_{\text{off}}, t_f]$  but not on  $[0, t_{\text{on}})$ .

Necessary conditions for a touch point can be obtained analogously, resulting in a (downward) jump of  $p_3$  at  $t_{\text{touch}}$ . So just like before, we can always expect an adjoint  $p_3$  not identical to zero between  $t = 0$  and the first point of time  $t^*$  with  $T\left(\frac{l}{2}, t^*\right) = T_{\text{max}}$ , and via (4.7a) and (4.7h) this will again influence the control  $u$  in  $[0, t^*)$ , preventing a linear behaviour.

### 4.3 Problem 1 as PDE optimal control problem

The third alternative finally is to replace the ODE and arrive at a nonstandard state-constrained PDE optimal control problem with a control embedded in integral terms:

$$\min_{u \in U} \left\{ t_f + \frac{1}{2} \lambda \int_0^{t_f} u^2 dt \right\}, \quad \lambda > 0, \quad (4.8)$$

subject to

$$T_t(x, t) - T_{xx}(x, t) = g \left( \dot{w}_0 + \int_0^t u(s) ds \right) \quad \text{in } (0, l) \times (0, t_f), \quad (4.9a)$$

$$-T_x(0, t) + T(0, t) = 0, \quad T_x(l, t) + T(l, t) = 0 \quad \text{in } [0, t_f], \quad (4.9b)$$

$$T(x, 0) = T_0(x) := 0 \quad \text{on } [0, l], \quad (4.9c)$$

$$\int_0^{t_f} u(t) dt = -\dot{w}_0, \quad (4.9d)$$

$$\int_0^{t_f} \int_0^t u(s) ds dt = -w_0 - \dot{w}_0 t_f \xrightarrow{\text{part. int.}} \int_0^{t_f} t u(t) dt = w_0, \quad (4.9e)$$

$$T(x, t) \leq T_{\max} \quad \text{in } [0, l] \times [0, t_f]. \quad (4.9f)$$

The two isoperimetric conditions (4.9d, e) comprise the original ODE as well as its initial and terminal conditions.

(4.9a) once more plainly shows the dependence of the temperature on the history of  $u$ .

Additional results regarding the existence of solutions, the properties of the solution operator etc. are going to be published in [26].

Under basically the same necessary assumptions and with the same catches as in the ODE-PDE case we can again formally proceed with

$$\begin{aligned} \mathcal{L} &= \int_0^{t_f} \left( 1 + \frac{\lambda}{2} u^2(t) \right) dt - \int_0^{t_f} \int_0^l \left( T_t - T_{xx} - g \left( \dot{w}_0 + \int_0^t u(s) ds \right) \right) q dx dt \\ &\quad - \int_0^{t_f} (-T_x(0, t) + T(0, t)) q(0, t) dt - \int_0^{t_f} (T_x(l, t) + T(l, t)) q(l, t) dt \\ &\quad + \nu_1 \left( \int_0^{t_f} u(t) dt + \dot{w}_0 \right) + \nu_2 \left( \int_0^{t_f} t u(t) dt - w_0 \right) \\ &\quad + \int_0^{t_f} \int_0^l (T - T_{\max}) \bar{\mu} dx dt, \end{aligned} \quad (4.10)$$

and with the usual partial integration in space and time and appropriate directional derivatives one finally arrives at the adjoint equations

### 4.3 Problem 1 as PDE optimal control problem

---

$$-q_t - q_{xx} = \bar{\mu} \text{ in } (0, l) \times (0, t_f). \quad (4.11a)$$

$$-q_x(0, t) = -q(0, t), \quad q_x(l, t) = -q(l, t) \text{ on } [0, t_f] \quad \text{and} \quad q(x, t_f) = 0 \text{ on } [0, l] \quad (4.11b)$$

and the now rather involved projection formula

$$u(t) = P_{[-u_{\max}, u_{\max}]} \left\{ -\frac{1}{\lambda} \left( \nu_1 + \nu_2 t + \int_t^{t_f} g' \left( \dot{w}_0 + \int_0^s u(\tilde{s}) d\tilde{s} \right) \cdot \left( \int_0^l q(x, s) dx \right) ds \right) \right\}. \quad (4.12)$$

Equations (4.11) are again to be understood in the weak sense, but as before this version is preferable for our aims.

It should also be observed, that (4.12) has the same structure as (4.7h), but in integro form with a kernel depending on all values of  $u$  on the interval  $[0, t]$ , forward in time, as well as on all values of  $q$  on  $[t, t_f]$ , backward in time.

The complementarity condition stays the same as in the ODE-PDE context:

$$\int_0^l \int_0^{t_f} (T - T_{\max}) \bar{\mu} dt dx = 0, \quad \bar{\mu} \geq 0,$$

and for the terminal time condition we arrive at

$$1 + \frac{\lambda}{2} u^2(t_f) + u(t_f)(\nu_1 + \nu_2 t_f) - \underbrace{\int_0^l T_x(x, t_f) q_x(x, t_f) dx}_{=0, (4.11b)} = 0, \quad (4.13)$$

also very much reminiscent of its ODE-PDE version pendant (4.3).

Indeed with a closer look at all 3 sets of necessary conditions, the following relations catch our eye:

$$p_1(t) \hat{=} -\nu_2, \quad (4.14a)$$

$$p_2(t) \hat{=} \nu_1 + \nu_2 t + \int_t^{t_f} g' \left( \dot{w}_0 + \int_0^s u(\tilde{s}) d\tilde{s} \right) \cdot \left( \int_0^l q(x, s) dx \right) ds, \quad (4.14b)$$

$$p_2(t_f) \hat{=} \nu_1 + \nu_2 t_f, \quad (4.14c)$$

$$p_3(t) - \int_t^{t_f} \sum_{n=1}^{\infty} k_n^2 \alpha_n e^{-k_n^2 (s-t)} p_3(s) ds \hat{=} \int_0^l q(x, t) dx. \quad (4.14d)$$

Those connect the interchanging adjoints of the 3 versions: the ODE-adjoints  $p_1$  and  $p_2$ , the multipliers  $\nu_1$  and  $\nu_2$  associated with the integro equations (4.9d,e) replacing the ODE in the PDE version, the temperature's adjoint  $q$  and  $p_3$ , the adjoint of the auxiliary state  $w_3$  replacing  $T$  in the ODE version.

Just as the different sets of optimality conditions, the relations (4.14) will be picked up in the next chapter, where we will try to numerically verify all of the above a posteriori.



## Chapter 5

# Numerical solution of the hypersonic rocket car problems

After having already deduced some of the new mathematical effects of the hypersonic rocket car problems analytically and having derived at least tentative optimality conditions of the problem's different formulations, the current chapter, which can be seen as the main chapter of the thesis, will contain the numerical computations accompanying all ruminations of chapter 1 to 3 as well as the already promised a posteriori verification of the different optimality conditions from chapter 4.

For numerical computations one has to choose between two major sets of methods: the direct approach of *first discretize then optimize* (FDTO), or the indirect alternative *first optimize, then discretize* (FOTD). From a practical point of view, i.e. if one is just interested in obtaining a solution, FDTO is clearly the method of choice. All one has to do, is to find a proper discretization of both the ODE (1.2) and PDE (1.3) resp. (1.4) and a numerical approximation of the objective functional (1.1) via a quadrature formula and hand it all over to a nonlinear optimization program. This is relatively easily done and the computations for a problem of the magnitude of the hypersonic rocket car are not too taxing even for an average machine. The main drawback is of course the possibility, that the solution of the discretized problem does not converge against the solution of the continuous problem.

FOTD on the other hand, despite being the in a theoretical sense more sound and save method, is the remarkably more stony road. As the name suggests, this methods starts with setting up the (first order) optimality conditions as already seen in previous sections, which then have to be discretized and numerically solved. In spite of sounding on the first impression like doing nearly the same thing but in reversed order, the difference in implementation and especially performance of those two methods is far from marginal.

Therefore our first attempt shall be FDTO. A posteriori we could at least offer a partial remedy for the lack of a convergence proof by approximately verifying the first-order optimality conditions.

With those in mind we only utilized the ODE formulation of a system of two first order equations instead of the second order ODE (1.2). This offers the additional comfort of having the velocity  $w_2$  of the car explicitly given for the source term of the PDE. In addition, the free terminal time has been transformed by  $\tau := \frac{t}{t_f}$  at the cost of spawning an additional optimization variable  $t_f$ <sup>1</sup>.

---

<sup>1</sup>Practically speaking, one could of course do without the transformation: implementing the untransformed version with a (time) steplength of  $t_f$  times the transformed one yields exactly the same numerics wise. The important point is really just to include  $t_f$  as an additional optimization variable. The transformation is nevertheless the mathematically "proper" way.

This leads to a problem with a normalized time  $\tau$  running in a fixed interval  $[0,1]$ . Problem 1 for example takes the new form below:

$$\min_{u \in U} \left\{ t_f + \frac{t_f}{2} \lambda \int_0^1 u^2(\tau) d\tau \right\}, \quad \lambda > 0,$$

subject to

$$\begin{aligned} \frac{1}{t_f} \dot{w}_1(\tau) &= w_2(\tau) \quad \text{in } (0, 1), \\ \frac{1}{t_f} \dot{w}_2(\tau) &= u(\tau) \quad \text{in } (0, 1), \\ w_1(0) &= w_0, \quad w_2(0) = \dot{w}_0, \\ w_1(1) &= 0, \quad w_2(1) = 0, \\ U &:= \{u \in L^2(0, 1) : |u(\tau)| \leq u_{\max} \text{ in } [0, 1]\}, \end{aligned}$$

$$\begin{aligned} \frac{1}{t_f} T_\tau(x, \tau) - T_{xx}(x, \tau) &= g(w_2(\tau)) \quad \text{in } (0, l) \times (0, 1), \\ -T_x(0, \tau) + T(0, \tau) &= 0, \quad T_x(l, \tau) + T(l, \tau) = 0 \quad \text{in } [0, 1], \\ T(x, 0) &= 0 \quad \text{in } [0, l], \\ T(x, \tau) &\leq T_{\max} \quad \text{in } [0, l] \times [0, 1], \\ t_f &> 0. \end{aligned}$$

We now discretized the heat equation with the well-known Crank-Nicolson scheme, known to be unconditionally stable and second-order in space and time, and the ordinary differential equations by simple forward difference quotients. The boundary conditions have always been incorporated by suitable second-order schemes. Finally the integral term of the objective functional is approximated with a basic quadrature formula (more on that in section 5.3) and one obtains the following nonlinear programming problem (NLP, again only demonstrated for Problem 1):

$$\min_{u \in U} \left\{ t_f + \frac{\lambda}{2} \frac{t_f}{n_1} \sum_{j=0}^{n_1-1} \mathbf{u}(j)^2 \right\}$$

$$\frac{n_1}{t_f} (\mathbf{w}_1(j+1) - \mathbf{w}_1(j)) = \mathbf{w}_2(j) \quad j = 0, \dots, n_1 - 1,$$

$$\frac{n_1}{t_f} (\mathbf{w}_2(j+1) - \mathbf{w}_2(j)) = \mathbf{u}(j) \quad j = 0, \dots, n_1 - 1,$$

$$\mathbf{w}_1(0) = w_0, \quad \mathbf{w}_2(0) = \dot{w}_0,$$

$$\mathbf{w}_1(n_1) = 0, \quad \mathbf{w}_2(n_1) = 0,$$

$$U := \{\mathbf{u} \in \mathbb{R}^{n_1-1} : |\mathbf{u}(j)| \leq u_{\max} \quad j = 0, \dots, n_1 - 1\},$$

---


$$\begin{aligned}
& \frac{n_1}{t_f} (\mathbf{T}(i, j+1) - \mathbf{T}(i, j)) \\
& - \frac{n_2^2}{2} (\mathbf{T}(i-1, j+1) - 2 \cdot \mathbf{T}(i, j+1) + \mathbf{T}(i+1, j+1) \\
& \quad + \mathbf{T}(i-1, j) - 2 \cdot \mathbf{T}(i, j) + \mathbf{T}(i+1, j)) = \frac{1}{2} (\mathbf{w}_2(j+1)^2 + \mathbf{w}_2(j)^2), \\
& \hspace{15em} j = 0, \dots, n_1 - 1 \\
& \hspace{15em} i = 1, \dots, n_2 - 1 \\
& \frac{n_2}{2} (-3 \cdot \mathbf{T}(0, j) + 4 \cdot \mathbf{T}(1, j) - \mathbf{T}(2, j)) = \mathbf{T}(0, j), \\
& \frac{n_2}{2} (3 \cdot \mathbf{T}(n_2, j) - 4 \cdot \mathbf{T}(n_2 - 1, j) + \mathbf{T}(n_2 - 2, j)) = \mathbf{T}(n_2, j), \quad j = 1, \dots, n_1 \\
& \mathbf{T}(i, 0) = 0, \quad i = 0, \dots, n_2 \\
& \mathbf{T}(i, j) \leq T_{\max}, \quad j = 0, \dots, n_1 \\
& \hspace{15em} i = 0, \dots, n_2 \\
& t_f > 0.
\end{aligned}$$

*Remark:*

The additional condition  $t_f > 0$  is essentially just a precaution to avoid possible nonsense solutions. As the utilized software AMPL/IPOPT cannot handle strict constraints this can be implemented as  $t_f \geq \varepsilon$  ( $\varepsilon$  sufficiently small), or even plainly  $t_f \geq 0$  (as done in the according AMPL program), because  $t_f = 0$  only allows for viable solutions in trivial cases.

This resulting NLP has been solved via the algebraic modelling language AMPL [1] ("A Mathematical Programming Language" developed at Bell Laboratories by Robert Fourer, David Gay and Brian Kernighan), featuring fast automatic differentiation.

The choice for the nonlinear optimization software fell on IPOPT [13] ("Interior Point OPTimizer", developed by A. Wächter and Biegler [32], [33] as part of the COIN-OR project. Being a freeware program of quite some renown, IPOPT is able to exploit first and second derivative information provided by AMPLs automatic differentiation.

The according AMPL program `rocketcar_ode_pde.txt` as well as the Matlab [20] program `rocketcar_ode_pde.m` (only necessary for plotting, as this is not possible with AMPL/IPOPT itself) are located in the folder `Programs/Direct approach`. The respective programs for the other versions, `rocketcar_pde.txt` and `rocketcar_ode.txt`, can be found in the same folder.

In the neighboring folder `Programs/Comsol test` one can additionally find a Comsol Multiphysics<sup>2</sup> program named `comsoltest.m`. As its name suggests, it was used to check the accuracy of the solution of the heat equation as well as creating the small video clip `temperature.avi`, showing the development of the constrained temperature for Problem 1. The very same development is also shown in the first figure of the next section.

---

<sup>2</sup>A widely used finite element solver.

## 5.1 Results for Problem 1

In the following (both for Problem 1 and 2) it shall hold  $\lambda = 10^{-1}$ ,  $w_0 = -6$ ,  $g(z) = h(z) := z^2$  and  $l = 1$ . In the control constrained cases  $u_{\max}$  is always set to 1.

Figure (5.1) shows the same setup as figure (2.3) (left) with the additional heat constraint  $T(x, t) \leq T_{\max} = 1.5$ .

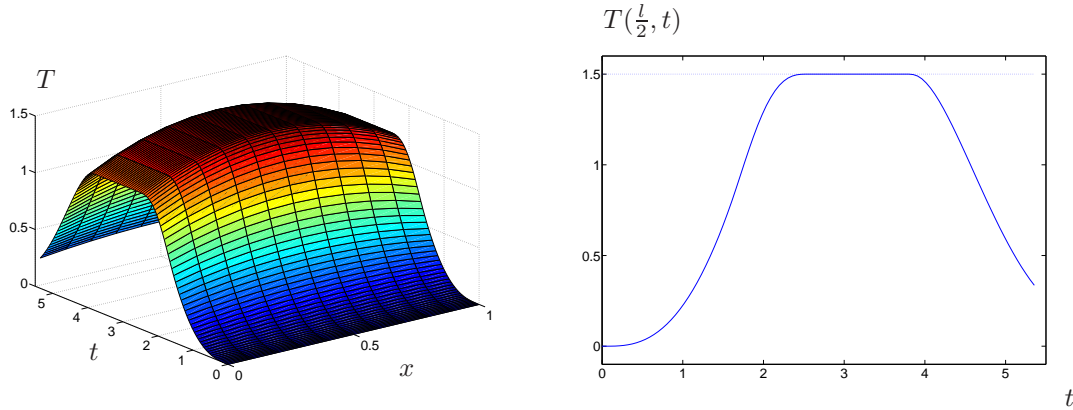


Figure 5.1: Temperature  $T(x, t)$  (left) and cross-section  $T(\frac{l}{2}, t)$  (right) for Problem 1 along a state- and control-constrained trajectory.

Data:  $\lambda = 10^{-1}$ ,  $u_{\max} = 1$ ,  $w_0 = -6$ ,  $\dot{w}_0 = 0$  and  $g(z) := z^2$ ; cf. Fig. (2.3) (left).

The results are as anticipated: symmetry with respect to  $x = \frac{l}{2}$ , the position of the maximal temperature for each respective time  $t$ . As can be observed in the cross-section on the right,  $T(\frac{l}{2}, t)$  goes straight up to  $T_{\max}$ , followed by a boundary arc. Basically, the peak of figure (2.3) (left) just got capped due to the temperature constraint. The more restrictive this constraint gets, the longer the boundary arc will be.

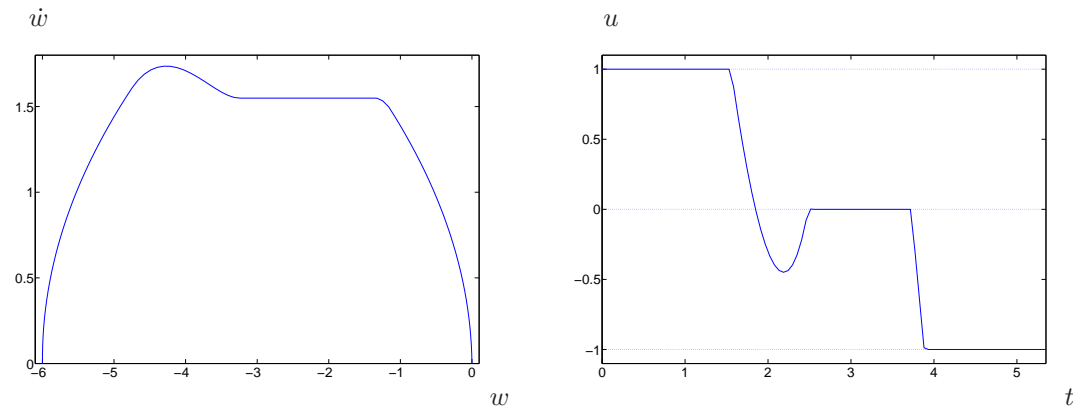


Figure 5.2: State-constrained control-constrained optimal trajectory for Problem 1 in the phase-plane (left) with associated optimal control  $u$  (right).

Data:  $\lambda = 10^{-1}$ ,  $w_0 = -6$ ,  $\dot{w}_0 = 0$ ,  $u_{\max} = 1$ ,  $T_{\max} = 1.5$ , and  $g(z) := z^2$ ; cf. Fig. (2.1) resp. (2.2) (left).

## 5.1 Results for Problem 1

In figure (5.2) (right) we can clearly see the predicted nonlinearity of the control  $u$  before  $t_{\text{on}}$ . Please note, that the seemingly linear behaviour of  $u$  up to roughly  $t = 1.7$  is solely caused by the controls constraint and the resulting projection on  $u_{\text{max}} = 1$ . In a scenario without constraints for  $u$  we would witness nonlinearity on the entire interval  $[0, t_{\text{on}}]$  with the effect being most prominent close to  $t_{\text{on}}$  while fading close to 0.

Consequently the phase diagram on the left of figure (5.2) is not just a capped version of the one in figure (2.1), as there remains a little hump created by the controls behaviour.

Interestingly  $u$  seems to approach 0 in  $[t_{\text{on}}, t_{\text{off}}]$ , which means the temperature is at least close to a state of equilibrium there.

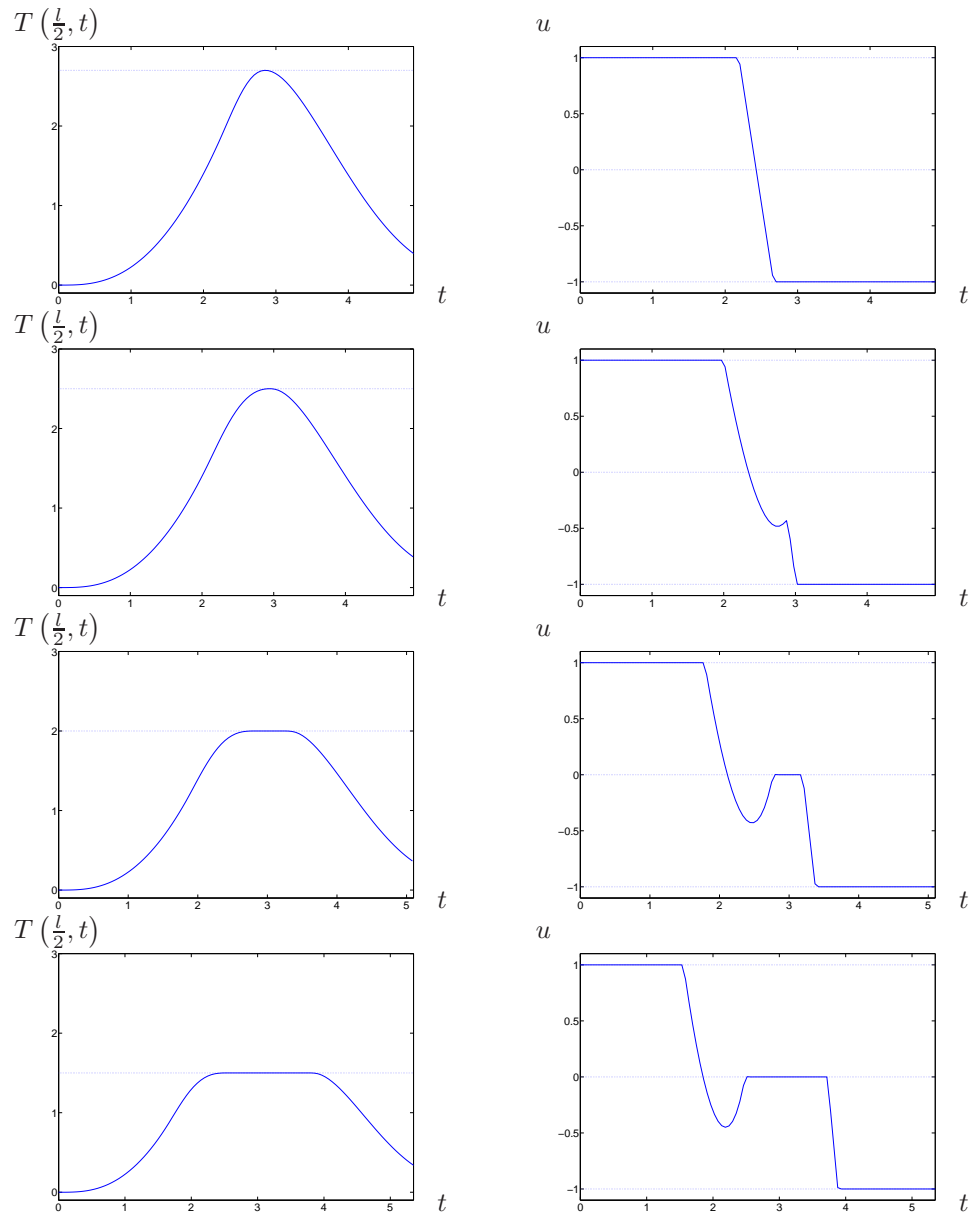


Figure 5.3: Cross-sections of the temperature profiles at  $\frac{l}{2}$  and according optimal controls  $u$  for Problem 1 featuring different values for  $T_{\text{max}}$   
 Data:  $\lambda = 10^{-1}$ ,  $w_0 = -6$ ,  $\dot{w}_0 = 0$ ,  $u_{\text{max}} = 1$ ,  $T_{\text{max}} = 2.7, 2.5, 2.0, 1.5$ , and  $g(z) := z^2$ ;

Fig. (5.3) shows the development for increasingly stricter constraints. On the left side one can observe the growth of the boundary arc, while the right side displays the according controls.

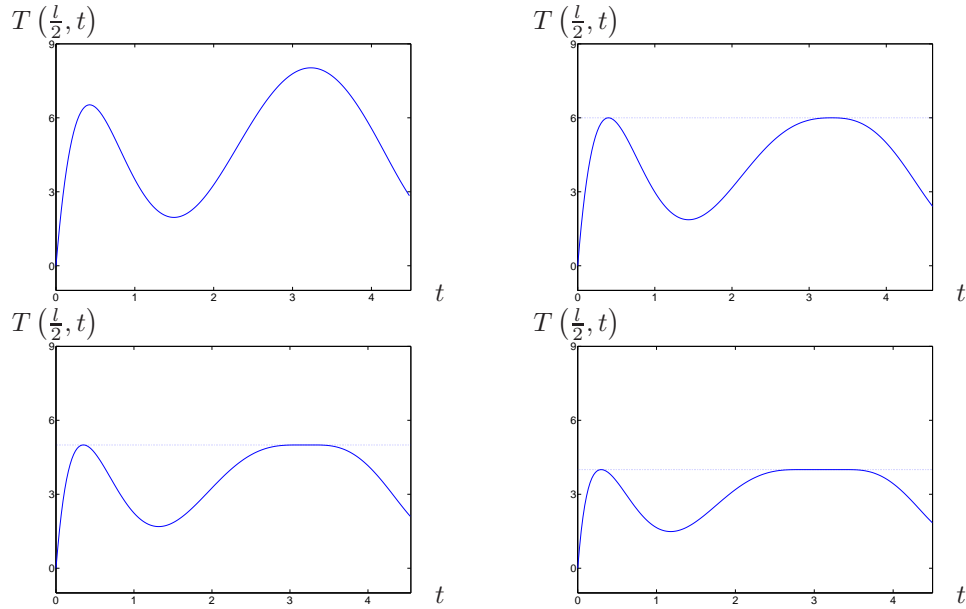


Figure 5.4: Cross-sections of the temperature profiles at  $x = \frac{l}{2}$  for Problem 1 featuring different values for  $T_{\max}$

Data:  $\lambda = 10^{-1}$ ,  $w_0 = -6$ ,  $\dot{w}_0 = -6$ ,  $u_{\max} = \infty$ ,  $T_{\max} = \infty, 6, 5, 4$ , and  $g(z) := z^2$ ; cf. Fig. (2.3) (right).

In Fig. (5.4) one can witness the influence of increasingly stricter heat constraints on the double-hump structure from (2.3) (right). While the second hump is flattened out into a boundary arc like seen before, the first one just yields a touch point, as predicted by the order of Problem 1. This will be of special interest, when compared to the same setting with Problem 2.

Please note that in order to prevent infeasibility, the control constraint had to be dropped. As the double-hump structure stems from the initial conditions  $w_0 = -6$  and  $\dot{w}_0 = -6$ , the car initially drives in the wrong direction and has to slow down and turn around first, creating the first peak. However with active control constraints one could face the situation, that even maximum allowed deceleration still leads to a violation of the heat constraint.

This “double hump” case can also exhibit some rather unpredictable results regarding computation time versus initial guesses for  $t_f$ .

## 5.2 Results for Problem 2

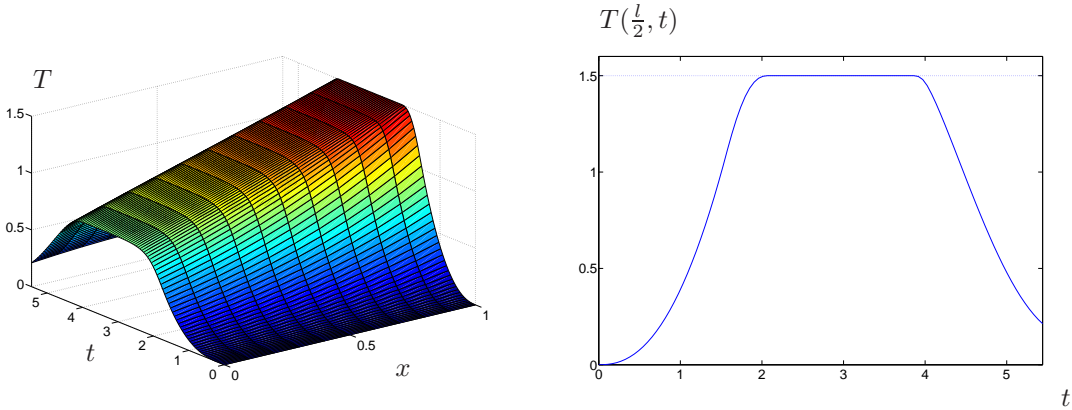


Figure 5.5: Temperature  $T(x,t)$  (left) and cross-section  $T(l,t)$  (right) for Problem 2 along a state- and control-constrained trajectory.  
 Data:  $\lambda = 10^{-1}$ ,  $u_{\max} = 1$ ,  $w_0 = -6$ ,  $\dot{w}_0 = 0$  and  $h(z) := z^2$ ; cf. Fig. (2.4) (left).

Just like Fig. (5.1) for Problem 1, Fig. (5.5) shows the "one hump" temperature profile and its cross-section (this time at  $x = l$ ) for Problem 2. Below in Fig. (5.6) are shown the according phase diagram and optimal control. While the first looks pretty similar to its Problem 1 counterpart, the latter is distinctively different: contrary to the optimal control for Problem 1 being nearly zero on the boundary arc, the beginning of the arc corresponds here with a cusp in  $u$  before it approaches 0.

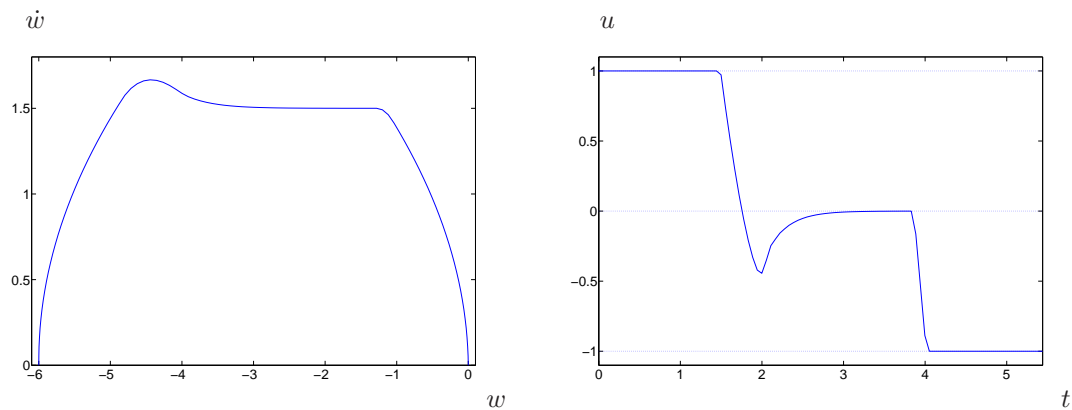


Figure 5.6: State-constrained control-constrained optimal trajectory for Problem 2 in the phase-plane (left) with associated optimal control  $u$  (right).  
 Data:  $\lambda = 10^{-1}$ ,  $w_0 = -6$ ,  $\dot{w}_0 = 0$ ,  $u_{\max} = 1$ ,  $T_{\max} = 1.5$ , and  $h(z) := z^2$ ; cf. Fig. (2.1) resp. (2.2) (left) and (5.2).

Additionally it is worth noting, that there is a considerable discrepancy in the profoundness of the impacts of the nonlinearity of  $u$  in  $[0, t_{\text{on}}]$ . Especially shortly before  $t_{\text{on}}$  the same effect with Problem 1 was way more pronounced. An explanation might be the location of the respective

temperature maximums at any given point of time. While in Problem 2 it was located at the edge at  $x = l$ , where there is immediate cooling through the Robin-type boundary conditions available, Problem 1 has its maximum seated right in the middle at  $x = \frac{l}{2}$ , the point that will be least effected by (symmetric) cooling induced via the boundaries and therefore requires greater foresight in driving.

As already hinted previously, another marked difference can be observed in the "double hump" case:

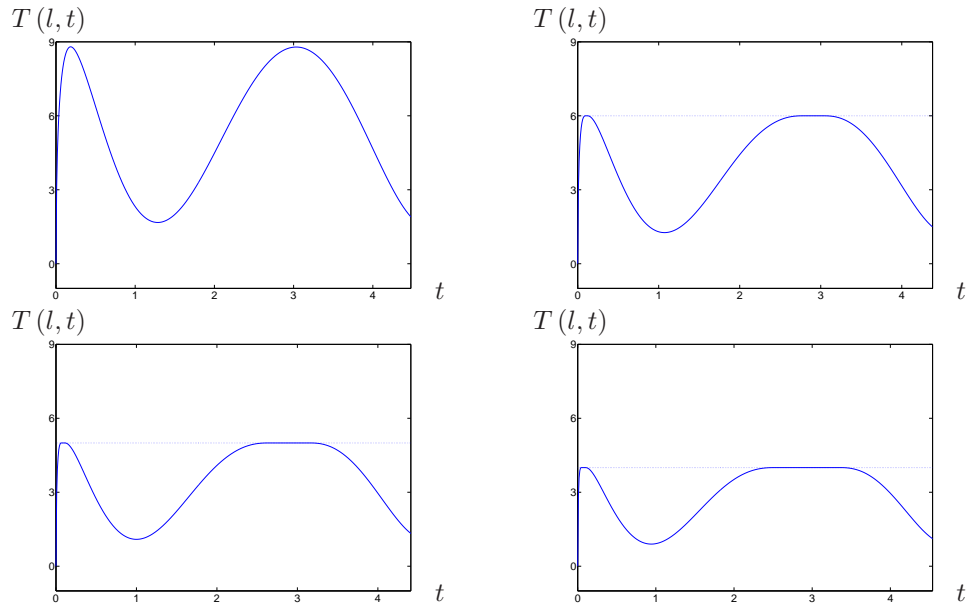


Figure 5.7: Cross-sections of the temperature profiles at  $x = l$  for Problem 2 featuring different values for  $T_{\max}$   
 Data:  $\lambda = 10^{-1}$ ,  $w_0 = -6$ ,  $\dot{w}_0 = -6$ ,  $u_{\max} = \infty$ ,  $T_{\max} = \infty, 6, 5, 4$ , and  $h(z) := z^2$ ; cf. Fig. (2.4) (right) and (5.4).

Fig. (5.7) shows the Problem 2 counterpart to Fig. (5.4). Just like before, the control constraint had to be dropped here. While with Problem 1 increasingly stricter heat constraints in the "double hump" case led to a touch point and a boundary arc (in accordance to Problem 1 having a second order state constraint), we now obtain two boundary arcs as Problem 2 features a first order state constraint. For better illustration the differing parts have been magnified below:

## 5.2 Results for Problem 2

---

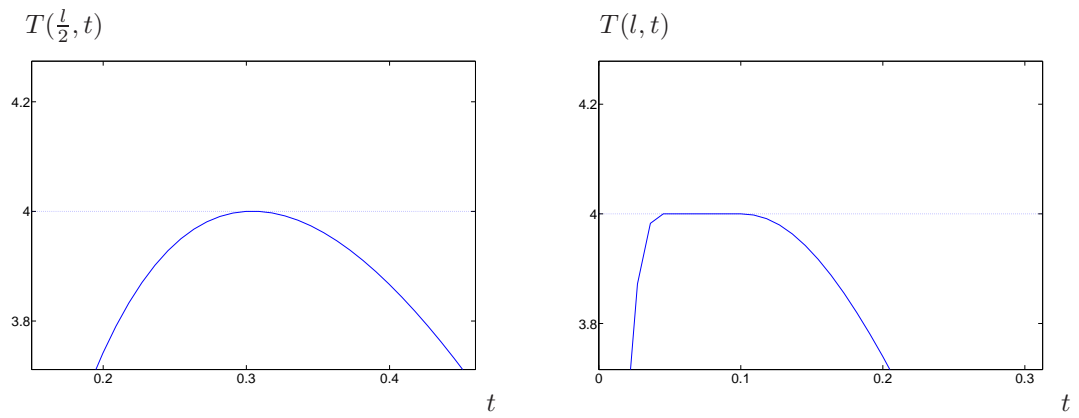


Figure 5.8: Closeups of the "first hump" of the bottom right pictures of Fig. (5.4) (left) resp. (5.7) (right).

With those we would like to end the examination of the primal variables. Before jumping to the dual ones and the according necessary conditions, first a small interlude considering the numerical approximation of the objective functional.

### 5.3 A side note on discretizations

As mentioned in the beginning of the chapter, the objective functional has been numerically approximated with a very basic quadrature formula, i.e. summing up (function value) times (step length). Despite its crudeness this offers some advantage in our special case (apart from being very easy to implement of course). Before any further elaboration let's first look at the following, very simple example:

$$\begin{aligned} \min J(y, u) &= \frac{1}{2} \int_0^1 y^2 + u^2 dx \\ \text{s.t. } -y_{xx} + y - 1 &= -u \quad \text{in } ]0, 1[ \\ y_x(0) = y_x(1) &= 0 \end{aligned} \quad (5.3)$$

Together with the adjoint equations and the gradient equation

$$\begin{aligned} -p_{xx} + p &= y \quad \text{in } ]0, 1[ \\ p_x(0) = p_x(1) &= 0 \\ u &= p \end{aligned}$$

one gets the optimality system, which has the unique solution  $\bar{u} = \bar{p} = \bar{y} \equiv \frac{1}{2}$ ,  $J(\bar{y}, \bar{u}) = \frac{1}{4}$ . Numerically integrating the objective functional with the trapezoidal resp. simpson rule however yields some unexpected results:

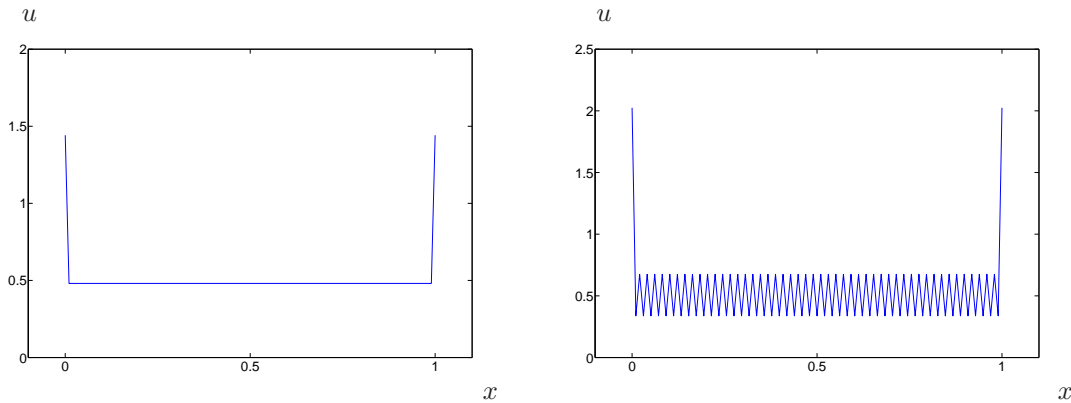


Figure 5.9: Optimal control  $u$  of (5.3) with trapezoidal (left) and simpson rule (right)

Increasing the number of discretization points additionally only makes the simpson result worse. The basic problem here is not a straightforward numerics error. Both the integral in the objective and the ODE are solved within acceptable error margins. But as AMPL tries to minimize  $\frac{1}{2} \int_0^1 y^2 + u^2 dx$  the different weighting factors employed in the trapezoidal rule (only 1st and last point) and simpson rule (every other point), as well as virtually every other higher quadrature formula, develop a life on their own: Due to the fact that some points are cheaper (lesser weighting factor) than others it is now possible to reduce the objective functional even “beyond optimality” by favouring those cheaper points. Optimal objective functional values obtained are:

### 5.3 A side note on discretizations

Quadrature formula	objective
weighted equally	0.249392
Trapezoidal	0.245243
Simpson	0.224972

Just to emphasize, this phenomenon has absolutely nothing to do with AMPL or IPOPT, those just optimize the NLP handed over to them, as they are supposed to do. Due to the inhomogeneous weighting said NLP really has a better optimum than the analytical problem it is meant to approximate.

To obtain an unobstructed view at this effect, the whole example was of course especially designed to exhibit this behaviour very blatantly.  $u$  can only exploit the weighting nearly fully by jumping around, because the associated state  $y$  is extremely placid. As it also appears in the objective it would (together with possible other effects) normally at least dull the controls excentric behaviour. However this effect will in any case be an additional source of error and introduce at least some noise into the solution.

The AMPL/IPOPT program `discr.txt` used for those little experiments and the accompanying Matlab plot program `discr.m` can be found in the folder `Programs/discretisation test`.

For the rocketcar a similar effect can be observed if one chooses the simpson rule for the objective functional:

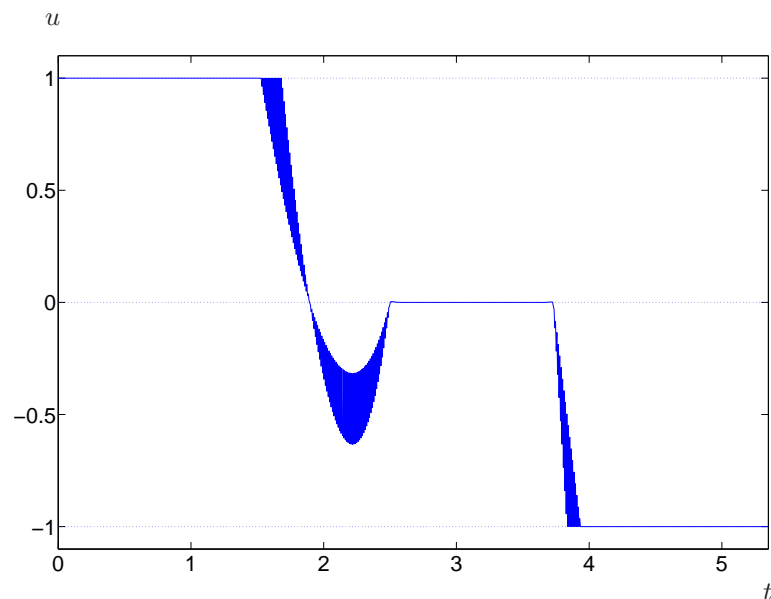


Figure 5.10: Optimal control  $u$  for Problem 1 with simpson rule as quadrature formula  
Data:  $\lambda = 10^{-1}$ ,  $u_{\max} = 1$ ,  $w_0 = -6$ ,  $\dot{w}_0 = 0$  and  $g(z) := z^2$ ; cf. Fig. (5.2) (right).

The zigzagging control "improves" the overall objective from 5.52017 to 5.51901. As in the case of the rocketcar the control constraints are active in the beginning and end, the effect of the trapezoidal rule in the same scenario is negligible.

## 5.4 Approximate verification of optimality conditions

After figuring out some of the properties of the solution itself it is now time to have a look at the adjoint variables. Those can be obtained the same way as normal ones. Their names are given by the names of the respective constraints in AMPL. However it is important to note, that the program yields adjoints with the opposite sign of our notation. With those it is now possible to check the optimality conditions at least a posteriori as announced before. To cover the various versions however, the AMPL/IPOPT program used so far (rocketcar\_ode\_pde.txt, can be found in Programs/Direct approach) is not sufficient. To obtain for example the auxiliary variable p3, one has to rewrite the above program utilising the analytical solution formula (2.3) for  $T$ . This has been done in rocketcar\_ode.txt, also to be found in Programs/Direct approach. Please note that in order to use the solution formula, one has to provide the parameters  $k_n$  from (2.2). Those are stored in the files kn10.dat, kn30.dat and kn60.dat (containing the first 10, 30 or 60  $k_n$  as the names suggest). With them it is now possible to solve the rocketcar problem with an even more compact program. However the performance of rocketcar\_ode.txt is considerably inferior to the original rocketcar\_ode\_pde.txt, see tables (5.1) and (5.2), which is, given the fact that it uses quite some prior knowledge, somewhat counterintuitive. Unfortunately the evaluation of the solution formula proves to be more intricate than the solution of the discretized heat equation it replaces.

$n_1$	$n_2$	$t_{\text{on}}$	$t_{\text{off}}$	$t_f$	CPU secs
100	10	2.410	3.749	5.35640	0.29
100	20	2.518	3.803	5.35688	0.80
1000	10	2.458	3.781	5.35616	7.76
1000	100	2.453	3.782	5.35683	675.86
3000	200	2.453	3.782	5.35696	14488.65

Table 5.1: Performance and accuracy of rocketcar\_ode\_pde.txt with various discretizations for Problem 1

Data:  $\lambda = 10^{-1}$ ,  $u_{\text{max}} = 1$ ,  $w_0 = -6$ ,  $\dot{w}_0 = 0$  and  $g(z) := z^2$ ; Initial values given to rocketcar\_ode\_pde.txt were identical with those used in table (5.2)

$n_1$	$t_{\text{on}}$	$t_{\text{off}}$	$t_f$	CPU secs
100	2.464	3.750	5.35706	23.95
1000	2.453	3.777	5.35689	75118.20
3000	—	—	—	computation not possible

Table 5.2: Performance and accuracy of rocketcar\_ode.txt with various discretizations for Problem 1

Data:  $\lambda = 10^{-1}$ ,  $u_{\text{max}} = 1$ ,  $w_0 = -6$ ,  $\dot{w}_0 = 0$  and  $g(z) := z^2$ ; Initial values given to rocketcar\_ode.txt were identical with those used in table (5.1)

For Problem 2 we face an additional difficulty here:

While the analytical handling of the  $\beta_n$  of (3.17) was much easier compared to the  $\alpha_n$  of (3.15), the situation is reversed when it comes to numerics:

The term  $\int_0^t h(\dot{w}(s)) e^{-k_n^2(t-s)} ds$  is very difficult to tackle for standard quadrature schemes.

$e^{-k_n^2(t-s)}$  is always 1 at  $s = t$  and drops very sharply towards 0 as  $(t - s)$  gets bigger, especially for higher  $k_n$  (which behave roughly like  $(n - 1)\pi$ ). For Problem 1 this was not such a big deal. As this effect only gets problematic for the bigger  $k_n$ , the special structure of the  $\alpha_n$  in (3.15) compensated most of it. Now however the whole convergence of (3.17) is hinged on the exponential term alone.

## 5.4 Approximate verification of optimality conditions

The most obvious remedy here of course would be the application of adaptive methods. Unfortunately (3.17) depends on input from the rest of the NLP and we are therefore bound to a fixed grid. Even more unfortunately the refining of said grid is prohibitively expensive.

A relatively simple and easy to implement solution here is to shift the problematic term a bit. Integration by parts yields

$$\int_0^t h(\dot{w}(s)) e^{-k_n^2(t-s)} ds = \frac{h(\dot{w}(t))}{k_n^2} - \frac{h(\dot{w}_0)}{k_n^2} e^{-k_n^2 t} - \frac{1}{k_n^2} \int_0^t h'(\dot{w}(s)) \cdot u(s) e^{-k_n^2(t-s)} ds \quad (5.4)$$

While the integral in (5.4) still causes a significant numerical error for bigger  $k_n$ , its pre-factor  $\frac{1}{k_n^2}$  is enough to make it manageable. Yet still (5.4) requires a finer time discretization compared to (3.15) to yield reliable results.

Nonetheless all previously obtained necessary conditions could be verified numerically. In the following we will have a look at the more intriguing of them. Lets start with the projection formula (4.7h) for the optimal control  $u$ : as figure (5.11) shows, the control is indeed the projection of the adjoint state  $p_2$  times  $(\frac{-1}{\lambda})$  onto the admissible set of controls (here  $[-1, 1]$ ).

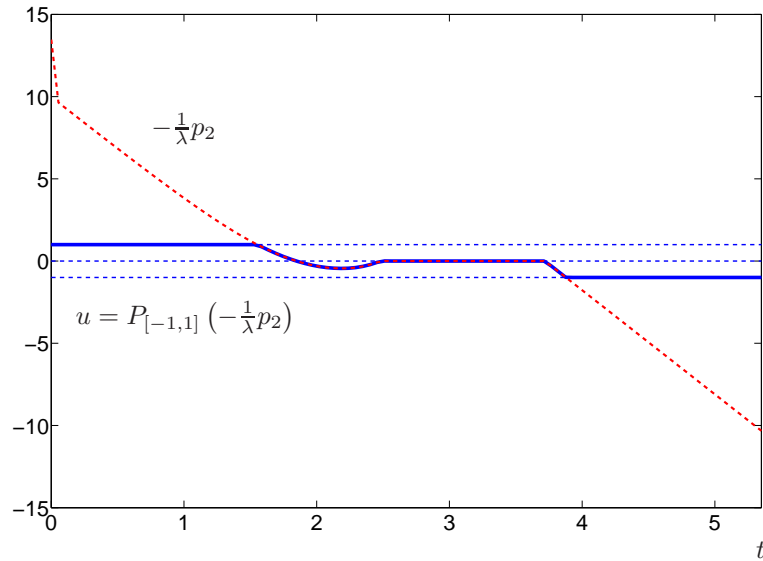


Figure 5.11: Optimality check showing the perfect coincidence with the projection formula (4.7h). Data:  $\lambda = 10^{-1}$ ,  $u_{\max} = 1$ ,  $w_0 = -6$ ,  $\dot{w}_0 = 0$  and  $g(z) := z^2$ ; cf. Fig. (5.2) (right).

Equation (4.7a), no doubt the most intricate of the whole set (4.7) is also fulfilled nearly perfectly. To discern the tiny differences in figure (5.12) left and right one has to open the files p2dot.fig and p2dot\_recon.fig in Text/Figures with matlab and use the data cursor.

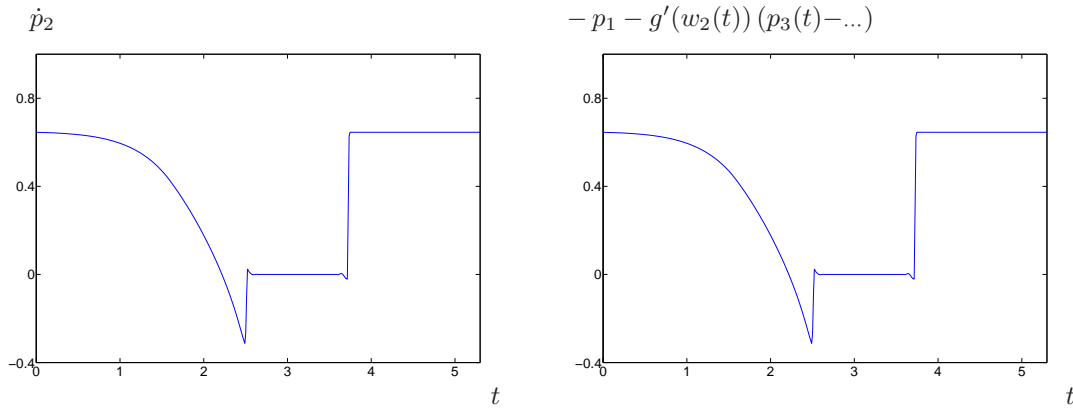


Figure 5.12: Illustration of the left and right hand side of equation (4.7a).  
 Data:  $\lambda = 10^{-1}$ ,  $u_{\max} = 1$ ,  $w_0 = -6$ ,  $\dot{w}_0 = 0$  and  $g(z) := z^2$ .

Finally there remains the adjoint  $p_3$  and its associated measure  $\mu$ .  $p_3$  can in some sense be seen as the most important adjoint of the whole lot, as its behaviour directly stems from the temperature constraint. As such it also very nicely reflects the influence of the latter even before  $T$  resp.  $w_3$  in the ODE formulation hits  $T_{\max}$ : figure (5.13) (depicting again the “single-hump” case with only a boundary arc) shows  $p_3 > 0$  for  $t < t_{\text{on}}$ ,  $p_3$  linear for  $t_{\text{on}} < t < t_{\text{off}}$  and  $p_3 = 0$  for  $t > t_{\text{off}}$ , just as predicted. So the only part, where the constraint exerts absolutely no influence is just the last stretch from  $t_{\text{off}}$  to  $t_f$ , where the car has to slow down anyway to fulfill the ODE constraints at  $t_f$  and overheating is therefore no concern anymore.

$p_3$  also exhibits the expected jump behaviour at  $t_{\text{on}}$  and  $t_{\text{off}}$ , mirrored in the respective peaks of  $\mu$ . This effect is even more evident in figure (5.14), the “double-hump” case counterpart to figure (5.13). The touch point appearing in this scenario causes a massive jump in  $p_3$ . Please also note that the difference in scale between figure (5.13) (left) and figure (5.14) (left) is roughly factor 10. This rise in magnitude is due to the dominant effect the temperature constraint possesses right before the touch point. As the starting velocity (and as a consequence also the influx of heat) in this case was rather high it is imperative to decelerate at any cost to avoid violating said constraint (just to remember:  $u_{\max}$  had to be set to  $\infty$  to create this scenario).

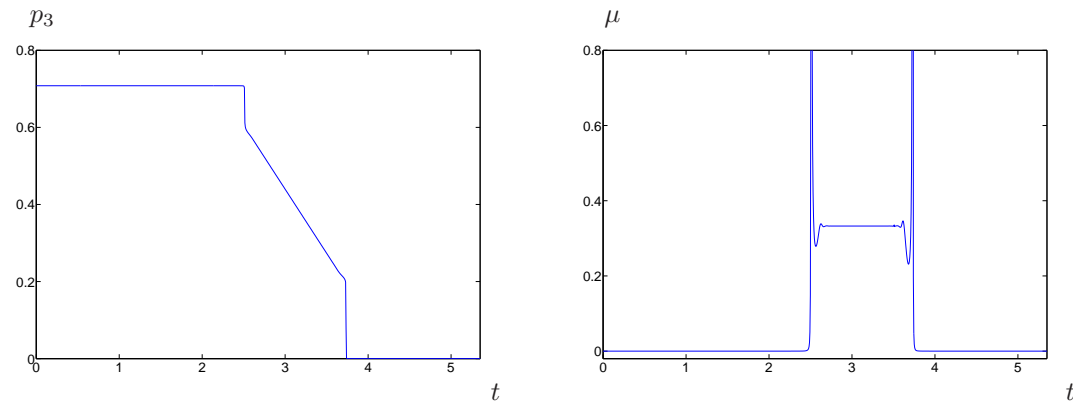


Figure 5.13: Adjoint state  $p_3$  and associated measure  $\mu$  for Problem 1  
 Data:  $\lambda = 10^{-1}$ ,  $u_{\max} = 1$ ,  $T_{\max} = 1.5$ ,  $w_0 = -6$ ,  $\dot{w}_0 = 0$  and  $g(z) := z^2$

## 5.4 Approximate verification of optimality conditions

---

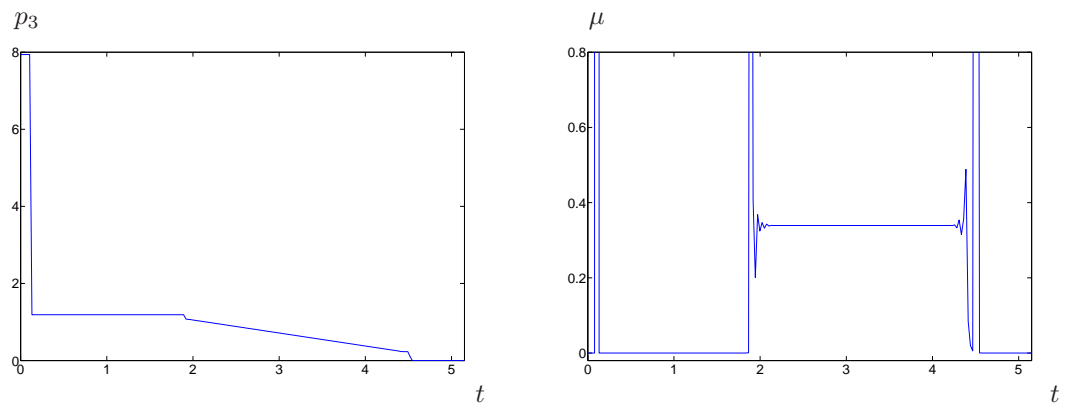


Figure 5.14: Adjoint state  $p_3$  and associated measure  $\mu$  for Problem 1 (“double-hump” case)  
 Data:  $\lambda = 10^{-1}$ ,  $u_{\max} = \infty$ ,  $T_{\max} = 3$ ,  $w_0 = -6$ ,  $\dot{w}_0 = -6$  and  $g(z) := z^2$

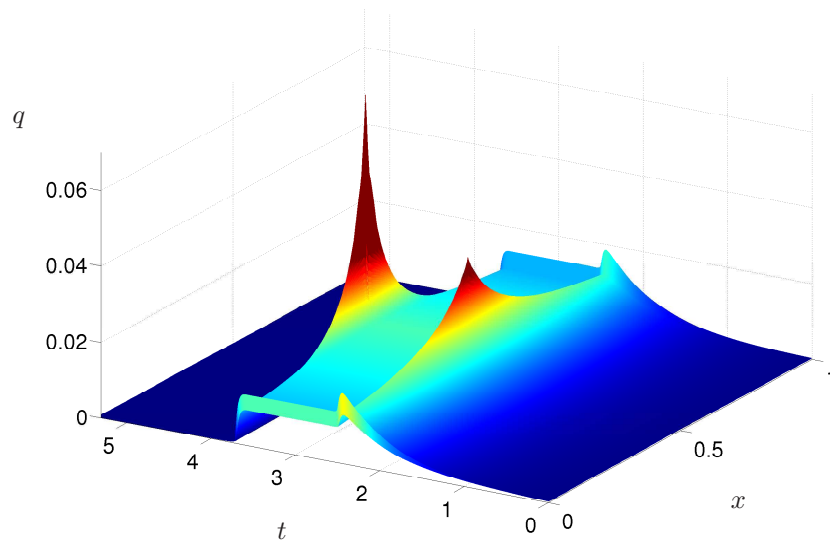


Figure 5.15: Adjoint state  $q$  of the temperature  $T$ .  
 Data:  $\lambda = 10^{-1}$ ,  $u_{\max} = 1$ ,  $w_0 = -6$ ,  $\dot{w}_0 = 0$  and  $g(z) := z^2$ ; cf. Fig. (5.1).

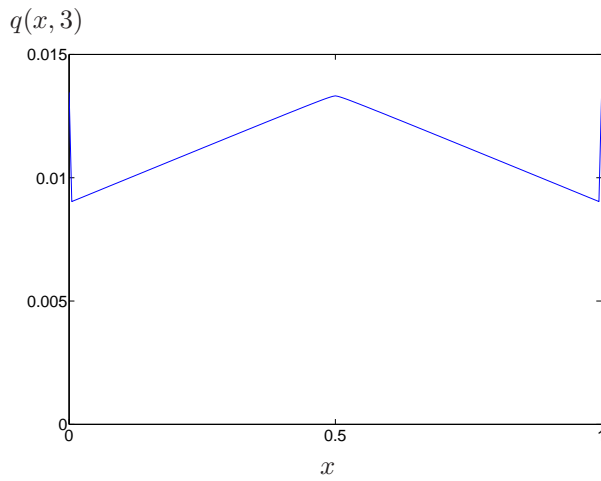


Figure 5.16: Cross section of  $q$  at  $t = 3$ .  
 Data:  $\lambda = 10^{-1}$ ,  $u_{\max} = 1$ ,  $w_0 = -6$ ,  $\dot{w}_0 = 0$  and  $g(z) := z^2$ ; cf. Fig. (5.1) and Fig. (5.15).

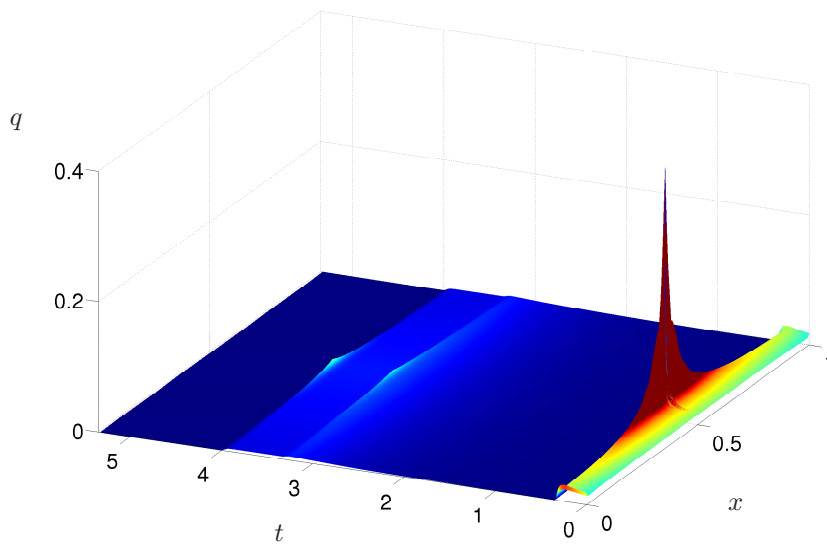


Figure 5.17: Adjoint state  $q$  of the temperature  $T$ , “double hump“ case.  
 Data:  $\lambda = 10^{-1}$ ,  $u_{\max} = \infty$ ,  $w_0 = -6$ ,  $\dot{w}_0 = -6$  and  $g(z) := z^2$ ; cf. Fig. (5.4), bottom right.

## 5.4 Approximate verification of optimality conditions

Figure (5.15) depicts the adjoint state  $q$  of the temperature  $T$ . Like its ODE formulation counterpart  $p_3$  (cf. figure (5.13), left),  $q$  vanishes after  $t_{\text{off}}$ , i.e. when the temperature constraint loses its influence. In contrast the latter's growing influence before  $t_{\text{on}}$  can be clearly observed.

But no doubt the most distinctive features of figure (5.15) are its peaks at  $(\frac{1}{2}, t_{\text{on}})$  and  $(\frac{1}{2}, t_{\text{off}})$ , reflecting the structure of the measure  $\bar{\mu}$  in (4.4c). While those are the result of  $\bar{\mu}$  being a measure in space and time at  $(\frac{1}{2}, t_{\text{on}})$  and  $(\frac{1}{2}, t_{\text{off}})$ ,  $\bar{\mu}$  is only a measure in space in  $(\frac{1}{2}, ]t_{\text{on}}, t_{\text{off}}[)$ . As this section is rather obscured in figure (5.15), figure (5.16) provides a cross-section at  $t = 3 \in ]t_{\text{on}}, t_{\text{off}}[$  showing the expected sharp bend at  $x = \frac{1}{2}$ .

The adjoint  $q$  for the "double hump" case can be seen in figure (5.17) again demonstrating the dominant influence of the touch point, just as figure (5.14) did for  $p_3$ .

For Problem 2 the "single hump" case leads to according peaks at  $x = l$  (figure (5.18) below). Here however the observations are a bit blurred due to the numerical artifacts at  $x = 0$  and  $x = l$ , which can also be seen in the previous figures.

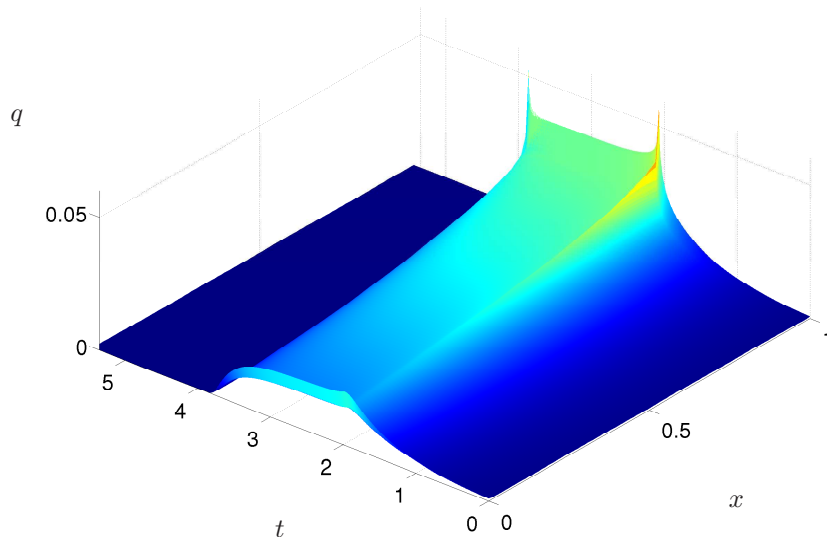


Figure 5.18: Adjoint state  $q$  of the temperature  $T$  for Problem 2.  
Data:  $\lambda = 10^{-1}$ ,  $u_{\text{max}} = 1$ ,  $w_0 = -6$ ,  $\dot{w}_0 = 0$  and  $g(z) := z^2$ ; cf. Fig. (5.1).

Before going any further however, some preliminary elaboration might be prudent: the adjoint  $q$  (among others) delivered by AMPL/IPOPT strongly depends on the discretization. To be more precise it depends on the ratio of discretization in time versus discretization in space. A prime example can be found in [29], page 68. Abbildung 3.4 there shows, except for A. Rund's use of the transformed time  $\tau$ , basically the same as figure (5.15) here. However the values of  $q$  seem to differ by roughly a magnitude of factor 10. The reason for this apparent discrepancy is solely the different ratio of time versus space discretization, which is  $3001 \times 21$  in A. Rund's thesis while figure (5.15) features  $3001 \times 201$ . All other data used for the two figures is absolutely identical. To understand this on the first view rather surprising and erratic behaviour one has to contemplate how for example doubling of the spatial discretization (and leaving time fixed) alters the NLP solved by AMPL/IPOPT: while a change in time discretization would affect both the

ODE and PDE components of the system, the PDE alone benefits from a higher discretization in space. To follow the above example, twice as many equations of the system are now devoted to the PDE, while the rest sports the same amount as before, making the PDE now a lot more predominant. This very effect leads to an according diminishing of the PDE's adjoint state  $q$ . This rather annoying dependency of the adjoints on the discretization had to be taken care of in order to verify equations (4.14b, d), which contain both  $p_2$  and  $q$  resp.  $p_3$  and  $q$ . With that in mind equations (4.14) (a-d) now can be understood as

$$\begin{aligned}
 p_1(t) &\hat{=} -\nu_2, \\
 p_2(t) &\hat{=} \nu_1 + \nu_2 t + \int_t^{t_f} g' \left( \dot{w}_0 + \int_0^s u(\bar{s}) d\bar{s} \right) \cdot \left( \int_0^l \gamma \hat{q}(x, s) dx \right) ds, \\
 p_2(t_f) &\hat{=} \nu_1 + \nu_2 t_f, \\
 p_3(t) - \int_t^{t_f} \sum_{n=1}^{\infty} k_n^2 \alpha_n e^{-k_n^2 (s-t)} p_3(s) ds &\hat{=} \int_0^l \gamma \hat{q}(x, t) dx,
 \end{aligned}$$

with  $\hat{q}$  being the adjoint delivered by the program `rocketcar_ode_pde.txt` and  $q = \gamma \hat{q}$  being the "real" adjoint.

Identification and elimination of the unwanted proportionality factor, dubbed  $\gamma$ , was done in program `rocketcar_adjoints.m`, which can be found in Programs/Direct approach. This Matlab program also contains the subsequent calculations necessary for this section.

As a last remark here, the higher spatial discretization does absolutely not pay off in terms of increased accuracy, as the heat equation is really very placid with respect to space, see for example table (5.1) or again [29], page 68, Tabelle 3.2. The main benefit one gets in exchange for the steep increase in computation time is merely a nicer picture.

With that nuisance taken care of we are now able to tackle equations (4.14), matching the adjoints of the different variants. This is done in the second half of program `rocketcar_adjoints.m`<sup>3</sup>.

Figure (5.19) shows the left and right hand side of equation (4.14b) linking the adjoints  $p_2$  (appearing in the ODE as well as in the ODE-PDE variant),  $\nu_{1,2}$  (appearing in the PDE variant) and  $q$  (of the PDE and ODE-PDE variant). For in depths scrutiny one may again use matlab's data cursor on the files `p2.fig` and `p2_recon.fig`, also to be found in Text/Figures.

---

<sup>3</sup>This program checks the relations between the adjoints of the different rocketcar versions. Prior to running it, please be sure to run the corresponding AMPL programs `rocketcar_ode.txt`, `rocketcar_pde.txt` and `rocketcar_ode_pde.txt` with decent and matching discretizations to create the necessary data input!

## 5.4 Approximate verification of optimality conditions

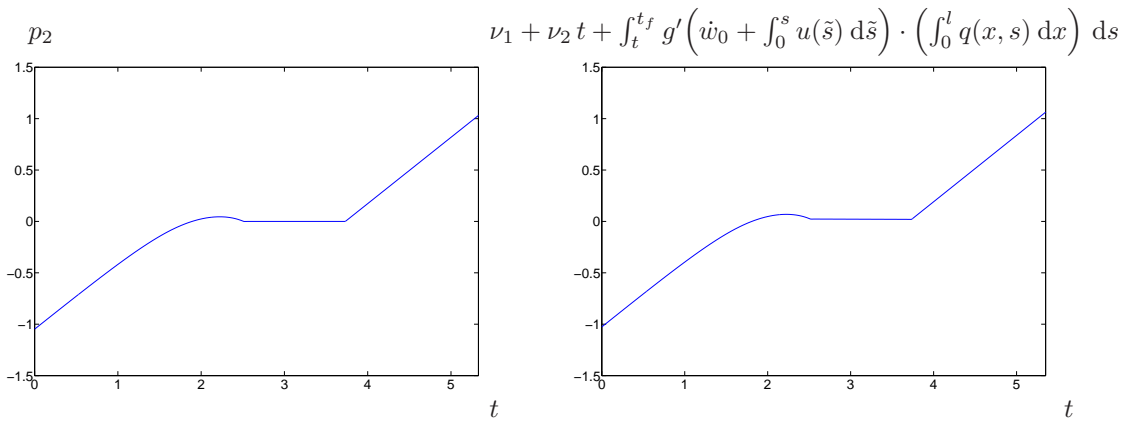


Figure 5.19: Illustration of the left and right hand side of equation (4.14b).  
 Data:  $\lambda = 10^{-1}$ ,  $u_{\max} = 1$ ,  $w_0 = -6$ ,  $\dot{w}_0 = 0$  and  $g(z) := z^2$ .

Both sides of equation (4.14d) are depicted in figure (5.20) below. The according files are named intq\_recon.fig and intq.fig.

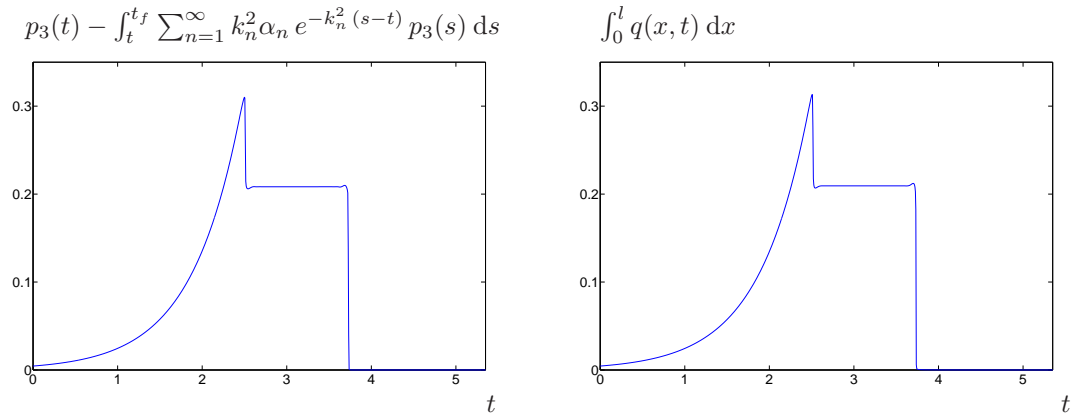


Figure 5.20: Illustration of the left and right hand side of equation (4.14d).  
 Data:  $\lambda = 10^{-1}$ ,  $u_{\max} = 1$ ,  $w_0 = -6$ ,  $\dot{w}_0 = 0$  and  $g(z) := z^2$ .

And last but not least the Hamiltonian fulfills  $H(t_f^*) = 0$  and is continuous at  $t_{\text{on/off/touch}}$ :

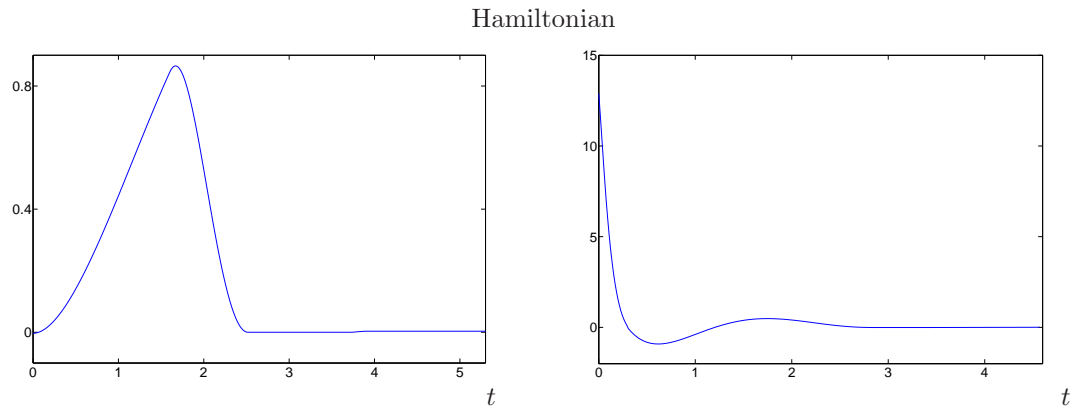


Figure 5.21: Hamiltonian for Problem 1 ("single-hump" case left, "double-hump" case right)  
 Data:  $w_0 = -6$ ,  $\dot{w}_0 = 0$  (left), resp.  $\dot{w}_0 = -6$  (right)

## 5.5 Solution via an indirect method

Solving the rocket car problem with a direct method went remarkably smooth. The mathematically more intriguing way however is an indirect (FOTD) approach, even despite AMPLs convenient feature of delivering the adjoints. As we will soon see, this will be considerably more frustrating and time consuming, both in terms of computing and programming time. First of all we now have to depart from AMPL-IPOPT for this section and switch to Matlab for computation due to the change in nature of the underlying problem. With FDTO we had to implement an NLP of only the primal variables. FOTD now "only" demands the solving of a nonlinear equation system of primal and dual variables, being (of course) about twice the size of the NLPs system of constraints and a far cry more complicated, no matter the formulation one chooses ( $\implies$  Appendix A).

Just as a remark: theoretically it is possible to solve a system of nonlinear equations with AMPL-IPOPT. A straightforward method would for example be to introduce residuum terms into each equation and define the objective functional as the sum of their squares. However this makeshift approach is anything but efficient and really only advisable if one has no other software options. In the course of this thesis, a brief attempt was made, but quickly abandoned and will not be included here in any detail.

### 5.5.1 Primal dual active set strategy

The first, yet unfortunately abortive attempt was made with the well known primal dual active set strategy (PDAS) [3]. PDAS is a method originally meant for control constrained problems, which can (with some difficulties) be adapted for state constraints, see for example [5]<sup>4</sup>.

Of the rocket car's control and state constraint the latter is the by far more demanding one, so it will be the "target" of PDAS, while the relatively harmless control constraint will be left to the underlying nonlinear solver (in this case matlab's `fsolve` routine). The basic concept now works as follows<sup>5</sup>:

*PDAS* (basic concept):

1. Initial guess  $(T^0, q^0, w_1^0, p_1^0, \dots)$
2. i-loop:
  - a) Determine current active set  $\mathcal{A}^i$  via  $(T^i, q^i, w_1^i, p_1^i, \dots)$
  - b) Stop if  $\mathcal{A}^i \equiv \mathcal{A}^{i-1}$
  - c) Solve the optimality system with  $T^i \equiv T_{\max}$  on  $\mathcal{A}^i$  and  $\mu \equiv 0$  on the inactive set  $(\mathcal{A}^i)^C$
  - d)  $i = i + 1$

As mentioned above, the optimality system in (2c) will be solved with matlab's `fsolve` functionality. This poses a bit of a problem/inconvenience: `fsolve` is called via `fsolve(@function, x0)`, where `@function` is the (external) definition of the nonlinear system to be solved and `x0` is a vector containing the initial guess for its variables. All variables in the optimality system now have to be written in the form of one huge vector, which is rather cumbersome, especially for  $T$  and  $q$ , as they are 2D. The main program `indirect.m` can be found in `Programs/Indirect_approach`. The nonlinear system itself is contained in the function `f.m`. There the incoming vector of data was as a first step split into its original components. While this is anything but optimal from a programming point of view (it introduces a lot of new, redundant equations), it was the only

---

<sup>4</sup>While [3] and [5] can more or less be seen as primary sources on the matter, the author mainly utilized [2] for its comprehensive yet easily accessible overview of the subject.

<sup>5</sup>Just to avoid confusion, the problem formulation used for the PDAS approach is the ODE-PDE Version, see Appendix A3.

## 5.5 Solution via an indirect method

---

way to maintain some degree of readability.

fsolve contains 3 different algorithms: Trust-Region-Reflective, Trust-Region-Dogleg and Levenberg-Marquardt. As the nonlinear equation system resulting from the optimality system is non-square, the latter algorithm was utilized here. Being a blending of a Gauss-Newton method and gradient decent the Levenberg-Marquardt algorithm (aka damped least squares method) is a lot more robust than pure Gauss-Newton with the downside of being somewhat slower.

Unfortunately the results were not very encouraging. Those familiar with PDAS might first suspect the notorious chattering effect (simply put one gets locked in an eternal loop by constantly jumping back and forth between the same two active sets, a rather common problem with PDAS). Here however the trouble starts much earlier: even after lengthy computations fsolve is not able to solve the optimality system, so PDAS itself as the outer loop doesn't even come properly into play. Luckily it is not necessary to fully solve the optimality system in step 2c). It can even be advantageous to just do a few iterations in 2c), determine the new active set and start anew. The idea is to invest less time into solving the optimality system to the last  $\varepsilon$  so to speak, but instead do more outer active set steps <sup>6</sup>.

So a new try was implemented, were fsolve was limited to a fixed and relatively small number of iterations and would yield whatever it got after those were done. The hope was, that even if the optimality system wasn't solved, the current iteration would be close enough to warrant a useful active set update for the next outer iteration.

But that hope too was dashed, no matter how many iterations fsolve undertook, the results were not even remotely useable. Now the task at hand was to somehow alleviate fsolve's chore. The first thing, that comes into mind, is obviously to provide a better starting guess for the variables. In all the previous tries  $\mathbf{x0}$  for the first call of fsolve has simply been set to  $\mathbf{0}$ . To obtain a better start, the system was broken down and solved in several steps, each increasing the complexity. Therefore the auxiliary functions f1.m and f2.m were introduced: f1 just contains the ODE part of the problem <sup>7</sup>, f2 additionally incorporates the temperature  $T$ , albeit without its constraint. Results from the lesser versions yielded the initial guesses for the next higher ones, where the missing pieces were still initialized with zeros. After f2 is successfully completed one now has a viable solution for the rocket car without state constraints which serves as a start for the full version ( $T$ 's adjoint  $q$  is added manually after the completion of f2, as it is at that time  $\equiv 0$ , due to the missing constraint on  $T$ ).

Yet even that was not enough. While f1/2 were solved in a breath, the gap in complexity between f2 and f was still too big, which is not to surprising considering the responsible equations (4.4) (b-f), with (4.4c) featuring the measure  $\bar{\mu}$  being the most likely candidate for the culprit.

To bridge this final gap the choice fell on an approach with homotopies. After obtaining the unconstrained  $T$  from f2 one determines its maximum, denoted with  $T_m$  and solves a series of problems with increasingly strict temperature constraint  $T_{\max}^i$  defined by  $T_m$ , the original constraint  $T_{\max}$  and a set number  $h$  of homotopy steps:

$$T_{\max}^i = T_m - i/h \cdot (T_m - T_{\max}), \quad i \in [1..h]$$

Thereby one tightens the temperature constraint until one finally reaches the desired  $T_{\max}$ , each iteration providing the initial guess for its successor.

Even this attempt ended in failure <sup>8</sup>. As even with a considerable number of homotopy steps and therefore a very small difference from the state unconstrained to the first state constrained version this step proved to be an insurmountable obstacle, the only open route left here was to utilize the best possible initial guess, i.e. the solution (plus its adjoints) from the direct method. The according software indirect.m (main program), f1.m, f2.m and f.m (external functions) are located in Programs/Indirect\_approach. Taking about one night of computation time, this

---

<sup>6</sup>For more detail see [2] p. 69, section PDAS als halbglatte Newton-Verfahren (PDAS as semismooth newton method).

<sup>7</sup>Basically the original "rocket car on a rail track problem" without any heating or state constraint, as done by Bushaw in the 1950s.

<sup>8</sup>Further brief attempts at modifying the current version were made, for example augmenting the standard PDAS with a Moreau-Yosida-regularisation among others, but all met a similar fate.

already nearly perfect initial guess finally led to an acceptable result.

Obviously this was nevertheless anything but satisfying. Having to more or less already exactly know the solution, to finally achieve it is itself rather unrealistic if not downright cheesy. It is also defying the whole point of PDAS, as except for very minor fluctuations (no more than a hand full of grid points, even on relatively high discretizations) the final active set is already defined by the initial guess.

It was clear that something radically different had to be tried.

### 5.5.2 Switching point optimization

As evident now the “only“ problem was to help fsolve cope with the difficult structure of equation (4.4c) (i.e. the temperature’s adjoint  $q$ ) with its measure valued right hand side. The approach for this new attempt now is twofold:

- a) Utilizing the problem’s special properties and any beforehand knowledge one can obtain. While this may sound awfully akin to the previous attempt of solving indirectly with the direct solution as initial guess, it means something entirely different here, namely simply using all the beforehand knowledge about the solutions structure already derived in chapters 2 to 4.
- b) Breaking down the equation system into three different phases, thereby of course not really avoiding but hopefully alleviating the problem with the jumps in  $q$ . Additionally this also allows a more profound exploitation of point a).

A further necessary change is to depart from the ODE-PDE formulation and instead switch to the ODE version. While ODE-PDE was no doubt the version most easy on the eye and also relatively easy to program (solving however was an entirely different matter as seen before), the ODE version offers some distinct advantages here. For example the temperature  $T$  and its adjoint  $q$ , which are both 2D are replaced with  $w_3 \hat{=} T(\frac{l}{2}, \cdot)$  and its adjoint  $p_3$ , which are both just 1D. Albeit this is a tremendous reduction in the number of variables in the system, it of course comes with an equally big catch: one now has to deal with the integro state constraint (4.6). As shown before it is numerically more efficient to deal with the PDE directly than to use the solution formula (2.3) which is also present in (4.6a). Essentially one gets less equations which will be a lot more time consuming to evaluate, and of course the new adjoint  $p_3$  will feature jumps just like the old adjoint  $q$  it substitutes.

After we split the whole system into three different sections<sup>9</sup>, namely

- a)  $0 - t_{on}$ : state constraint exerts indirect influence,
- b)  $t_{on} - t_{off}$ : state constraint is active,
- c)  $t_{off} - t_f$ : state constraint is inactive,

one can see that  $p_3$ ’s equations (4.7c) and (4.7i) however fall apart quite nicely. They can be completely replaced by assuming the right structure for  $p_3$  as already deduced for this case in section 4.2.(in the following the 3 subscripts a,b and c shall denote the variable in the respective section, see above):

$$\begin{aligned} p_{3a}(t) &= \text{const}, \\ p_{3b}(t) &\text{ is determined as before,} \\ p_{3c}(t) &\equiv 0. \end{aligned}$$

With the aim in mind, to make the final nonlinear equation system as easy as possible for the solver, one can implement this as follows:

---

<sup>9</sup>Obviously one has to deduce/guess the switching structure as before in order to do this.

## 5.5 Solution via an indirect method

---

- Introduce  $p_{3a}(t)$  simply as one skalar variable (instead of a vector, like one would normally do for a time dependent variable).
- $p_{3b}(t)$  remains a vector in the program.
- $p_{3c}(t)$  is omitted and set to 0 in all other formulas it appeared in.

As  $p_{3a-c}$  are now, at least for the solver, distinct and unrelated entities, one can completely omit the measure structure of  $\mu$  by simply not demanding continuity between them.

While it is obviously necessary to evaluate the solution formula (2.3) to observe the heat constraint, it is not necessary to explicitly include  $w_3$  as a variable in the program (it is of course computed a posteriori).

Additionally said unwieldy temperature formula is fortunately only relevant in section b and can be completely omitted in a and c.

$p_1$ 's equation is simply  $\dot{p}_1 = 0$ , so the self-evident idea is to skip the equation and introduce  $p_1$  as a skalar variable, just like  $p_{3a}$  before.

Another variable that does not have to be explicitly included is the control  $u$ , as it is determined via  $p_2$  and the projection formula. With this in mind one should also take a closer look at the Hamiltonian:

$$\begin{aligned} H(\mathbf{w}, \mathbf{p}, u) &= 1 + \frac{1}{2} \lambda u^2 + p_1 w_2 + p_2 u \\ &= 1 + \frac{1}{2} \lambda \left( P_{[-u_{\max}, u_{\max}]} \left( -\frac{p_2}{\lambda} \right) \right)^2 + p_1 w_2 + p_2 P_{[-u_{\max}, u_{\max}]} \left( -\frac{p_2}{\lambda} \right) \end{aligned}$$

Here  $\lambda$  and  $p_1$  are simple constants and  $w_2$  is continuous, because  $u$  is constrained (jumps in the velocity would be a violation of physical laws anyway). So under the assumption, that  $t_{\text{on/off}}$  are not in an area, where the control constraint is active, the required continuity of the Hamiltonian at  $t_{\text{on/off}}$  just translates into continuity of  $p_2$ .

The new optimality system one obtains contains significantly less, albeit more elaborate equations and most noticeably no measures. Programming of course gets somewhat more confusing and cumbersome, mostly because of the Volterra terms (which on top have to be split up, as for example  $w_{2a}$  and  $w_{2b}$  are now different entities) as well as the necessity of a distinct time transformation for each of the 3 sections with  $t_{\text{on}}$  and  $t_{\text{off}}$  being spawned as new optimization variables.

Nevertheless there is some additional fringe benefit in this: as  $t_{\text{on}}$  and  $t_{\text{off}}$  are now variables in their own right, they are no longer tied to the grid, like in previous versions.

All in all one now gets the rather ugly but hopefully easier to solve system below:

**Section a** ( $0 - t_{\text{on}}$ ):

$$\begin{aligned}
 \dot{w}_{1a}(t) &= w_{2a}(t) \\
 \dot{w}_{2a}(t) &= P_{[-u_{\text{max}}, u_{\text{max}}]} \left( -\frac{p_{2a}(t)}{\lambda} \right) \\
 w_{1a}(0) &= w_0 \\
 w_{2a}(0) &= \dot{w}_0 \\
 \dot{p}_{2a}(t) &= -p_1 - g'(w_{2a}(t)) \left( p_{3a} \sum_{n=1}^{\infty} \tilde{\gamma}_n e^{-k_n^2(t_{\text{on}}-t)} - \int_{t_{\text{on}}}^{t_{\text{off}}} \sum_{n=1}^{\infty} k_n^2 \tilde{\gamma}_n e^{-k_n^2(s-t)} p_{3b}(s) ds \right)
 \end{aligned}$$

**Section b** ( $t_{\text{on}} - t_{\text{off}}$ ):

$$\begin{aligned}
 \dot{w}_{1b}(t) &= w_{2b}(t) \\
 \dot{w}_{2b}(t) &= P_{[-u_{\text{max}}, u_{\text{max}}]} \left( -\frac{p_{2b}(t)}{\lambda} \right) \\
 w_{1b}(t_{\text{on}}) &= w_{1a}(t_{\text{on}}) \\
 w_{2b}(t_{\text{on}}) &= w_{1a}(t_{\text{on}}) \\
 T_{\text{max}} &= \int_0^{t_{\text{on}}} \sum_{n=1}^{\infty} \tilde{\gamma}_n g(w_{2a}(s)) e^{-k_n^2(t-s)} ds + \int_{t_{\text{on}}}^t \sum_{n=1}^{\infty} \tilde{\gamma}_n g(w_{2b}(s)) e^{-k_n^2(t-s)} ds \quad \forall t \in [t_{\text{on}}, t_{\text{off}}] \\
 &\quad (\text{i.e. } T \equiv T_{\text{max}}) \\
 \dot{p}_{2b}(t) &= -p_1 - g'(w_{2b}(t)) \left( p_{3b}(t) - \int_t^{t_{\text{off}}} \sum_{n=1}^{\infty} k_n^2 \tilde{\gamma}_n e^{-k_n^2(s-t)} p_{3b}(s) ds \right) \\
 \dot{p}_{3b}(t) &= \mu \\
 p_{2b}(t_{\text{on}}) &= p_{2a}(t_{\text{on}})
 \end{aligned}$$

**Section c** ( $t_{\text{off}} - t_f$ ):

$$\begin{aligned}
 \dot{w}_{1c}(t) &= w_{2c}(t) \\
 \dot{w}_{2c}(t) &= P_{[-u_{\text{max}}, u_{\text{max}}]} \left( -\frac{p_{2c}(t)}{\lambda} \right) \\
 w_{1c}(t_{\text{off}}) &= w_{1b}(t_{\text{off}}) \\
 w_{2c}(t_{\text{off}}) &= w_{1b}(t_{\text{off}}) \\
 w_{1c}(t_f) &= 0 \\
 w_{2c}(t_f) &= 0 \\
 \dot{p}_{2c}(t) &= -p_1 \\
 p_{2c}(t_{\text{off}}) &= p_{2b}(t_{\text{off}}) \\
 H(t_f) &= 0
 \end{aligned}$$

## 5.5 Solution via an indirect method

---

The according programs `indirect2.m` (main program) and `findirect2.m` (external function) can be found in `Programs/Indirect_approach`. The additional function `myfun.m` was utilized to generate the modes  $k_n$ , it is identical to the one used during the direct approach.

Despite all this shuffling around, convergence was still not possible to achieve with a generic initial guess. The approach via homotopies as before was dismissed in this attempt, as its first crucial steps down from the unconstrained maximum of  $T$  would mean an interval  $[t_{\text{on}}, t_{\text{off}}]$  of length close to 0 with quite some accompanying numerical inconveniences. But fortunately the functions `f1` and `f2` of the previous attempt could be recycled to generate the solution of the state unconstrained problem, which provided a sufficiently close initial guess for surprisingly swift convergence. Computation times however skyrocket with only relatively moderate increases in discretization as can be seen in table (5.3) below. In the program, the discretizations of the 3 aforementioned sections are denoted with  $n_1$ - $n_3$ . As the last point of section a resp. b is identical with the first point of section b resp. c, this can be seen as an overall discretization of  $n_1 + n_2 + n_3 - 2$ .

$n_1 + n_2 + n_3 - 2$	$t_{\text{on}}$	$t_{\text{off}}$	$t_f$	CPU secs
97	2.3949	3.7628	5.3728	248.85
298	2.4814	3.7374	5.3621	7973.40
898	2.3974	3.7162	5.3655	216280.00

Table 5.3: Performance and accuracy of `indirect2.m` with various discretizations for Problem 1  
Data:  $\lambda = 10^{-1}$ ,  $u_{\text{max}} = 1$ ,  $w_0 = -6$ ,  $\dot{w}_0 = 0$  and  $g(z) := z^2$ ;

Unfortunately  $n_{1,2,3} = 300$  already translates into roughly a weekend of computation time. Even compared to the slower version of the direct approach, that also utilizes the heat equations solution formula, this is a steep cost (compare table (5.2), however it should be noted that those 2 sets of computations were done with different programs and on different, though comparable, computers). Additional consideration of the amount of a priory knowledge and "educated guesses", that were necessary to come this far, paints an even bleaker picture of the indirect methods performance.



## Chapter 6

# Conclusion and outlook

The main aim of this thesis was to create and analyze a prototype problem of ODE-PDE optimal control with both state and control constraints that, while still being manageable in a mathematical way, retains a certain extent of comprehensible physical background. Additionally said ODE-PDE optimal control problem could be transformed into either a ODE optimal control problem whose state constraints are in integro form or a PDE optimal control problem with a control featured in integral terms.

Those same integral terms of the two (highly nonstandard) alternative formulations also serve to explain the main new aspect of ODE-PDE optimal control compared to standard ODE or PDE optimal control: while at least in conventional (i.e. without the integro terms mentioned above) examples of those fields things usually got interesting when the state constraint got active, resulting in singular control etc., the state constraint here exerts its influence straight from the get-go.

We have described this phenomenon as the state constraint being indirectly active. While it is barely discernible when the temperature is still far from its threshold and also obscured by the projection caused by the (altogether less interesting) control constraint, we could nevertheless prove that no point of time between the start and the beginning of the traditional direct effect of the state constraint is free of its indirect influence.

On the numerical side it was possible to at least a posteriori verify all necessary first order optimality conditions of the 3 different versions and also to match them with each other.

While the straightforward solution of the hypersonic rocketcar was quickly and easily obtained via a direct FDTO method, the alternative indirect FOTD approach was considerably more demanding, both in terms of programming as well as computation time versus accuracy. Curiously enough FOTD was only successful while employing an explicit solution formula for the PDE. Contrary to a laymans intuition, evaluating such an explicit solution formula is usually far less efficient than utilizing some numerical scheme. Here however, the considerable advantage of having an optimality system without any directly appearing measures caused by the state constraint more than outweighs this disadvantage. It nevertheless comes at a price: the scalability of the FOTD program is far inferior to its FDTO counterpart.

This does however not mean that FDTO is a fast and convenient solution to all problems. One has to bear in mind that the hypersonic rocketcar, despite all the difficulties it posed and all its intriguing effect is a mere academical example with only one ODE and one PDE involved. On top of that both differential equations were relatively benign specimen of their respective kind and current multiphysics problems tend to be a really far cry more elaborate.

Future tasks among others include the rigorous analytical proof of the relations (4.14), which is one of the major so far unresolved issues of [26].

Despite those shortcomings, we nevertheless hope to have given some first insight and maybe also some thought-provoking impulses for the fascinating field of ODE-PDE optimal control. Well that, and perhaps an incentive to drive with foresight.

## Appendix A

# Compact overview over the different optimality systems

This part of the appendix is solely meant to alleviate looking things up and keeping an oversight over the different formulations of the rocket car problems and the resulting adjoint equations.

### A.1 Problem 1: ODE formulation

$$\min_{u \in U} \left\{ t_f + \frac{1}{2} \lambda \int_0^{t_f} u^2(t) dt \right\}, \quad \lambda > 0,$$

subject to

$$\begin{aligned} \dot{w}_1(t) &= w_2(t) \quad \text{in } (0, t_f), \\ \dot{w}_2(t) &= u(t) \quad \text{in } (0, t_f), \\ \dot{w}_3(t) &= \frac{d}{dt} T\left(\frac{l}{2}, t\right) = \frac{d}{dt} \int_0^t \sum_{n=1}^{\infty} \alpha_n g(w_2(s)) e^{-k_n^2(t-s)} ds \quad \text{in } (0, t_f), \\ w_1(0) &= w_0, \quad w_2(0) = \dot{w}_0, \\ w_1(t_f) &= 0, \quad w_2(t_f) = 0, \\ w_3(0) &= 0, \\ w_3(t_{\text{on/off/touch}}) &= T_{\text{max}}, \\ w_3(t) - T_{\text{max}} &\leq 0 \quad \text{in } (0, t_f), \\ U &:= \{u \in L^2(0, t_f) : |u(t)| \leq u_{\text{max}} \text{ in } [0, t_f]\} \end{aligned}$$

$$\begin{aligned} \dot{p}_1(t) &= 0 \quad \text{in } (0, t_f), \\ \dot{p}_2(t) &= -p_1(t) - g'(w_2(t)) \left( p_3(t) - \int_t^{t_f} \sum_{n=1}^{\infty} k_n^2 \alpha_n e^{-k_n^2(s-t)} p_3(s) ds \right) \quad \text{in } (0, t_f), \\ \dot{p}_3(t) &= \mu, \quad p_3(t_f) = 0, \\ p_3(t_{\text{on/off/touch}}^+) &= p_3(t_{\text{on/off/touch}}^-) - \sigma_{\text{on/off/touch}}, \quad \sigma_{\text{on/off/touch}} > 0, \\ \mu \cdot (w_3(t) - T_{\text{max}}) &= 0, \quad \mu \geq 0, \\ H[t_f] &= 0, \quad H[t_{\text{on/off/touch}}^+] = H[t_{\text{on/off/touch}}^-] \\ u(t) &= P_{[-u_{\text{max}}, u_{\text{max}}]} \left( -\frac{p_2(t)}{\lambda} \right) \end{aligned}$$

## A.2 Problem 1: PDE formulation

$$\min_{u \in U} \left\{ t_f + \frac{1}{2} \lambda \int_0^{t_f} u^2(t) dt \right\}, \quad \lambda > 0,$$

subject to

$$\begin{aligned} T_t(x, t) - T_{xx}(x, t) &= g \left( \dot{w}_0 + \int_0^t u(s) ds \right) \quad \text{in } (0, l) \times (0, t_f), \\ -T_x(0, t) + T(0, t) &= 0, \quad T_x(l, t) + T(l, t) = 0 \quad \text{in } [0, t_f], \\ T(x, 0) &= 0 \quad \text{in } [0, l], \\ T(x, t) &\leq T_{\max} \quad \text{in } [0, l] \times [0, t_f], \\ \int_0^{t_f} u(t) dt &= -\dot{w}_0, \\ \int_0^{t_f} t u(t) dt &= w_0. \\ \\ -q_t(x, t) - q_{xx}(x, t) &= \bar{\mu} \quad \text{in } (0, l) \times (0, t_f), \\ q(x, t_f) &= 0 \quad \text{in } [0, l], \\ q_x(0, t) &= q(0, t) \quad \text{in } [0, t_f], \\ q_x(l, t) &= -q(l, t) \quad \text{in } [0, t_f], \\ u(t) &= P_{[-u_{\max}, u_{\max}]} \left\{ -\frac{1}{\lambda} \left( \nu_1 + \nu_2 t \right. \right. \\ &\quad \left. \left. + \int_t^{t_f} g' \left( \dot{w}_0 + \int_0^s u(\tilde{s}) d\tilde{s} \right) \cdot \left( \int_0^l q(x, s) dx \right) ds \right) \right\}, \\ 0 &= 1 + \frac{\lambda}{2} u^2(t_f) + (\nu_1 + \nu_2 t_f) u(t_f), \\ 0 &= \int_0^{t_f} \int_0^l (T - T_{\max}) \bar{\mu} dx dt, \quad \bar{\mu} \geq 0. \end{aligned}$$

### A.3 Problem 1: ODE-PDE formulation

$$\min_{u \in U} \left\{ t_f + \frac{1}{2} \lambda \int_0^{t_f} u^2(t) dt \right\}, \quad \lambda > 0,$$

subject to

$$\begin{aligned} \dot{w}_1(t) &= w_2(t) && \text{in } (0, t_f), \\ \dot{w}_2(t) &= u(t) && \text{in } (0, t_f), \\ w_1(0) &= w_0, \quad w_2(0) = \dot{w}_0, \\ w_1(t_f) &= 0, \quad w_2(t_f) = 0, \\ U &:= \{u \in L^2(0, t_f) : |u(t)| \leq u_{\max} \text{ in } [0, t_f]\}, \end{aligned}$$

$$\begin{aligned} T_t(x, t) - T_{xx}(x, t) &= g(w_2(t)) && \text{in } (0, l) \times (0, t_f), \\ -T_x(0, t) + T(0, t) &= 0, \quad T_x(l, t) + T(l, t) = 0 && \text{in } [0, t_f], \\ T(x, 0) &= 0 && \text{in } [0, l], \\ T(x, t) &\leq T_{\max} && \text{in } [0, l] \times [0, t_f]. \end{aligned}$$

$$\begin{aligned} \dot{p}_1(t) &= 0 && \text{in } [0, t_f], \\ \dot{p}_2(t) &= -p_1(t) - g'(w_2(t)) \int_0^l q(x, t) dx && \text{in } [0, t_f], \\ -q_t(x, t) - q_{xx}(x, t) &= \bar{\mu} && \text{in } (0, l) \times (0, t_f), \\ q(x, t_f) &= 0 && \text{in } [0, l], \\ q_x(0, t) &= q(0, t) && \text{in } [0, t_f], \\ q_x(l, t) &= -q(l, t) && \text{in } [0, t_f], \\ u &= P_{[-u_{\max}, u_{\max}]} \left( -\frac{p_2(t)}{\lambda} \right) \\ 0 &= \int_0^{t_f} \int_0^l (T - T_{\max}) \bar{\mu} dx dt, \quad \bar{\mu} \geq 0. \end{aligned}$$

## A.4 Problem 2: ODE formulation

$$\min_{u \in U} \left\{ t_f + \frac{1}{2} \lambda \int_0^{t_f} u^2(t) dt \right\}, \quad \lambda > 0,$$

subject to

$$\begin{aligned} \dot{w}_1(t) &= w_2(t) \quad \text{in } (0, t_f), \\ \dot{w}_2(t) &= u(t) \quad \text{in } (0, t_f), \\ \dot{w}_3(t) &= \frac{d}{dt} T(l, t) = \frac{d}{dt} \int_0^t \sum_{n=1}^{\infty} \beta_n h(w_2(s)) e^{-k_n^2(t-s)} ds \quad \text{in } (0, t_f), \\ w_1(0) &= w_0, \quad w_2(0) = \dot{w}_0, \\ w_1(t_f) &= 0, \quad w_2(t_f) = 0, \\ w_3(0) &= 0, \\ w_3(t_{\text{on/off}}) &= T_{\text{max}}, \\ w_3(t) - T_{\text{max}} &\leq 0 \quad \text{in } (0, t_f), \\ U &:= \{u \in L^2(0, t_f) : |u(t)| \leq u_{\text{max}} \text{ in } [0, t_f]\} \end{aligned}$$

$$\begin{aligned} \dot{p}_1(t) &= 0 \quad \text{in } (0, t_f), \\ \dot{p}_2(t) &= -p_1(t) - h'(w_2(t)) \left( p_3(t) - \int_t^{t_f} \sum_{n=1}^{\infty} k_n^2 \beta_n e^{-k_n^2(s-t)} p_3(s) ds \right) \quad \text{in } (0, t_f), \\ \dot{p}_3(t) &= \mu, \quad p_3(t_f) = 0, \\ p_3(t_{\text{on/off}}^+) &= p_3(t_{\text{on/off}}^-) - \sigma_{\text{on/off}}, \quad \sigma_{\text{on/off}} > 0, \\ \mu \cdot (w_3(t) - T_{\text{max}}) &= 0, \quad \mu \geq 0, \\ H[t_f] &= 0, \quad H[t_{\text{on/off}}^+] = H[t_{\text{on/off}}^-] \\ u(t) &= P_{[-u_{\text{max}}, u_{\text{max}}]} \left( -\frac{p_2(t)}{\lambda} \right) \end{aligned}$$

## A.5 Problem 2: PDE formulation

$$\min_{u \in U} \left\{ t_f + \frac{1}{2} \lambda \int_0^{t_f} u^2(t) dt \right\}, \quad \lambda > 0,$$

subject to

$$\begin{aligned} T_t(x, t) - T_{xx}(x, t) &= 0 \quad \text{in } (0, l) \times (0, t_f), \\ -T_x(0, t) + T(0, t) &= 0, \quad T_x(l, t) + T(l, t) = h \left( \dot{w}_0 + \int_0^t u(s) ds \right) \quad \text{in } [0, t_f], \end{aligned}$$

$$T(x, 0) = 0 \quad \text{in } [0, l],$$

$$T(x, t) \leq T_{\max} \quad \text{in } [0, l] \times [0, t_f],$$

$$\int_0^{t_f} u(t) dt = -\dot{w}_0,$$

$$\int_0^{t_f} t u(t) dt = w_0.$$

$$-q_t(x, t) - q_{xx}(x, t) = \bar{\mu} \quad \text{in } (0, l) \times (0, t_f),$$

$$q(x, t_f) = 0 \quad \text{in } [0, l],$$

$$q_x(0, t) = q(0, t) \quad \text{in } [0, t_f],$$

$$q_x(l, t) = -q(l, t) \quad \text{in } [0, t_f],$$

$$u(t) = P_{[-u_{\max}, u_{\max}]} \left\{ -\frac{1}{\lambda} \left( \nu_1 + \nu_2 t + \int_t^{t_f} h' \left( \dot{w}_0 + \int_0^s u(\tilde{s}) d\tilde{s} \right) \cdot q(l, s) ds \right) \right\},$$

$$0 = 1 + \frac{\lambda}{2} u^2(t_f) + (\nu_1 + \nu_2 t_f) u(t_f),$$

$$0 = \int_0^{t_f} \int_0^l (T - T_{\max}) \bar{\mu} dx dt, \quad \bar{\mu} \geq 0.$$

## A.6 Problem 2: ODE-PDE formulation

$$\min_{u \in U} \left\{ t_f + \frac{1}{2} \lambda \int_0^{t_f} u^2(t) dt \right\}, \quad \lambda > 0,$$

subject to

$$\begin{aligned} \dot{w}_1(t) &= w_2(t) && \text{in } (0, t_f), \\ \dot{w}_2(t) &= u(t) && \text{in } (0, t_f), \\ w_1(0) &= w_0, \quad w_2(0) = \dot{w}_0, \\ w_1(t_f) &= 0, \quad w_2(t_f) = 0, \\ U &:= \{u \in L^2(0, t_f) : |u(t)| \leq u_{\max} \text{ in } [0, t_f]\}, \end{aligned}$$

$$\begin{aligned} T_t(x, t) - T_{xx}(x, t) &= 0 && \text{in } (0, l) \times (0, t_f), \\ -T_x(0, t) + T(0, t) = 0, \quad T_x(l, t) + T(l, t) &= h(w_2(t)) && \text{in } [0, t_f], \\ T(x, 0) &= 0 && \text{in } [0, l], \\ T(x, t) &\leq T_{\max} && \text{in } [0, l] \times [0, t_f]. \end{aligned}$$

$$\begin{aligned} \dot{p}_1(t) &= 0 && \text{in } [0, t_f], \\ \dot{p}_2(t) &= -p_1(t) - h'(w_2(t)) \cdot q(l, t) && \text{in } [0, t_f], \\ -q_t(x, t) - q_{xx}(x, t) &= \bar{\mu} && \text{in } (0, l) \times (0, t_f), \\ q(x, t_f) &= 0 && \text{in } [0, l], \\ q_x(0, t) &= q(0, t) && \text{in } [0, t_f], \\ q_x(l, t) &= -q(l, t) && \text{in } [0, t_f], \\ u &= P_{[-u_{\max}, u_{\max}]} \left( -\frac{p_2(t)}{\lambda} \right) \\ 0 &= \int_0^{t_f} \int_0^l (T - T_{\max}) \bar{\mu} \, dx \, dt, \quad \bar{\mu} \geq 0. \end{aligned}$$

# Appendix B

## List of symbols and abbreviations

$\mathcal{A}_{1,2}$	active set of Problem 1 resp. 2
$\mathcal{A}^C$	complement of an active set
$C^k(Q)$	set of all $k$ -times continuously differentiable functions on $Q$ , $C^0(Q) := C(Q)$
$C([0, t_f], L^2(0, l))$	space of abstract continuous functions with values in $L^2(0, l)$
FDTO	first discretize, then optimize aka direct method
FOTD	first optimize, then discretize aka indirect method
$\mathcal{L}$	Lagrangian
$H$	Hamiltonian
$L^2(0, t_f)$	Lebesgue space
min / max	minimum / maximum
NLP	nonlinear program
ODE	ordinary differential equation
PDE	partial differential equation
part. int.	partial integration
PDAS	primal dual active set strategy
$P_{[a,b]}$	projection onto the interval $[a, b]$ , $P_{[a,b]}(f) = \max(a, \min(b, f))$
$\mathbf{v}$	bold print indicates $\mathbf{v}$ is a vector
$\lambda$	Tychonoff parameter
$W_p^{k,m}(Q)$	Sobolev space
s.t.	subject to



## Appendix C

# On a Prototype Class of ODE-PDE State-constrained Optimal Control Problems Part 1: Analysis of the State-unconstrained Problems

H. J. PESCH<sup>1</sup>, A. RUND<sup>2</sup>, W. VON WAHL<sup>3</sup>, AND S. WENDL<sup>4</sup>

---

<sup>1</sup>Full Professor, Chair of Mathematics in Engineering Sciences, University of Bayreuth, Bayreuth, Germany. Corresponding author: [hans-josef.pesch@uni-bayreuth.de](mailto:hans-josef.pesch@uni-bayreuth.de)

<sup>2</sup>Research Assistant, Chair of Mathematics in Engineering Sciences, University of Bayreuth, Bayreuth, Germany.

<sup>3</sup>Full Professor, Chair of Mathematics VI (Partial Differential Equations and Mathematical Physics), University of Bayreuth, Bayreuth, Germany.

<sup>4</sup>Research Assistant, Chair of Mathematics in Engineering Sciences, University of Bayreuth, Bayreuth, Germany.

**Abstract.** In this bipartite paper, we investigate a new class of optimal control problems with constraints in form of a coupled system of ordinary and partial differential equations. We call this kind of problems hypersonic rocket car problems, since they are inspired, on the one hand, by the well-known rocket car problem, and, on the other hand, by a recently investigated flight path trajectory optimization problem for a hypersonic aircraft.

The hypersonic rocket car problems can be considered as undressed abstract examples for a class of staggered state-constrained ODE-PDE-constrained optimal control problems with a coupling structure similar to the hypersonic aircraft problem. This simplification allows to obtain analytical solutions to a certain extent which is prohibited by the enormous complexity of the flight path optimization problem.

The analysis of structural questions concerning the existence of boundary arcs and touch points of state constraints is the aim of the second part of this paper and is novel in the context of PDE-constrained optimal control. We obtain results, which are, at a first glance, similar to state-constrained ODE optimal control problems and show their relation to the differentiation index of the related partial differential algebraic equation system along state-constrained subarcs. At a second glance, new phenomena are observed caused by the non-local character of the state constraint in the ODE context leading to additional constraints on the ODE states from the beginning of the process on.

**Key Words.** Optimal control of partial differential equations, ODE-PDE-constrained optimization, state constraints, partial differential algebraic equations.

---

## Introduction

Realistic mathematical models of dynamical processes from scientific or engineering background may often have to consider different physical phenomena leading to coupled systems of equations that include partial and ordinary differential equations as well as algebraic equations. Frequently, their numerical solution is only the first step. The identification of system parameters and the control of such systems are tackled subsequently. Mathematically one obtains optimization problems where the constraints are given by the underlying dynamical process. Because of their complexity such optimization problems are not widely studied in literature, neither theoretically nor numerically.

One such example was an optimal control problem recently studied by Chudej et. al. [12]<sup>5</sup> and M. Wächter [34]. It describes the flight of a hypersonic aircraft under the objective of minimum fuel consumption. The flight trajectory is described, as usual, by a system of ordinary differential equations (ODE). However, due to the hypersonic flight conditions a thermal protection system is indispensable and must therefore be taken into account in the model. This leads to a quasi-linear heat equation with non-linear boundary conditions, which is coupled with the ODE. A major goal of the optimization is limiting the peak temperature of the thermal protection system, inducing a pointwise state constraint, which couples the PDE with the ODE reversely.

However there is little to no hope to achieve any insight in the structure of this problem and its solution due its enormous complexity, which makes anything beyond numerical analysis nigh impossible. To obtain an unobstructed view, we decided to design a model problem as simple as possible, yet containing the key features of ODE-PDE optimal control.

This model problem we would like to call the *hypersonic rocket car* problem. Its ODE-part consists of the *rocket car on a rail track* problem, first studied by Bushaw [8] in the pioneering days of ODE optimal control and is augmented by a heat equation, mimicing heating due to friction.

The subject of the paper is the theoretical and numerical analysis of this prototype of an ODE-PDE optimal control problem, with the major aim to answer structural questions about the existence of state-constrained subarcs or touch points. With view on complex real-life problems we focus on first-order necessary conditions only. Even these conditions are hardly manageable for problems of this kind not to mention second-order sufficiency conditions.

The paper may also lead to new contributions in the field of state-constrained optimal control problems with PDEs in particular with view to the connection of state-constrained optimal control problems to free boundary problems, where the boundary (interface) between the active and inactive sets is treated as optimization variable; cf. Hintermüller, Ring [15]. This approach contains the spirit of determining the junction points in ODE state-constrained problems as optimization parameters of a multi-point boundary value problem; cf. [23].

The paper is divided into two parts. Part 1 will , as a prelude and for better comparison and illustration, shed some light on the state-unconstrained problem and provide the necessary theory for Part 2, which deals with the full state-constrained problem and is more numerically oriented.

---

<sup>5</sup>To avoid unnecessary confusion, the bibliography of this preprint has been included into the main bibliography of the entire thesis. All references can be found there.

## The hypersonic rocket car problems

As mentioned before the *hypersonic rocket car* problem is based on the classical *rocket car on a rail track* problem, whose aim it is to drive a rocket car from a given starting position and velocity to the origin of the phase plane by controlling its acceleration. Additionally, the cars temperature  $T$  is calculated with its speed entering the source term of the heat equation. In case of Coulomb, Stokes or Newton friction the source term of the PDE has to be proportional to the vehicle's speed, its square or cube. This temperature finally is not allowed to exceed a certain threshold  $T_{\max}$ .

For the heating we consider two cases. In the first case, it is assumed to be induced over the entire length  $l$  of the car. This leads to an ODE-PDE-constrained optimization problem with an indirectly distributed control of the PDE via the ODE state variables by a semi-linear coupling term, subsequently referred to as Problem 1. In the second case, the PDE is controlled through a type of boundary control indirectly introduced by the ODE state variables, subsequently referred to as Problem 2. Here, the heat flux is assumed to be dependent also on the car's speed according to the aforementioned friction laws.

In view of the hypersonic aircraft problem, these two problems constitute extremely simplified versions of the optimal control of the instationary heat flux into the thermal protection system of the aircraft's body, resp., at its stagnation point.

In the following, the ODE state variable  $w$  denotes the one-dimensional position of the car depending on time  $t$  with the terminal time  $t_f$  unspecified. The PDE state variable  $T$  stands for the temperature and depends on time as well as the spatial coordinate  $x$  describing the position within the car. The control is denoted by  $u$  and stands for the acceleration of the car. The PDE is controlled only indirectly via the velocity  $\dot{w}$  of the car.

The hypersonic rocket car problems are now given as follows:

$$\min_{u \in U} \left\{ t_f + \frac{1}{2} \lambda \int_0^{t_f} u^2 dt \right\}, \quad \lambda \geq 0, \quad (\text{C.1})$$

subject to

$$\ddot{w}(t) = u(t) \quad \text{in } (0, t_f), \quad (\text{C.2a})$$

$$w(0) = w_0, \quad \dot{w}(0) = \dot{w}_0, \quad (\text{C.2b})$$

$$w(t_f) = 0, \quad \dot{w}(t_f) = 0, \quad (\text{C.2c})$$

$$U := \{u \in L^2(0, t_f) : |u(t)| \leq u_{\max} \text{ almost everywhere in } [0, t_f]\}, \quad (\text{C.2d})$$

and either

1st Problem: *Distributed control of the PDE via an ODE state variable:*

$$\frac{\partial T}{\partial t}(x, t) - \frac{\partial^2 T}{\partial x^2}(x, t) = g(\dot{w}(t)) \quad \text{in } (0, l) \times (0, t_f), \quad (\text{C.3a})$$

$$T(x, 0) = T_0 \quad \text{on } (0, l), \quad (\text{C.3b})$$

$$-\frac{\partial T}{\partial x}(0, t) = -(T(0, t) - T_0), \quad \frac{\partial T}{\partial x}(l, t) = -(T(l, t) - T_0) \quad \text{on } [0, t_f], \quad (\text{C.3c})$$

or

2nd Problem: *Boundary control of the PDE via an ODE state variable:*

$$\frac{\partial T}{\partial t}(x, t) - \frac{\partial^2 T}{\partial x^2}(x, t) = 0 \quad \text{in } (0, l) \times (0, t_f), \quad (\text{C.4a})$$

$$T(x, 0) = T_0 \quad \text{on } (0, l), \quad (\text{C.4b})$$

$$-\frac{\partial T}{\partial x}(0, t) = -(T(0, t) - T_0), \quad \frac{\partial T}{\partial x}(l, t) = -(T(l, t) - T_0) + h(\dot{w}(t)) \quad \text{on } [0, t_f], \quad (\text{C.4c})$$

---

with non-negative continuously differentiable functions  $g$  and  $h$  satisfying  $g(z) = 0$  and  $h(z) = 0$ , if and only if  $z = 0$ , and finally subject to a pointwise state constraint of type

$$T(x, t) \leq T_{\max} \text{ in } [0, l] \times [0, t_f]. \quad (\text{C.5})$$

Physically reasonable choices for  $g$  and  $h$  are, for example,  $z \mapsto |z|^n$ ,  $n = 1, 2, 3$ , according to Coulomb, Stokes, and Newton friction. Negative values for  $z$ , i. e., when the rocket car drives backward, require some additional devices of the rocket car, in order to preserve the physical interpretability, such as a front and a rear engine in case of Problem 1 or the ability of instantaneous turns. (Take it with a grain of salt.)

## The state-unconstrained hypersonic rocket car problem

For better illustration and to allow comparison with the results of the full-blown ODE-PDE problem lets first have a brief look at the state-unconstrained problem:

### 3.1 Solution of the ODE-part. Inactive state constraint

Rewriting the second-order ODE as a system of two first-order ODEs in  $\mathbf{w} := (w_1, w_2) := (w, \dot{w})$ ,  $\dot{w}_1 = w_2$ ,  $\dot{w}_2 = u$ , and defining the Hamiltonian by

$$H(\mathbf{w}, \mathbf{p}, u) = 1 + \frac{1}{2} \lambda u^2 + p_1 w_2 + p_2 u,$$

the ODE adjoint equations are

$$\dot{p}_1 = -H_{w_1} = 0, \quad \dot{p}_2 = -H_{w_2} = -p_1.$$

The minimum principle yields

$$u(t) = P_{[-u_{\max}, u_{\max}]} \left( -\frac{1}{\lambda} p_2 \right),$$

where  $P_{[a,b]}(z) := \min \{b, \max \{a, z\}\}$  denotes the projection of  $\mathbb{R}$  onto the interval  $[a, b]$ . Furthermore, the terminal time  $t_f$  is determined by

$$H|_{t_f} = 1 + \frac{1}{2} \lambda u(t_f)^2 + p_1(t_f) \underbrace{w_2(t_f)}_{=0} + p_2(t_f) u(t_f) = 0.$$

An elementary calculation shows that  $p_2(t) = -C(t - t_f) + p_2(t_f)$  with  $p_1(t) = C = \text{const}$ . Hence  $p_2$  is linear; cf. [24]. Due to this linearity, the optimal control law induces at most two junction points, when taking box constraints on the control  $u$  into account. If  $\lambda$  is sufficiently small, the switching structure generally consists either of the three subarcs  $u(t) = u_{\max}$ ,  $u(t) = u^{\text{free}}(t) := -\frac{1}{\lambda} p_2(t)$ , and  $u(t) = -u_{\max}$  with the two junction points  $t_1$  and  $t_2$  or the other way around. Herewith, an analytical solution of the state-unconstrained problem can be obtained, however the necessary computations are rather longsome yet basic and are therefore omitted here. Their results are shown in the following phase diagram:

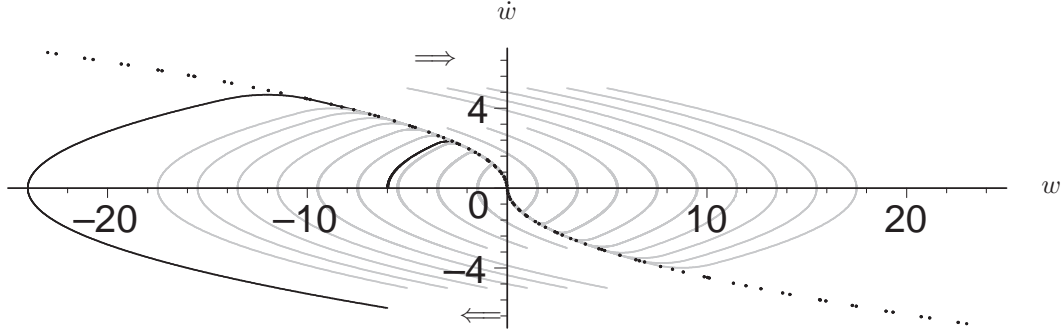


Figure C.1: Optimal trajectories of the regularized minimum-time problem in the phase plane (grey) with  $\lambda = 10^{-1}$  and box constraints  $|u| \leq u_{\max} = 1$ . The dotted black curve is the envelope curve and coincides with the switching curve for  $\lambda = 0$ . The black curves are the optimal solutions for the starting conditions  $w_0 = -6$  and  $\dot{w}_0 = 0$  resp.  $w_0 = -6$  and  $\dot{w}_0 = -6$ . Those will be picked up again later on.

### 3.2 Solution of the heat equation. Inactive state constraint

Furthermore it is also possible to derive a semi-analytical solution of the heat equation for both problems (of course still depending on the input  $\dot{w} = w_2$  from the ODE).

Without loss of generality, we may choose  $T_0 := 0$ . Additionally, in the second problem a transformation to homogeneous Robin conditions can be achieved by  $\hat{T} := T - \frac{1}{2} e^{x-l} h(\dot{w})$ .

Then the second problem reads, again replacing  $\hat{T}$  by  $T$ , as

$$T_t(x, t) - T_{xx}(x, t) = \frac{1}{2} e^{x-l} (h(\dot{w}(t)) - \frac{d}{dt} h(\dot{w}(t))) \text{ in } (0, l) \times (0, t_f), \quad (\text{C.6a})$$

$$T(x, 0) = -\frac{1}{2} e^{x-l} h(\dot{w}(0)) \text{ on } (0, l), \quad (\text{C.6b})$$

$$-T_x(0, t) = -T(0, t), \quad T_x(l, t) = -T(l, t) \text{ on } [0, t_f]. \quad (\text{C.6c})$$

Considering the homogeneous parts of the PDEs of the two problems, a separation of variables,  $T(x, t) = \xi(x) \tau(t)$ , leads to the eigenvalue problem

$$\xi'' + \mu \xi = 0 \quad \text{with} \quad 0 < \mu =: k^2$$

with the associated boundary conditions  $-\xi'(0) = -\xi(0)$  and  $\xi'(l) = -\xi(l)$ . In addition, one obtains a differential equation for  $\tau$ ,  $\dot{\tau} + \mu \tau = 0$ . For both problems, the analysis yields the same eigenfunctions

$$\varphi_n(x) = k_n \cos k_n x + \sin k_n x$$

and the same eigenvalues determined by either

$$\frac{2k}{k^2 - 1} = \tan kl \quad (\text{if } l \neq \frac{1}{2k} (2m - 1)\pi) \quad (\text{C.7a})$$

or

$$\frac{k^2 - 1}{2k} = \cot kl \quad (\text{if } l \neq \frac{1}{2k} (2m + 1)\pi). \quad (\text{C.7b})$$

They satisfy the asymptotic behaviour

$$\lim_{n \rightarrow \infty} \left( \mu_n - (n - 1)^2 \left( \frac{\pi}{l} \right)^2 \right) = 0.$$

Their dependence on  $l$  will furtheron be suppressed.

Because of the symmetry of the boundary conditions, these eigenfunctions are orthogonal, but not normalized with respect to the usual Hilbert space scalar product. To facilitate further calculations, we mainly use the normalized eigenfunctions from now on,

$$\phi_n(x) = \frac{1}{N_n} (k_n \cos k_n x + \sin k_n x) \quad \text{with } N_n^2 := \|\varphi_n\|_{L^2(0,l)}^2 = \int_0^l \varphi_n^2(x) dx = \frac{l}{2} k_n^2 + \frac{l}{2} + 1.$$

By Fourier's method one finally obtains the following solutions, which can be easily evaluated: For the 1st problem, Eqs. (C.3):

$$\begin{aligned} T(x, t) &= \sum_{n=1}^{\infty} \left[ \int_0^t g(\dot{w}(s)) e^{-k_n^2 (t-s)} ds \right] \cdot \left( \int_0^l \phi_n(y) dy \right) \phi_n(x) \\ &= \sum_{n=1}^{\infty} \left[ \int_0^t g(\dot{w}(s)) e^{-k_n^2 (t-s)} ds \right] \cdot \frac{1}{N_n} \left[ \sin k_n l + \frac{1}{k_n} (1 - \cos k_n l) \right] \phi_n(x). \end{aligned} \quad (\text{C.8})$$

For the 2nd problem, Eqs. (C.6):

$$\begin{aligned} T(x, t) &= -\frac{1}{2} e^{-l} \sum_{n=1}^{\infty} \left[ h(\dot{w}(0)) e^{-k_n^2 t} - \int_0^t (h(\dot{w}(s)) - \frac{d}{ds} h(\dot{w}(s))) e^{-k_n^2 (t-s)} ds \right] \\ &\quad \cdot \left( \int_0^l e^y \phi_n(y) dy \right) \phi_n(x) + \frac{1}{2} h(\dot{w}(t)) e^{x-l} \end{aligned} \quad (\text{C.9a})$$

$$= \frac{1}{2} \sum_{n=1}^{\infty} \left[ (1 + k_n^2) \int_0^t h(\dot{w}(s)) e^{-k_n^2 (t-s)} ds \right] \frac{1}{N_n} \sin k_n l \phi_n(x). \quad (\text{C.9b})$$

The representation (C.9b) is obtained by partial integration and explicit computation of the  $y$ -integral. Despite of its compact form, the series representation (C.9b) converges slower compared to (C.9a). This is caused by the  $\mathcal{O}(n^2)$ -term  $(1 + k_n^2)$ . In Theorem 4.9, this will later be explained in more detail. Moreover, the jump discontinuities of  $\ddot{w} = u$  always cancel each other in (C.9b).

Herewith one can compute the temperature profiles for the trajectories of Fig. C.1 for the problems 1 and 2 (In all computations the length  $l$  of the car has been set to 1):

All graphical results shown here were obtained by symbolic computations using the mathematical and analytical software package MAPLE 10.

Please note that for Problem 1 the temperature is symmetric in space with respect to  $x = \frac{l}{2}$ , where the spatial maximum for each time  $t$  is situated. For Problem 2 there is unfortunately no such symmetry, but one can observe that the absolute maximum of the temperature is always at  $x = l$ . The latter implies that the coordinate  $x^*$  of the maximum of  $T$  for arbitrary  $t \in [0, t_f]$  satisfies  $x^* < l$ , if and only if the state constraint is not active. Those observations will be proven in the course of the next chapter and will come in very handy in Part 2 of the paper.

## Theoretical analysis of the coupled ODE-PDE system

In the following we summarize some properties, the solutions of the two different ODE-PDE systems have, independent of the choice of the control  $u \in U$ . Firstly, we present the main result:

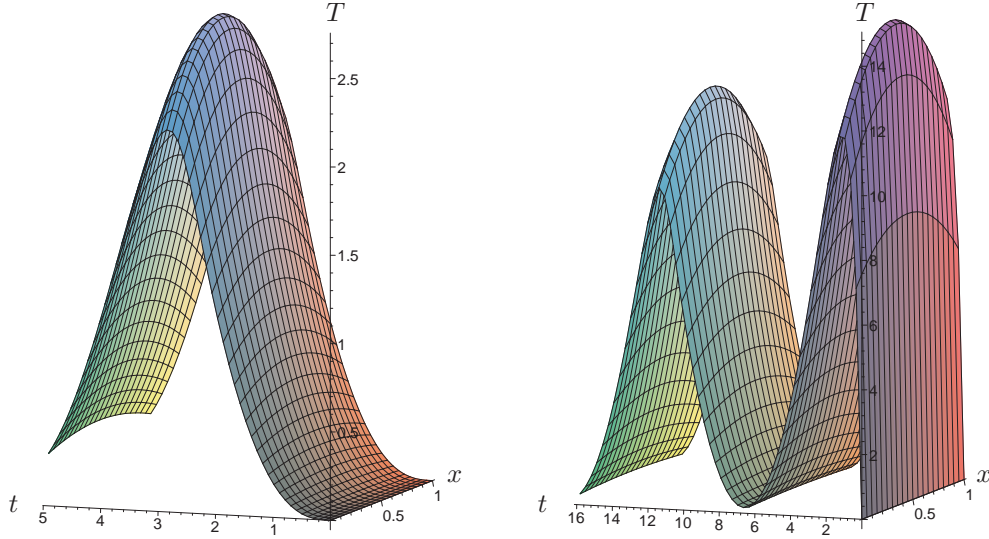


Figure C.2: Temperature profiles for Problem 1 along state-unconstrained trajectories; cf. Fig. C.1. Data:  $\lambda = 10^{-1}$ ,  $u_{\max} = 1$ ,  $w_0 = -6$ ,  $\dot{w}_0 = 0$  (left), resp.  $\dot{w}_0 = -6$  (right), and  $g(z) := z^2$ .

**Theorem 4.1.** *Let  $g$  and  $h$  be continuously differentiable real valued functions satisfying  $g(0) = h(0) = 0$ . Let  $t_f$  be fixed. Then Problems 1 and 2 given by Eqs. (C.2), (C.3), resp. (C.2), (C.4) possess each one and only one solution  $(w, T)$  in the space  $W_2^1(0, t_f) \times W_2^{1,0}(Q)$ . This solution also belongs to the space  $W_2^1(0, t_f) \times (W_2^{1,0}(Q) \cap C([0, t_f], L^2(0, l)))$  for all  $u \in U$ . Moreover, the solutions depend continuously on the data, for example,*

$$\begin{aligned} & \|w\|_{W_2^1(0, t_f)} + \max_{[0, t_f]} \|T(\cdot, t)\|_{L^2(0, l)} + \|T\|_{W_2^{1,0}(Q)} \\ & \leq c_{\text{ODE}} (|w_0| + |\dot{w}_0| + \|u\|_{L^2(0, t_f)}) + c_{\text{PDE}} \|g(\dot{w})\|_{L^2(0, t_f)} \end{aligned}$$

with constants  $c_{\text{ODE}}$ , resp.  $c_{\text{PDE}}$  independent of  $u$ , resp.  $g$  or  $h$ .

As usual we define the Banach spaces  $W_p^m(0, t_f) := \{w \in L^p(0, t_f) : \frac{d^m}{dt^m} w \in L^p(0, t_f)\}$ . In particular,  $W_p^1(0, t_f)$ ,  $p = 2$ , resp.  $p = \infty$ , denote the Banach space of all absolutely continuous functions, both equipped with the usual norms. Moreover,  $W_2^{1,0}(Q)$  denotes the Banach space of all functions in  $L^2(Q)$  with weak first-order partial derivative w.r.t.  $x$  in  $L^2(Q)$ , and  $C([0, t_f], L^2(0, l))$  is the space of abstract continuous functions with values in  $L^2(0, l)$ .  $Q$  stands for the space-time cylinder  $(0, l) \times (0, t_f)$ . For later use, we define  $V_2^{1,0}(Q) := W_2^{1,0}(Q) \cap C([0, t_f], L^2(0, l))$ .

**Proof.** According to standard Theorems of existence, uniqueness and continuous dependence on data, the ODE (C.2) possesses one and only one solution for all  $u \in U$ , which depends continuously on the data:

$$\|w\|_{W_2^1(0, t_f)} \leq c_{\text{ODE}} (|w_0| + |\dot{w}_0| + \|u\|_{L^2(0, t_f)}),$$

since

$$\begin{aligned} \ddot{w}(t) = u(t) & \implies \dot{w}(t) = \dot{w}_0 + \int_0^t u(s) ds \implies \dot{w}(t)^2 \leq (|\dot{w}_0| + \|u\|_{L^1(0, t_f)})^2 \\ & \implies \|\dot{w}\|_{L^2(0, t_f)}^2 \leq c (|\dot{w}_0| + \|u\|_{L^2(0, t_f)})^2. \end{aligned}$$

Analogously we obtain  $\|w\|_{L^2(0, t_f)}^2 \leq c (|w_0| + \|\dot{w}\|_{L^2(0, t_f)})^2$ .

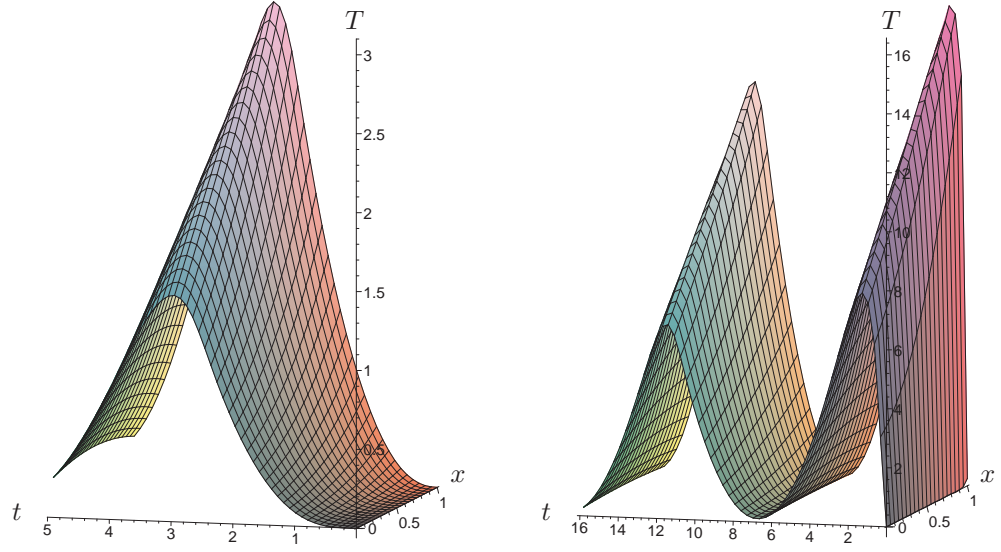


Figure C.3: Temperature profiles for Problem 2 along state-unconstrained trajectories; cf. Fig. C.1. Data:  $\lambda = 10^{-1}$ ,  $u_{\max} = 1$ ,  $w_0 = -6$ ,  $\dot{w}_0 = 0$  (left), resp.  $\dot{w}_0 = -6$  (right), and  $h(z) := z^2$ .

Here and in the following,  $c$  always denotes a generic constant.

Then, according to [31], Satz 7.6, p. 280, based on Chapter III of [18], both initial-boundary value problems possess unique solutions in the spaces stated. Moreover, the solutions depend continuously on all data of the problem, e.g. for Problem 1,

$$\max_{[0, t_f]} \|T(\cdot, t)\|_{L^2(0, l)} + \|T\|_{W_2^{1,0}(Q)} \leq c \|g(\dot{w})\|_{L^2(0, t_f)}.$$

Combining the two estimates completes the proof.  $\diamond$

*Remarks:* Theorem 4.1 gives rise to continuous, generally non-linear solution operators

$$S: U \rightarrow W_2^1(0, t_f) \times V_2^{1,0}(Q), \quad u \mapsto (w, T).$$

Note that the nonlinearity of  $S$  is solely induced by the nonlinearities of  $g$ , resp.  $h$ . In the second part of this paper, we will show that  $S$  is even continuously Fréchet differentiable which will be used to prove the existence of a Lagrange multiplier associated with the state constraint (C.5). The solutions are explicitly given by the formulae (C.8) and (C.9).

If the terminal time is unprescribed, we can linearly transform the time interval  $[0, t_f]$  into a fixed interval  $[0, 1]$  for a normalized time. This introduces a factor  $\frac{1}{t_f}$  in front of each time derivative of the ODE-PDE system. By a boundedness assumption on the optimal time  $t_f \leq t_f^{\max}$ , the proof applies accordingly.

#### 4.1 Problem 1: Distributed control of the PDE by the ODE

Next we will show that solutions of Problem 1, Eqs. (C.3), are positive in  $[0, l] \times (0, t_f]$  and possess strong maxima w. r. t.  $x$  for all  $t > 0$  on the vertical line  $x = \frac{l}{2}$ . Moreover, we will investigate their regularity properties.

**Theorem 4.2.** *Let  $T(x, t)$  be a solution of Problem 1, Eqs. (C.3), with  $T_0 = 0$  in  $[0, l] \times [0, t_f]$  and with the following properties,*

- (A1)  $T$  is continuous in  $[0, l] \times [0, t_f]$ ,  $\partial_x^i T$ ,  $i = 1, \dots, 3$ , as well as  $\partial_x^i T_t$ ,  $i = 0, 1$ , exist and are continuous in  $[0, l] \times (0, t_f]$ ;

(A2)  $T_x$  possesses a continuation in  $C^0([0, l] \times [0, t_f])$ , also denoted by  $T_x$ .

Then there holds:

- a) If  $g(\dot{w}) > 0$  for  $[0, l] \times (0, t_f]$ , then  $T \geq 0$  in  $[0, l] \times [0, t_f]$ .
- b) If  $g(\dot{w}) > 0$  for  $[0, l] \times (0, t_f]$ , then  $T > 0$  in  $[0, l] \times (0, t_f]$ .

**Proof of a).** We assume that  $T$  has a negative minimum in  $(x_0, t_0) \in [0, l] \times [0, t_f]$ . Then  $t_0 > 0$ .

- (i) Let  $(x_0, t_0)$  be an interior point of  $[0, l] \times (0, t_f]$ . Because of  $T_t(x_0, t_0) = T_x(x_0, t_0) = 0$ , Eq. (C.3a) yields  $T_{xx}(x_0, t_0) < 0$ , which contradicts to  $(x_0, t_0)$  being a minimizer. For,  $T(x, t_0) = T(t_0, x_0) + \frac{1}{2} T_{xx}(x_0, t_0) (x - x_0)^2 + \mathcal{O}((x - x_0)^3)$ .
- (ii) Let  $x_0 = 0$ . Then Eq. (C.3c) yields  $T(x, t_0) = T(0, t_0) + T_x(0, t_0) x + \mathcal{O}(x^2) = T(0, t_0) (1 + x) + \mathcal{O}(x^2)$ , which also leads to a contradiction.
- (iii) Let  $x_0 = l$ . Then Eq. (C.3c) yields  $T(x, t_0) = T(l, t_0) + T_x(l, t_0) (x - l) + \mathcal{O}((x - l)^2) = T(l, t_0) (1 + l - x) + \mathcal{O}((x - l)^2)$ , which leads to a contradiction, too.
- (iv) Let  $t_0 = t_f$  and  $0 < x_0 < l$ . Then we have  $T_t(x_0, t_f) \leq 0$ . For,  $T_t(x_0, t_f) > 0$  would imply  $T(x_0, t) = T(x_0, t_f) + T_t(x_0, s) (t - t_f) < T(x_0, t_f)$  for  $t < s < t_f$  and  $t_f - t$  sufficiently small, thus a contradiction.

Therefore, by Eq. (C.3a) there must hold  $T_{xx}(x_0, t_f) < 0$ . The expansion  $T(x, t_f) = T(x_0, t_f) + \frac{1}{2} T_{xx}(x_0, t_f) (x - x_0)^2 + \mathcal{O}((x - x_0)^3)$  then leads again to a contradiction.

Hence,  $T$  cannot have a negative minimum. ◇

**Proof of b).** We assume that  $T$  has a minimum in  $(x_0, t_0) \in [0, l] \times (0, t_f]$ , which equals zero. As in the proof of Part a), (i), (iv), we can immediately exclude  $0 < x_0 < l$ .

Let  $x_0 = 0$ . Because of  $T(0, t_0) = 0$  and Eq. (C.3c), there holds  $T(x, t_0) = \frac{1}{2} T_{xx}(0, t_0) x^2 + \mathcal{O}(x^3)$ . Since Eq. (C.3a) yields  $T_{xx}(0, t_0) < 0$ , the last equation leads to a contradiction. We proceed analogously if  $x_0 = l$ . ◇

**Theorem 4.3.** *There holds  $T(x, t) = T(l - x, t)$ .*

**Proof.** Under the assumptions (A1), Problem 1 (C.3) possesses one and only one solution, since  $\mathcal{L}$  defined by

$$\begin{aligned} \mathcal{L}y &:= -y_{xx}, \\ \mathcal{D}(\mathcal{L}) &:= \{y : y \in H^2(0, l), (-y_x + y)(0) = 0, (y_x + y)(l) = 0\} \end{aligned}$$

is a positive definite self-adjoint operator in  $L^2(0, l)$ . Here,  $H^2(0, l)$  denotes the Hilbert space of all functions having square integrable weak derivatives up to order 2.

If  $T$  solves Problem 1, then  $\hat{T}(x, t) := T(l - x, t)$  solves it, too. ◇

**Theorem 4.4.**  *$T$  takes its strong maximum in  $x = \frac{l}{2}$  for each  $t_0 \in (0, t_f)$ .  $T(x, t_0)$  increases strictly monotonic in  $[0, \frac{l}{2}]$  and decreases strictly monotonic in  $[\frac{l}{2}, l]$ .*

**Proof.** Because of Theorem 4.3 there holds

$$T_x\left(\frac{l}{2}, t\right) = 0, \quad 0 \leq t \leq t_f.$$

Since there holds  $T_{xt} - T_{xxx} = 0$ ,  $T_x$  takes its maximum and minimum on the parabolic boundary of  $[0, \frac{l}{2}] \times [0, t_f]$ . Because of Theorem 4.2 a) and Eq. (C.3b), we obtain  $T_x(x, t) \geq 0$  in  $[0, \frac{l}{2}] \times [0, t_f]$ . Because of Theorem 4.2 b) and Eq. (C.3c),  $T_x(0, t_0) > 0$ . Hence,  $T$  at first increases strictly monotonic.

Let us assume that  $T_x(x, t_0)$  possesses its first zero in  $x_0$ ,  $0 < x_0 < \frac{l}{2}$ . There holds  $T_x$  is real analytic in  $(0, l) \times (0, t_f)$ , i. e.,

$$T_x(x, t_0) = T_{xx}(x_0, t_0) (x - x_0) + \sum_{k=2}^{\infty} \frac{1}{k!} \partial_x^k T_x(x_0, t_0) (x - x_0)^k \quad \text{in } |x - x_0| < \varepsilon.$$

Because of  $T_x(x, t_0) > 0$  in  $x_0 - \varepsilon < x < x_0$ , the first non-vanishing coefficient of the preceding expansion must have the form  $\frac{1}{(2l)!} \partial_x^{2l} T_x(x_0, t_0) > 0$ . Hence  $T(x, t_0)$  passes strictly monotonic increasing through  $(x_0, t_0)$ . Since only a finite number of zeros can lie in each interval  $(\eta, l - \eta)$ , the proposition follows immediately.  $\diamond$

**Theorem 4.5.** *Let  $T$  be the unique weak solution of*

$$T_t + \mathcal{L}T = g(\dot{w}), \quad (\text{C.10a})$$

$$T(0) = 0, \quad (\text{C.10b})$$

*i. e.,  $T \in C^0([0, t_f], L^2(0, l)) \cap L^2(0, t_f; \mathcal{D}(\mathcal{L}^{\frac{1}{2}}))$ , such that*

$$-\int_0^{t_f} (T, \psi_t) ds + \int_0^{t_f} (\mathcal{L}^{\frac{1}{2}} T, \mathcal{L}^{\frac{1}{2}} \psi) ds = \int_0^{t_f} (g(\dot{w}), \psi) ds + (T(0) = 0, \psi(0)) \quad (\text{C.11})$$

*for all test functions  $\psi \in C^1([0, t_f], \mathcal{D}(\mathcal{L}^{\frac{1}{2}}))$  with  $\psi(t_f) = 0$ .*

*Then*

$$T(t) = \int_0^t e^{-(t-s)\mathcal{L}} g(\dot{w}(s)) ds, \quad (\text{C.12})$$

*and  $T$  has the following additional regularity properties:*

$$T(t) \in \mathcal{D}(\mathcal{L}), \quad 0 \leq t \leq t_f, \quad (\text{C.13a})$$

$$\mathcal{L}T \in C^0([0, t_f], L^2(0, l)), \quad (\text{C.13b})$$

$$T \in C^1([0, t_f], L^2(0, l)), \quad (\text{C.13c})$$

$$T \in \bigcap_{\eta, 0 \leq \eta < \frac{1}{2}} C^0((0, t_f], C^{3+\eta}([0, l])), \quad (\text{C.13d})$$

$$T_t \in \bigcap_{\eta, 0 \leq \eta < \frac{1}{2}} C^0((0, t_f], C^{1+\eta}([0, l])). \quad (\text{C.13e})$$

*In particular,  $T$  is a classical solution of (C.10) in  $[0, l] \times (0, t_f]$  and satisfies (C.10) in the strong sense, i. e.,  $\frac{d}{dt} T + \mathcal{L}T = g(\dot{w})$  in  $[0, t_f]$ .*

*Remark:* As for the definition of a weak solution, we refer to Lions [19], p. 44. There it is shown that the weak solution uniquely exists for right hand sides in (C.10) having even weaker regularity properties than  $g(\dot{w})$ .  $\diamond$

**Proof.** Since  $\dot{w} = u \in L^\infty(0, t_f)$ , the term  $g(\dot{w})$  is Lipschitzian from  $[0, t_f]$  into  $\mathbb{R}$ . Thus

$$g(\dot{w}) \in C^{0,1}([0, t_f], L^2(0, l)),$$

and integration by parts in (C.12) yields

$$T(t) = \mathcal{L}^{-1} g(\dot{w}(t)) - \mathcal{L}^{-1} e^{-t\mathcal{L}} g(\dot{w}(0)) - \int_0^t \mathcal{L}^{-1} e^{-(t-s)\mathcal{L}} \frac{d}{dt} g(\dot{w})|_{t=s} ds. \quad (\text{C.14})$$

This implies

$$\mathcal{L}T(t) = g(\dot{w}(t)) - e^{-t\mathcal{L}} g(\dot{w}(0)) - \int_0^t e^{-(t-s)\mathcal{L}} \frac{d}{dt} g(\dot{w})|_{t=s} ds,$$

$$\mathcal{L}T \in C^0([0, t_f], L^2(0, l)),$$

**On a Prototype Class of ODE-PDE State-constrained Optimal Control Problems**  
**Part 1: Analysis of the State-unconstrained Problems**

---

cf. [35], Sätze IV. 1.1 and IV. 1.2. In particular, the properties (C.13a, b, c) are satisfied and  $\frac{d}{dt}T + \mathcal{L}T = g(\dot{w})$  in  $[0, t_f]$ . Thus, the unique weak solution of (C.10) is given by (C.12). Since  $g(\dot{w})$  does not depend on  $x$ , we have

$$g(\dot{w}) \in C^0([0, t_f], C^2([0, l])) .$$

Moreover,

$$\mathcal{L}^\kappa e^{-t\mathcal{L}}g(\dot{w}(0)) \in C^0([0, t_f], L^2(0, l)) , \quad \kappa \in \mathbb{N} ,$$

thus

$$e^{-t\mathcal{L}}g(\dot{w}(0)) \in C^\infty([0, l] \times (0, t_f]) .$$

Since for any  $\varrho \in (0, 1]$  it holds

$$\mathcal{L}^{1-\varrho} \int_0^t e^{-(t-s)\mathcal{L}} \mathcal{L} \frac{d}{dt}g(\dot{w})|_{t=s} ds = \int_0^t \mathcal{L}^{1-\varrho} e^{-(t-s)\mathcal{L}} \mathcal{L} \frac{d}{dt}g(\dot{w})|_{t=s} ds$$

with an integrable and in  $0 \leq s < t$  continuous kernel, standard imbeddings furnish properties (C.13d, e). ◇

*Remark:* Property (C.13b) implies the continuity of  $T$  and  $T_x$  in  $[0, l] \times [0, t_f]$  as needed in Theorem 4.2. ◇

Next we deal with  $T_{tt}$  and  $\partial_x^4 T$ . To that end the concept of maximal regularity for parabolic equations can be used to advantage. We refer to [35], Chapter V. The functional-analytic version of this concept, as explained in this reference, is most easily applied to the present problem. First, we remark that  $\frac{d}{dt}g(\dot{w}(t)) = g'(\dot{w}(t))\ddot{w}(t)$ . Thus the chain rule holds. This is seen by taking appropriate approximations of  $w$ .

**Theorem 4.6.** *For any  $\varepsilon$ ,  $0 < \varepsilon < t_f$ , and any  $r \geq 2$  we have*

$$T_{tt} \in L^r(\varepsilon, t_f; L^2(0, l)) ,$$

$$\partial_x^4 T \in L^r(\varepsilon, t_f; L^2(0, l)) .$$

**Proof.** Let  $\varepsilon \in (0, t_f)$ . Let  $\zeta = \zeta_\varepsilon \in C^2([0, +\infty), \mathbb{R}^+)$  with  $\zeta(t) = 0$  in  $[0, \frac{\varepsilon}{2}]$ ,  $\zeta(t) = 1$  for  $t \geq \varepsilon$ . Let  $r \geq 2$ . Then

$$Z_t + \mathcal{L}Z = \zeta_t g(\dot{w}) + \zeta g'(\dot{w})\ddot{w} - \zeta_{tt}T - \zeta_t T_t ,$$

$$Z(0) = 0$$

has a unique solution  $Z$  with

$$Z_t \in L^r(0, t_f; L^2(0, l)) ,$$

$$Z \in L^r(0, t_f; \mathcal{D}(\mathcal{L})) ;$$

cf. [35], Satz V. 2.5. Setting

$$z = \int_0^t Z ds ,$$

we obtain

$$z_t + \mathcal{L}z = \zeta g(\dot{w}) - \zeta_t T ,$$

and, by uniqueness,  $z = \zeta T$ ,  $Z = (\zeta T)_t$ . ◇

---

## 4.2 Problem 2: Boundary control of the PDE by the ODE

We now deal with the second problem (C.4). As for the regularity question, the form (C.6) is more favourable for a first step. We start with these equations. In order to distinguish between  $T$  in (C.4) and  $T$  in (C.6) we set

$$\hat{T} = T - \frac{1}{2} e^{x-l} h(\dot{w}) \cong T \quad \text{in Eqs. (C.6),}$$

$$T \quad \text{as in Eqs. (C.4).}$$

Let us mention the interpolation space

$$\mathcal{I}_{1-\frac{1}{r},r} := \left\{ y : \int_0^\infty \frac{1}{t^r} \| (e^{-t\mathcal{L}} - I) y \|^r dt < \infty \right\}$$

as introduced in [35], Definition V.2.1, for any  $r > 1$ . Then  $\mathcal{I}_{1-\frac{1}{r},r}$  is close to  $\mathcal{D}(\mathcal{L}^{1-\frac{1}{r}})$ . More precisely, for any  $\varepsilon > 0$  we have

$$\mathcal{D}(\mathcal{L}^{1-\frac{1}{r}+\varepsilon}) \subset \mathcal{I}_{1-\frac{1}{r},r} \subset \mathcal{D}(\mathcal{L}^{1-\frac{1}{r}-\varepsilon}), \quad (\text{C.15})$$

$$\mathcal{I}_{1-\frac{1}{2},2} = \mathcal{D}(\mathcal{L}^{\frac{1}{2}})$$

with continuous imbeddings and equivalent norms, respectively; cf. [35], Chapter V., pp. 50, 59, Satz V.2.1. The appropriate first regularity Theorem for (C.6) is now at hand.

**Theorem 4.7.** *There is one and only one solution*

$$\hat{T} \in \bigcap_{r, r \geq 2} C^0([0, t_f], \mathcal{I}_{1-\frac{1}{r},r})$$

with

$$\hat{T}_t \in \bigcap_{r, r \geq 2} L^r(0, t_f; L^2(0, l)),$$

$$\hat{T} \in \bigcap_{r, r \geq 2} L^r(0, t_f; \mathcal{D}(\mathcal{L})),$$

$$\hat{T}_t(t) + \mathcal{L}\hat{T}(t) = \frac{1}{2} e^{x-l} \left( h(\dot{w}(t)) - \frac{d}{dt} h(\dot{w}(t)) \right) \quad \text{a. e. in } (0, t_f), \quad (\text{C.16})$$

$$\hat{T}(x, 0) = -\frac{1}{2} e^{x-l} h(\dot{w}(0)) \quad \text{on } [0, l].$$

**Proof.**  $\hat{T}(x, 0)$  is in  $\mathcal{D}(\mathcal{L})$ . The right hand side in (C.17) is in  $L^\infty(0, t_f; L^\infty(0, l))$  since  $h(\dot{w})$  has the distributional derivative  $h'(\dot{w}) \ddot{w} = h'(\dot{w}) u$ . Satz V.2.5 in [35] completes the proof.  $\diamond$

In the next step we again apply the maximum principle, now to Eqs. (C.4)

**Theorem 4.8.**  *$T$  as well as  $T_x$  of problem (C.4) are continuous in  $[0, l] \times [0, t_f]$ . Moreover,  $T - T_0 \geq 0$  in  $[0, l] \times [0, t_f]$  and assumes its global maximum in  $[0, l] \times [0, t_f]$  on  $x = l$ .*

**Proof.** Eq. (C.15), Theorem 4.7, and standard imbeddings show that  $T$  and  $T_x$  are continuous in  $[0, l] \times [0, t_f]$ . Indeed,  $T_x$  is even Hölder continuous in  $x$  and therefore in  $t$ ; cf. [18], pp. 78f. In particular,  $T$  is a classical solution of  $T_t - T_{xx} = 0$  in  $(0, l) \times (0, t_f)$  and therefore even real analytic there.

Assume now that  $T - T_0$  has a negative minimum in  $[0, l] \times [0, t_f]$ . Due to the maximum principle this is assumed on the parabolic boundary of  $[0, l] \times [0, t_f]$ . The only possibilities are  $x = 0$  and  $x = l$ . At a minimum point  $(0, t_0)$  on  $x = 0$ , we have, because of  $T(0, t_0) - T_0 < 0$ ,

$$\frac{\partial(T - T_0)}{\partial x}(0, t_0) = T(0, t_0) - T_0 < 0,$$

**On a Prototype Class of ODE-PDE State-constrained Optimal Control Problems**  
**Part 1: Analysis of the State-unconstrained Problems**

---

and, at a minimum point  $(l, t_0)$  on  $x = l$ , it holds, for the same reason,

$$\frac{\partial(T - T_0)}{\partial x}(l, t_0) = -(T(l, t_0) - T_0) + h(\dot{w}(t_0)) > 0.$$

However, both of these possibilities lead to a contradiction to  $T(0, t_0) - T_0$  and  $T(l, t_0) - T_0$  resp., being minimal.

Assume that  $T - T_0$  has a (global) positive maximum in  $(x_0, t_0)$ . It is assumed on  $\{0\} \times [0, t_f]$  or  $\{l\} \times [0, t_f]$ . For  $x_0 = 0$  we have

$$\frac{\partial(T - T_0)}{\partial x}(0, t_0) = T(0, t_0) - T_0 > 0$$

which is a contradiction. Hence, it must lie on  $\{l\} \times [0, t_f]$ . If the maximum of  $T - T_0$  vanishes, we have  $T \equiv T_0$ .  $\diamond$

*Remark:* Note that Theorem 4.8 does not imply that  $l = \arg \max_{x \in [0, l]} T(x, t)$  for all  $t \in [0, t_f]$ .

Finally, we investigate the convergence behaviour of the series (C.8) and (C.9), resp., representing the solutions of the two problems (C.3) and (C.4) or (C.6), resp.

**Theorem 4.9.**

a) *The (time dependent) coefficients*

$$a_n(t) := \left[ \int_0^t g(\dot{w}(s)) e^{-k_n^2(t-s)} ds \right] \cdot \left( \int_0^l \phi_n(y) dy \right) \frac{k_n}{N_n},$$

$$b_n(t) := \left[ \int_0^t g(\dot{w}(s)) e^{-k_n^2(t-s)} ds \right] \cdot \left( \int_0^l \phi_n(y) dy \right) \frac{1}{N_n}$$

of the series in  $\cos k_n x$  and  $\sin k_n x$  in the solution formula of Problem 1 are of order  $\mathcal{O}(n^{-4})$  uniformly in  $[0, t_f]$ . The coefficients associated with even modes vanish.

The series in  $\cos k_n x$  and  $\sin k_n x$  in the solution of Problem 1, Eq. (C.8), converge absolutely.

b) *The (time dependent) coefficients*

$$\bar{a}_n(t) := \left[ (1 + k_n^2) \int_0^t h(\dot{w}(s)) e^{-k_n^2(t-s)} ds \right] \cdot \left( \int_0^l e^y \phi_n(y) dy \right) \frac{k_n}{N_n},$$

$$\bar{b}_n(t) := \left[ (1 + k_n^2) \int_0^t h(\dot{w}(s)) e^{-k_n^2(t-s)} ds \right] \cdot \left( \int_0^l e^y \phi_n(y) dy \right) \frac{1}{N_n}$$

of the series in  $\cos k_n x$  and  $\sin k_n x$  in the solution formula of Problem 2 are of order  $\mathcal{O}(n^{-4})$  uniformly in  $[\varepsilon, t_f]$ ,  $0 < \varepsilon \leq t_f$ .

The series in  $\cos k_n x$  and  $\sin k_n x$  in the solution of Problem 2, Eq. (C.9), converge absolutely.

**Proof of a).** We investigate each factor of the coefficients separately. For  $t > 0$  we have

$$0 < \tau_n(t) := \int_0^t g(\dot{w}(s)) e^{-k_n^2(t-s)} ds < c \int_0^t e^{-k_n^2(t-s)} ds < c \frac{1}{k_n^2} = \mathcal{O}(n^{-2}).$$

Furthermore we obtain

$$\frac{1}{N_n^2} = \frac{1}{\frac{l}{2} k_n^2 + \frac{l}{2} + 1} = \frac{2}{l} \frac{1}{k_n^2} \frac{1}{1 + \frac{l+2}{l} \frac{1}{k_n^2}} = \frac{2}{l} \frac{1}{k_n^2} (1 + \mathcal{O}(k_n^{-2})) = \mathcal{O}(n^{-2}),$$

if  $|\frac{l+2}{l} \frac{1}{k_n^2}| < 1$ , which can always be fulfilled for sufficiently large  $n$ , e. g. for  $n \geq 2$ , if  $l = 1$ . Substituting (C.7b) in

$$\gamma_n := \int_0^l \phi_n(y) dy = \frac{1}{N_n} \left[ \sin k_n l + \frac{1}{k_n} (1 - \cos k_n l) \right],$$

one obtains

$$\gamma_n = \frac{1}{N_n} \left( \frac{2}{k_n} \cos k_n l + \frac{1}{k_n^2} \sin k_n l + \frac{1}{k_n} (1 - \cos k_n l) \right) = \mathcal{O}(k_n^{-2}) = \mathcal{O}(n^{-2}).$$

Because of  $a_n = \tau_n(t) \gamma_n \frac{1}{N_n} k_n$  and  $b_n = \tau_n(t) \gamma_n \frac{1}{N_n}$ , we at least have a decay of the order  $\mathcal{O}(n^{-4})$  of the coefficients of the cosine- and sine-terms of  $\varphi(x)$  uniformly in  $t$ . This also implies absolute convergence of the  $\cos k_n x - \sin k_n x$  series.

Moreover, the coefficients associated with even modes vanish due to the symmetry of the eigenfunctions. This can be seen as follows. For all  $n \in \mathbb{N}$  and all  $x \in [-\frac{l}{2}, \frac{l}{2}]$ , there holds, using the addition formulas of sine and cosine,

$$\begin{aligned} \varphi_n\left(\frac{l}{2} + x\right) &= \begin{cases} +\varphi_n\left(\frac{l}{2} - x\right) \\ -\varphi_n\left(\frac{l}{2} - x\right) \end{cases} &\iff \tan k_n \frac{l}{2} &= \begin{cases} \frac{1}{k_n} \\ -k_n \end{cases} \\ & &\iff \frac{2 \tan k_n \frac{l}{2}}{1 - \tan^2 k_n \frac{l}{2}} &= \frac{2 k_n}{k_n^2 - 1} = \tan k_n l. \end{aligned}$$

The upper branch holds if and only if  $n$  is odd, the lower one if and only if  $n$  is even. Hence, we have, for all  $\kappa \in \mathbb{N}$ ,

$$\varphi_{2\kappa-1}\left(\frac{l}{2} + x\right) = \varphi_{2\kappa-1}\left(\frac{l}{2} - x\right) \quad \text{and} \quad \varphi_{2\kappa}\left(\frac{l}{2} + x\right) = -\varphi_{2\kappa}\left(\frac{l}{2} - x\right) \quad \text{for} \quad -\frac{l}{2} \leq x \leq \frac{l}{2}, \quad (\text{C.17})$$

i. e., the eigenfunctions  $\varphi_{2\kappa-1}$ , resp.  $\phi_{2\kappa-1}$  are even, the eigenfunctions  $\varphi_{2\kappa}$ , resp.  $\phi_{2\kappa}$  are odd w. r. t.  $x = \frac{l}{2}$ . Therefore we have

$$\int_0^l \phi_{2\kappa-1}(y) dy = 2 \int_0^{\frac{l}{2}} \phi_{2\kappa-1}(y) dy \quad \text{and} \quad \int_0^l \phi_{2\kappa}(y) dy = 0.$$

**Proof of b).** For Problem 2, we proceed analogously and use the representation (C.9a). We now define  $\bar{\tau}_n$  by

$$\bar{\tau}_n(t) := h(\dot{w}(0)) e^{-k_n^2 t} - \int_0^t (h(\dot{w}(s)) - \frac{d}{ds} h(\dot{w}(s))) e^{-k_n^2 (t-s)} ds. \quad (\text{C.18})$$

Similarly to the first part of the proof, one obtains

$$\bar{\tau}_n(t) = \mathcal{O}(e^{-n^2 t}) + \mathcal{O}(n^{-2}) \quad \text{for} \quad t \in (0, t_f].$$

The rest of the proof proceeds analogously. By using (C.7b), one obtains

$$\bar{\gamma}_n := \int_0^l e^y \phi_n(y) dy = \frac{1}{N_n} e^l \sin k_n l = \frac{1}{N_n} e^l \cos k_n l \frac{2 k_n}{k_n^2 - 1} = \mathcal{O}(n^{-2}),$$

which also sums up to an asymptotic decay of the coefficients of order  $\mathcal{O}(n^{-4})$  at least, but now in  $[\varepsilon, t_f]$ ,  $0 < \varepsilon \leq t_f$ .  $\diamond$

*Remarks:* We now exploit Theorem 4.9. Since the  $\cos k_n x - \sin k_n x$  series are no longer orthogonal, we need to estimate the series of the absolute values for  $T$  and its derivatives.

According to Theorem 4.5, the solution of Problem 1 is in the class  $C^0((0, t_f], C^{3+\varepsilon}([0, l]))$ ,  $0 \leq \varepsilon < \frac{1}{2}$ , together with  $T_t \in C^0((0, t_f], C^{1+\varepsilon}([0, l]))$ ,  $0 \leq \varepsilon < \frac{1}{2}$ . As for the  $\cos k_n x - \sin k_n x$ -series we have absolute uniform convergence for the twice differentiated series  $T_{xx}$ .  $\diamond$

In Problem 2 however, the  $\cos k_n x - \sin k_n x$ -series improve on Theorem 4.7 for  $t > 0$ .

**Theorem 4.10.** *As for  $\hat{T}$  in Theorem 4.7, we have*

$$\hat{T} \in \bigcap_{\varepsilon, 0 \leq \varepsilon < 1} C^0([\delta, t_f], C^{2+\varepsilon}([0, l])),$$

$$\hat{T}_t \in L^\infty(\delta, t_f; C^\varepsilon([0, l])), 0 < \delta < t_f.$$

**Proof.** By Theorem 4.9 we have

$$\partial_x^2 \hat{T}(x, t) = - \sum_{n=1}^{\infty} k_n^2 (\bar{a}_n(t) \cos k_n x + \bar{b}_n(t) \sin k_n x)$$

with  $\bar{a}_n(t)$ ,  $\bar{b}_n(t)$  continuous in  $t$  and  $|\bar{a}_n(t)| \leq \frac{c}{k_n^4}$  as well as  $|\bar{b}_n(t)| \leq \frac{c}{k_n^4}$ . Now,

$$\frac{|\cos k_n x - \cos k_n x'|}{|x - x'|^\varepsilon} \leq c k_n^\varepsilon, \quad 0 \leq \varepsilon < 1, \quad x \neq x'.$$

A corresponding estimate holds for  $|\sin k_n x - \sin k_n x'|$ . This proves the first assertion. The second one follows from the equation for  $\hat{T}$ .  $\diamond$

## Conclusions and Outlook

This paper is inspired by several optimal control problems of real-life applications with side conditions in form of staggered systems of unilaterally coupled equations of different type, such as ordinary and partial differential equations, where a pointwise state constraint on variables of the highest level regenerates the dependency to the lowest level. We have studied a class of abstract optimal control problems, called hypersonic rocket car problems, for a controlled second-order ordinary differential equation, a state variable of which controls a heat equation through semi-linear coupling terms, either via a source term or a boundary condition. In the first part of this bipartite paper, theoretical results are obtained concerning existence and uniqueness of solutions of the state-unconstrained problems as well as the existence of a continuous control-to-state operator. Moreover, the positivity of the optimal solutions, their regularity properties and the existence of global maxima are thoroughly investigated.

Part 2 of the paper is then devoted to the state-constrained versions of the hypersonic rocket car problems. In particular, we will tighten the state constraint step by step. According to Theorem 4.4, resp. Theorem 4.8, the maximum temperature is attained either along  $x = \frac{l}{2}$  (for Problem 1) or  $x = l$  (for Problem 2). By means of those double hump solutions [Figs. C.2 (right), resp. C.3 (right)] the set of active constraints will be analyzed. In particular, the concept of order of a state constraint known in ODE optimal control will be generalized to PDE optimal control. For this analysis, the maximum regularity results of Theorems 4.6 (for Problem 1) and 4.10 (for Problem 2) turn out to be just sufficient to perform the successive differentiation process for determining the state constraint's order. Finally, Theorem 4.9, in particular the speed of convergence of the series representations will be of importance for obtaining the numerical results of Part 2.

# Bibliography

- [1] THE AMPL COMPANY, <http://www.ampl.com/>, 2013.
- [2] BECHMANN, S., FREY, M. *Regularisierungsmethoden für Optimalsteuerungsprobleme bei partiellen Differenzialgleichungen mit punktwweisen Zustandsbeschränkungen: Lavrentiev-Regularisierung und Moreau-Yosida-Reglarisierung*, Fakultät für Mathematik, Physik und Informatik, Universität Bayreuth, 2008.
- [3] BERGOUNIOUX, M., ITO, K., KUNISCH, K. *Primal-dual strategy for constrained optimal control problems*, SIAM Journal on Control and Optimization 37, No. 4, pp. 1176-1194, 1999.
- [4] BERGOUNIOUX, M., KUNISCH, K., *On the Structure of the Lagrange Multiplier for State-constrained Optimal Control Problems*, Systems and Control Letters, Vol. 48, 16–176, 2002.
- [5] BERGOUNIOUX, M., KUNISCH, K., *Primal-dual strategy for state-constrained optimal control problems*, Computational Optimization and Applications 22, No. 2, PP. 169-224, 2002.
- [6] BONNANS, J. F., DE LA VEGA, C., DUPUIS, X., *First- and Second-Order Optimality Conditions for Optimal Control Problems of State Constrained Integral Equations*, Journal of Optimization Theory and Applications, Vol. 159, pp. 1–41, 2013.
- [7] BRYSON, A. E., DENHAM, W. F., DREYFUS, S. E., *Optimal Programming Problems with Inequality Constraints, I*, AIAA Journal, Vol. 1, pp. 2544–2550, 1963.
- [8] BUSHAW, D. W., PhD Thesis, supervised by Solomon Lefschetz, Department of Mathematics, Princeton University, 1952, published as D. W. BUSHAW, *Differential Equations with a Discontinuous Forcing Term*. Experimental Towing Tank, Stevens Institute of Technology, Report No. 469, January 1953.
- [9] BUSHAW, D. W., *Optimal Discontinuous Forcing Terms*, Contributions to the Theory of Nonlinear Oscillations IV, Annals of Mathematics Studies 41, Princeton, 29–52, 1958.
- [10] CHUDEJ, K., *Effiziente Lösung zustandsbeschränkter Optimalsteuerungsaufgaben*, Habilitationsschrift, University of Bayreuth, Bayreuth, Germany, 2000.
- [11] Chudej, K., Günther, M.: *Global State Space Approach for the Efficient Numerical Solution of State-Constrained Trajectory Optimization Problems*, Journal of Optimization Theory and Applications, Vol. 103, No. 1, 75–93, 1999.
- [12] CHUDEJ, K., PESCH, H. J., WÄCHTER, M., SACHS, G., AND LE BRAS, F., *Instationary Heat Constrained Trajectory Optimization of a Hypersonic Space Vehicle*, in: A. Frediani, G. Butazzo (Eds.), Variational Analysis and Aerospace Engineering. — Berlin: Springer, 2009.
- [13] LAIRD, C. AND WÄCHTER, A., [www.coin-or.org/Ipopt/](http://www.coin-or.org/Ipopt/); for a documentation including a bibliography see [www.coin-or.org/Ipopt/documentation/](http://www.coin-or.org/Ipopt/documentation/), 2007.
- [14] HARTL, R. F., SETHI, S. P., VICKSON, R. G., *A Survey of the Maximum Principles for Optimal Control Problems with State Constraints*, SIAM Review, Vol. 37, 181–218, 1995.

- 
- [15] HINTERMÜLLER, M. AND RING, W., *A level set approach for the solution of a state-constrained optimal control problem*, Numerische Mathematik, Vol. 98, No. 1, 135–166, 2004.
- [16] JACOBSON, D. H., LELE, M. M., SPEYER, J. L., *New Necessary Conditions of Optimality for Control Problems with State-variable Inequality Constraints*, J. of Mathematical Analysis and Application, Vol. 35, 255–284, 1971.
- [17] KAPPEL, F., STETTNER, H., *Optimal Control Problems for Integrodifferential Equations of Volterra Type*, Technical Report, University of Graz, Dec. 1976.
- [18] LADYZHENSKAYA, O. A., SOLONNIKOV, V. A., AND URAL'CEVA, N. N., *Linear and Quasi-linear Equations of Parabolic Type*, American Mathematical Society, Providence, R. I., 1968.
- [19] LIONS, J. L., *Equations Differentielles Operationelles et Problèmes aux Limites*, Springer, Berlin, Heidelberg, New York, 1961.
- [20] MATLAB 2012A, <http://www.mathworks.com/>, 2012.
- [21] MAURER, H., *On the Minimum Principle for Optimal Control Problems with State Constraints*, Schriftenreihe des Rechenzentrums der Universität Münster, No. 41, Münster, Germany, 1979.
- [22] MAURER, H. AND OSMOLOVSKII, N., *Second order sufficient conditions for time-optimal bang-bang control problems*, SIAM J. Control and Optimization, Vol. 42, 2239–2263, 2004.
- [23] PESCH, H. J., *A practical guide to the solution of real-life optimal control problems*, Control and Cybernetics, Vol. 23, 7–60, 1994.
- [24] PESCH, H. J., *Schlüsseltechnologie Mathematik — Einblicke in aktuelle Anwendungen der Mathematik*, B. G. Teubner, Wiesbaden, Germany, 2002.
- [25] PESCH, H. J., RUND, A., VON WAHL, W., WENDL, S., *On a prototype class of ODE-PDE state-constrained optimal control problem, Part 1: Analysis of the state-unconstrained problem*, Preprint, University of Bayreuth (Attached in Appendix C)
- [26] PESCH, H. J., RUND, A., WENDL, S., *On a prototype class of ODE-PDE state-constrained optimal control problem, Part 2: Analysis of the state-constrained problem*, In Preparation, University of Bayreuth
- [27] PESCH, H. J., RUND, A., VON WAHL, W., WENDL, S., *On some new phenomena in state constrained optimal control if ODEs as well as PDEs are involved*, Control & Cybernetics, Vol. 39, 647-660, 2010.
- [28] PESCH, H. J., RUND, A., WENDL, S., *On a state constrained optimal control problem arising from ODE-PDE optimal control*, In Moritz Diehl, Francois Glineur, Elias Jarlebring und Wim Michiels, editors, Recent Advances in Optimization and its Applications in Engineering, pp. 429-438. Springer, Berlin, 2010.
- [29] RUND, A. *Beiträge zur Optimalen Steuerung partiell-differential algebraischer Gleichungen*, Fakultät für Mathematik, Physik und Informatik, Universität Bayreuth, 2012. (PDF version can be obtained via <http://opus.ub.uni-bayreuth.de/volltexte/2012/964/>)
- [30] SCHMIDT W., *Necessary Optimality Conditions for Control Processes Governed by Integro-differential Equations*, Trudy Institut Matematiki Minsk, Vol. 7(1), 151–158, 2001.
- [31] TRÖLTZSCH, F., *Optimal Control of Partial Differential Equations: Theory, Methods and Applications*, American Math. Society Graduate Studies in Mathematics, Providence 2010, Vol. 112, 399 pp.

## BIBLIOGRAPHY

---

- [32] WÄCHTER, A., *An Interior Point Algorithm for Large-Scale Nonlinear Optimization with Applications in Process Engineering*, Phd Thesis, Carnegie Mellon University, 2002.
- [33] WÄCHTER, A., BIEGLER, L. T., *On the Implementation of an Interior-point Filterline-search Algorithm for Large Scale Nonlinear Programing*, *Mathematical Programming*, Vol. 106, 25–57, 2006.
- [34] WÄCHTER, M., *Optimalflugbahnen im Hyperschall unter Berücksichtigung der instationären Aufheizung*, Phd Thesis, Technische Universität München, Faculty of Mechanical Engineering, Munich, Germany, 2004.
- [35] WAHL, W. VON, *Funktionalanalysis III, Kapitel 4, Kapitel 5*, [www.old.uni-bayreuth.de/departments/math/org/mathe6/publ/public.html](http://www.old.uni-bayreuth.de/departments/math/org/mathe6/publ/public.html).
- [36] WARGA, J., *Optimal control of differential and functional equations*, Academic Press, New York-London, 1972.



## Eidesstattliche Versicherung

Hiermit erkläre ich, dass ich die vorliegende Dissertation zum Thema "On a prototype of an optimal control problem governed by ordinary and partial differential equations" abgesehen von den Inhalten, welche in Zusammenarbeit mit H.J. Pesch, W. von Wahl und A. Rund entstanden und deshalb speziell gekennzeichnet sind, selbständig verfasst und keine anderen als die angegebenen Quellen und Hilfsmittel verwendet habe.

Diese Arbeit wurde weder in gleicher noch ähnlicher Form bei einem anderen Prüfungsverfahren zur Erlangung eines akademischen Grades eingereicht. Ich habe weder diese noch eine andere Promotionsprüfung an dieser oder einer anderen Hochschule endgültig nicht bestanden.

Die Hilfe von gewerblichen Promotionsberatern bzw. -vermittlern oder ähnlichen Dienstleistern habe ich nicht in Anspruch genommen und werde dies auch zukünftig nicht tun.

Bayreuth, den 06.12.2013

Stefan Wendl